University of Southern Queensland
Faculty of Engineering & Surveying

Instrumentation to Track the Southern Elephant Seal

A dissertation submitted by

Peter Deith

In fulfilment of the requirements of

ENG4112 Research Project

Towards the degree of

Bachelor of Electrical and Electronic Engineering

Submitted: October 2005

Abstract

Marine mammal researchers at the University of Tasmania actively study the southern elephant seal each year by attaching electronic instruments to the animal and recording environmental variables experience during their time spent at sea. When the animals return to land the instruments are recovered and the data downloaded.

To further this research effort a companion instrument capable of recording magnetic bearing Ψ, pitch Φ and roll Θ and has been designed and constructed in prototype. The instrument measures and logs the earth's magnetic field in three axis and the direction of gravity in two axis. Measuring the vector magnetic field strength is accomplished using a three axis (x,y,z) magnetoresistive device which produces analogue voltage outputs X^*, Y^* and Z^* representing its direction with respect to the earth's magnetic field. Measurement of orientation in terms of Φ and Θ is achieved by using an analogue two axis (x,y) micromachined accelerometer. The analogue signals are then converted to digital using a 10 bit analogue to digital converter. The data logging instrument is microcontroller controlled and incorporates flash memory capable of storing over 4 million bytes of information. This represents 97 days of directional data if sampled every 10 seconds. To link the data from the instrument with data gathered from other instruments, accurate timing is used, facilitated by a precision clocking oscillator with accuracy in the order of ± 1 minute per year.

Static and dynamic evaluation using a non aquatic testing regime has accurately quantified the discrimination achieved by the instrument. For magnetic bearing Ψ a discrimination of 1° is achievable. Acceleration can be measured to 0.5% of 1g and hence provides discrimination in pitch Φ and roll Θ of 5.3°. The uncertainty of Ψ, Φ and Θ measurements over the full range of orientation is quantified and reduced to predictable functions permitting compassing and orientation errors to be calculated for any position of the instrument.

In conclusion, the design of the instrument has reached a stage of development where discrimination of Ψ, Φ and Θ together with errors has been accurately assessed and data can be successfully recorded. Further work needed has been identified to develop the instrument into a form that marine mammal researchers can deploy and use in the field to achieve their research goals.

University of Southern Queensland
Faculty of Engineering & Surveying

ENG4111/2 Research Project

Limitations of Use

The Council of the University of Southern Queensland, its Faculty of Engineering and Surveying, and the staff of the University of Southern Queensland, do not accept any responsibility for the truth, accuracy or completeness of material contained within or associated with this dissertation.
Persons using all or any part of this material do so at their own risk, and not at the risk of the Council of the University of Southern Queensland, its Faculty of Engineering and Surveying or the staff of the University of Southern Queensland.

This dissertation reports a educational exercise and has no purpose or validity beyond this exercise. The sole purpose of the course pair entitled "Research Project" is to contribute to the overall education within the student's chosen degree program,. This document, the associated hardware, software, drawings, and other material set out in the associated appendices should not be used for any other purpose: if they are so used, it is entirely at the risk of the user.

Prof G Baker

Dean

Faculty of Engineering and Surveying

Certification

I certify that the ideas, designs and experimental work, results, analysis and conclusions set out in this dissertation are entirely my own effort, except where otherwise indicated and acknowledged.

I further certify that the work is original and has not been previously submitted for assessment in any other course or institution, except where specifically stated.

Peter Allan Deith

Student No.0019923017

______________________________Signature

______________________________Date

Acknowledgements

I would like to thank Steve Wall for asking,

"Do compasses work underwater?"

and my other biologist friends for providing the background, research documents and enlightening me to the world of marine mammal research.

Dr Nigel Hancock my supervisor for taking the reins and providing me with robust discussion, guidance and constructive criticism where I needed it most.

The staff of the FoES workshop, for the attention to detail in producing the prototype boards, fine work, well done.

Also Dr John Leis and Jeff Sinnamon who assisted in the early stage of developing a project proposal and for continued encouragement.

And my friends and family who tolerated the many late nights and preoccupation with study.

Contents

Abstract i

Limitations of Use ii

Certification........ iii

Acknowledgements iv

List of Figures ix

List of Tables xii

List of Tables xii

Chapter 1 Introduction 1

1.1 Project Aim........ 1
1.2 Specific Project Objectives........ 1
1.3 Chapter Overview........ 2

Chapter 2 The Southern Elephant Seal 4

2.1 The impetus for research 4
2.2 Biological Research Direction........ 5
2.3 Existing Trackers and Tags. 6
2.4 Velocity Time Depth Recorder (VTDR) data........ 8
2.5 Satellite Linked Time Depth Recorder (LTDR). 9
2.6 Limitations of current trackers........ 10
2.7 Demand from the Scientific Community........ 11

Chapter 3 Hardware Development........ 12

3.1 Introduction-The Component Selection Process 12
3.2 Plausible Components Selection Criteria. 12
3.2.1 Battery Operated Power Supply 12
3.2.2 Micro-Controller Selection. 13
3.2.3 Non-volatile memory selection........ 15
3.2.4 Oscillator........ 16
3.2.5 Communications Interface 17
3.3 Sensors........ 17
3.3.1 Exploring existing compassing solutions........ 18
3.3.2 Magnetic Sensing. 20
3.3.3 Gravitational Sensing. 21
3.4 Component Selection - an iterative process........ 23

Chapter 4 Circuit Schematic Design........ 24

4.1 Schematic Design Methodology........ 24
4.2 Power Supply........ 25
4.3 Microcontroller........ 25
4.4 Memory. 29
4.5 Precision Oscillator........ 31
4.6 Magnetic Sensor 31
4.7 The Accelerometer 34
4.8 The Communications Interface........ 34

Chapter 5 Software Design Requirements........ 37

5.1 Software Specification........ 37
5.2 Software Approach. 38

5.2.1 Initialisation Module. 39
5.2.2 Sample Sensors Module 40
5.2.3 Store Data Module 41
5.2.4 Decision Module 42
5.3 Structured Programming 43
5.3.1 Initialisation 43
Chapter 6 Prototype No.1 Construction. 45
6.1 PCB Layout and Construction 45
6.2 PCB Layout 46
6.3 PCB Construction. 47
6.4 Completion of Prototype No.1 48
Chapter 7 Prototype No.1 Evaluation 50
7.1 Prototype Evaluation Methodology. 50
7.2 Physical Inspection 50
7.3 Electrical Modules 51
7.3.1 Communication Board. 52
7.3.2 Power Supply 52
7.3.3 Microcontroller 53
7.3.4 Memory 53
7.3.5 Oscillator. 54
7.3.6 Accelerometer 54
7.3.6.1 'Static Testing' Regime 54
7.3.6.2 Accelerometer Static Resolution 55
7.3.6.3 Accelerometer low pass filtering 56
7.3.6.4 'Dynamic Testing' Regime 57
7.3.7 Magnetoresistive Stage. 57
7.4 Conclusions: Prototype No.1 58
Chapter 8 Prototype No.2 Construction 59
8.1 Adopting Recommendations from Prototype 1. 59
8.2 Design Improvements Prototype No.2 60
8.2.1 Physical Inspection 60
8.2.2 Communications 60
8.2.3 Power Supply 60
8.2.4 Oscillator 60
8.2.5 Accelerometer 61
8.2.5.1 Accelerometer resolution improvement 61
8.2.5.2 Accelerometer improved low pass filter 61
8.2.6 Magnetoresistive 62
8.3 Construction of Prototype No.2 62
Chapter 9 Prototype No.2 Evaluation. 64
9.1 Prototype Evaluation Methodology. 64
9.2 Physical Inspection 64
9.3 Electrical Modules 65
9.3.1 Communication Board 65
9.3.2 Power Supply 65
9.3.3 Microcontroller 65
9.3.3 Memory 65
9.3.4 Oscillator. 65
9.3.5 Accelerometer 66
9.3.5.1 'Static Testing' Regime 66
9.3.5.1 Static resolution 66
9.3.5.2 'Dynamic Testing' Regime 67
9.3.5.3 Dynamic Resolution 68
9.3.6 Magnetoresistive Stage 68
9.3.6.1 Offset Voltage Error 68
9.3.6.2 Magnetic Resolution and Voltage Output. 69

9.4 Energy Budget 70
9.5 Conclusions: Prototype No.2 70

Chapter 10 Instrument Performance 71

10.1 Why Performance Testing 71
10.2 Testing Methodology 71
10.3 Experimental Design 72
10.4 Testing Environment 73
10.5 Experiment No.1 75
10.5.1 Error due to amplifier offset 76
10.5.2 Adjusting sensor offset 76
10.6 Determining magnetic resolution 76
10.7 Determining the variability in the responses 77
10.8 Experimental Investigation 78
10.9 Determining sources of variation 80
10.10 Determining repeatability of readings 81
10.11 Electrical Investigation into Noise 82

Chapter 11 Interpreting the Data 83

11.1 Output from instrument 83
11.2 Determining heading from the data. 84
11.3 Determining Pitch and Roll from the data 86
11.3.1 Determining pitch angle Φ 86
11.3.2 Determining roll angle Θ 87
11.3.3 Determining if the device is inverted 87
11.3.4 Interpreting the results pitch Φ and roll Θ 88
11.4 Treatment of Compassing Error 88
11.5 Discrimination Summary 89

Chapter 12 Conclusion 91

12.1 Conclusion 91
12.2 Achievement of Project Objectives 92
12.3 Further Work 94
12.4 Ethical Consideration 95

References 96

Appendix A Project Specification 98

A.1 Issue C, 17 March 2005. 99
A.2 Issue B , 13 March 2005 100
A.3 Issue A , 3 February 2005 101

Appendix B Prototype No.1 Drawings 102

Note. In each case the printed drawing is unavoidably compressed but may be viewed with clarity in the software (pdf) version of this dissertation
B.1 Microcontroller 102
B.1 Microcontroller 103
B.2 Flash Memory 104
B.3 Magnetoresistive Sensor 105
B.4 Accelerometer 106
B.5 Communication 107

Appendix C Prototype No.2 Drawings 108

Note. In each case the printed drawing is unavoidably compressed but may be viewed with clarity in the software (pdf) version of this dissertation
C.1 Microcontroller Board 108
C.1 Microcontroller Board 109
C.2 Sensor Board 110
C.3 Communications Board 111

Appendix D Code Listing 112

D.1 Code Modules. 113
D 1.1 Write to External Memory 113
D 1.2 Selected Read ADC Modules 117

Appendix E Experimental Method and Data 120

E.1 Laboratory testing of Tracker 122
E.1.1 Testing apparatus. 122
E.1.2. Testing Precautions 122
E.1.3. Controlling the testing environment. 122
E.1.4. Set Up Procedure 123
E.1.5 Experimental Method. 123
E 2.1 Experiment No.1 Magnetic X and Y axis. 125
E 2.2 Experiment No.2 Magnetic X and Y axis. 129
E 2.3 Experiment No.3. Magnetic X and Y axis. 135
E 2.4 Experiment No 4. Magnetic X and Y axis 141
E 2.5 Experiment No.5 Magnetic X and Y axis. 147
E 2.6 Experiment No.6 Magnetic X and Y axis. 149
E 2.7 Experiment No.7 Magnetic X axis. 155
E 2.8 Experiment No.8 Magnetic Y axis 157
E 2.9 Experiment No.9 Accelerometer Y axis and Magnetic Z axis 159
E 2.10 Experiment No.10 Accelerometer X axis and Magnetic Z axis 161

Appendix F Miscellaneous 163

List of Figures

FIGURE 1 ANNUAL CENSUS RESULTS SHOWS CLEARLY THE LONG TERM DECLINE IN THE FEMALE ELEPHANT SEAL POPULATION. THE FEMALE POPULATION NUMBERS ARE A CRUCIAL REFLECTION OF THE SPECIES ABILITY TO REGENERATE. HTTP://WWW.DPIWE.TAS.GOV.AU 4
FIGURE 2. THE WILDLIFE COMPUTERS MK8 VTDR IS CONFIGURED TO RECORD DEPTH, LIGHT LEVEL, TEMPERATURE AND VELOCITY AT 30 SECOND INTERVALS AND STORES THE INFORMATION USING 16MB OF MEMORY FOR LATER RETRIEVAL. 6
FIGURE 3 THE SERIES 7000 SLTDR USES THE ARGOS SATELLITE SYSTEM TO RELAY DATA FROM A SURFACED SEAL AND PROVIDES RESEARCHERS WITH CLOSE TO REAL TIME GEOGRAPHICAL POSITIONING VIA A SECURE WEB ADDRESS GENERATED AT THE SEA MAMMAL RESEARCH UNIT AT THE UNIVERSITY OF STANDREWS, SCOTLAND. TIME, DEPTH AND VELOCITY IS ALSO RECORDED ON BOARD AND DOWNLOADED WHEN THE UNIT IS RECOVERED. 7
FIGURE 4 SLTDR (L), VTDR (R) AND VHF LOCATOR BEACON (TOP R). THE SCIENTIFIC PAYLOADS ATTACHED TO SEALS ARE SMALL IN COMPARISON TO THE TARGET ANIMAL, AN ADULT COW BEING IN THE ORDER OF 300KG AND 2.5M IN LENGTH. 7
FIGURE 5 VTDR DATA. THE SCREENSHOT FRAME REPRESENTS EIGHT DIVES, THE DEEPEST BEING APPROXIMATELY 1350 METERS OF 37 MINUTE DURATION RECORDED ON APRIL 9TH 2004 AT 1.45AM. THE SEAL PROVIDING THIS DATA WAS B836, A MATURE FEMALE. DATA COURTESY OF DR M HINDELL. 8
FIGURE 6 VTDR DATA. THE SCREENSHOT FRAME REPRESENTS 9 DIVES ON THE 11TH APRIL 2004 AT 4AM. THE WATER TEMPERATURE IS PLOTTED AS THE LOWER CURVE TOWARDS THE BOTTOM OF THE FRAME. BY SUPERIMPOSING THE DIVE PROFILE, UPPER CURVE, ON THE SAME FRAME, THE RELATIONSHIP BETWEEN DEPTH AND TEMPERATURE CAN BE EXPLORED. DATA COURTESY OF DR M HINDELL. 9
FIGURE 7 SATELLITE TRACKS OF DEPLOYED SLTDR UNITS ON 18 MARCH 2005. ELEVEN TRACKS ARE RECORDED EMANATING FROM MACQUARIE ISLAND (CENTRE) EXTENDING WELL SOUTH TOWARDS ANTARCTICA, A DISTANCE TRAVELLED OF 2000KM. NEW ZEALAND IS VISIBLE AT THE TOP, ANTARCTICA AT THE BOTTOM OF THE FRAME WITH LATITUDE AND LONGITUDE INSCRIBED ON THE BOARDERS. IMAGE COURTESY OF S. WALL. 10
FIGURE 8 DISCHARGE CURVES OF DIFFERENT BATTERY CHEMISTRIES LISTED IN TABLE 3. THE CURVES ARE RECORDED AT 25°C AT THE 1000 HOUR RATE. A CUT AWAY DIAGRAM OF A LITHIUM BATTERY SHOWS THE STRUCTURAL ELEMENTS. DATA SHEET: SONNENSCHEIN LBT BROCHURE (2003)...13
FIGURE 9 THE DS32KHZ PRODUCES A TEMPERATURE COMPENSATED OUTPUT OF 32.768KZ. THE OSCILLATOR CORRESPONDS WITH THE SPECIFIED FREQUENCY NEEDED FOR THE RTC IN THE SELECTED MC68HC908LJ24 MICROCONTROLLER. DS32KHZ TCXO (2004).......................16
FIGURE 10 THE POSITION OF AN AIRCRAFT CAN BE DESCRIBED BY ROLL AND PITCH COMBINED WITH A COMPASS BEARING. PITCH IS THE POSITION OF THE NOSE, EITHER UP OR DOWN, ROLL IS THE AMOUNT OF TILT WITH RESPECT TO THE WINGS, EITHER LEFT OR RIGHT AND IS MOST COMMONLY REPRESENTED IN THE COCKPIT BY A GIMBALLED INSTRUMENT. COURSE IS DERIVED FROM A MAGNETIC COMPASS AND DISPLAYED WITH RESPECT TO MAGNETIC NORTH. CARUSO (2004) 18
FIGURE 11 THE HMR3000 PROVIDES COMPASSING INFORMATION BY COMBINING A TWO AXIS MAGNETORESISTIVE SENSOR IN CONJUNCTION WITH A TWO AXIS ELECTROLYTIC TILT SENSOR. HONEYWELL AUSTRALIA PROVIDED A DEMONSTRATION UNIT FOR EVALUATION PURPOSES. HMR3000 DCM (2004)..18
FIGURE 12 SCHEMATIC OF CONNECTING CABLE TO PROVIDE POWER AND COMMUNICATIONS LINES BETWEEN THE HMR3000 AND A PC. *DCM USERS GUIDE (2004)* 19
FIGURE 13 HX AND HY MAGNETOMETER READINGS FOR DIFFERENT COMPASS HEADINGS. A FULL EXPLANATION IS PROVIDED IN *COMPASS HEADING USING MAGNETOMETERS AN203 (2004).* .21
FIGURE 14 FUNCTIONAL BLOCK DIAGRAM OF ACCELEROMETER SHOWING THE COMPLEX STAGES WITHIN THE INTEGRATED CIRCUIT WHICH RESULT IN COMPACT SENSING SOLUTIONS REQUIRING LITTLE EXTERNAL BIASING CIRCUITRY. ±10G DUEL AXIS MICROMACHINED ACCELEROMETER (2004). 22
FIGURE 15 ANTICIPATED OUTPUT OF ACCELEROMETER TO THE EFFECT OF GRAVITY IN A STATIC APPLICATION. WHEN THE COMPONENT IS POSITIONED AS SHOWN THE X AND Y OUTPUT VOLTAGES REPRESENT A 1G OUTPUT. *±10G DUEL AXIS MICROMACHINED ACCELEROMETER (2004).* 22

FIGURE 16 TWO OPTIONS FOR EXTERNAL FILTERING WAS PROVIDED IN DATA SHEETS, OPTION (A) IS FOR APPLICATIONS WHERE STABLE PLL OPERATION IS IMPORTANT AND OPTION (B) IS SUGGESTED FOR APPLICATIONS WHERE STABILITY IS NOT CRITICAL AS DESCRIBED IN *MC68HC908LJ24 DATA SHEET (2004).* 26
FIGURE 17 POWER SUPPLY BYPASSING RECOMMENDED TO REDUCE NOISE EFFECTS ON THE MICROCONTROLLER. MC68HC908LJ24 DATA SHEET (2004). COPYRIGHT MATERIAL OWNED BY FREESCALE SEMICONDUCTOR, INC. USED WITH PERMISSION, 2005 26
FIGURE 18 MC68HC908LJ24 BLOCK DIAGRAM SHOWING PORT USAGE AND FUNCTIONAL BLOCKS. THIS CONTROLLER WAS SPECIFICALLY DESIGNED BY FREESCALE TO CONTROL LCD DISPLAYS AND ADAPTED FOR THIS PROJECT. COPYRIGHT MATERIAL OWNED BY FREESCALE SEMICONDUCTOR, INC. USED WITH PERMISSION, 2005 27
FIGURE 19 THE AT49BV322AT PROVIDES A CHOICE OF 16BIT WORD OR 8 BIT BYTE DATA BUS WIDTH, FOR THIS APPLICATION THE 8 BIT BYTE OPTION WAS SELECTED. *32MBIT FLASH MEMORY (2004).* 30
FIGURE 20 EACH OF THE BRIDGE NETWORKS IS ARRANGED TO REPRESENT ONE AXIS OF MAGNETIC DETECTION, EITHER *X,Y* OR *Z.* THE OUTPUT OF THE BRIDGE PROVIDES THE INPUT TO THE OPERATIONAL AMPLIFIER STAGE THEN DIRECTLY INTO AN ANALOGUE TO DIGITAL CONVERTER. *1,2 AND 3 AXIS MAGNETIC SENSORS (2004)* 32
FIGURE 21 OPERATIONAL AMPLIFIER USED AS A DIFFERENCE AMPLIFIER TO INCREASE THE OUTPUT OF THE MAGNETORESISTIVE BRIDGE CIRCUIT. IN THIS APPLICATION R1=R3=4.7K AND R2=R4=470K. *1,2 AND 3 AXIS MAGNETIC SENSORS (2004)* 33
FIGURE 22 THE ACCELEROMETER IC SAMPLES THE INTERNAL MICRO MACHINED SENSORS AT A RATE OF 52KHZ. THE OUTPUT FILTER CIRCUIT OF 1KΩ AND 0.1UF REMOVES THE NOISE GENERATED FROM THE INTERNAL SWITCHED CAPACITOR FILTER CIRCUIT. *±10G DUEL AXIS MICROMACHINED ACCELEROMETER (2004)* 34
FIGURE 23 CONDITIONS REQUIRED TO ENTER MONITOR MODE AS OUTLINED IN MC68HC908LJ24 DATA SHEET (2004). COPYRIGHT MATERIAL OWNED BY FREESCALE SEMICONDUCTOR, INC. USED WITH PERMISSION, 2005. 35
FIGURE 24 THE TOP DOWN APPROACH PROMOTES A MODULAR DESIGN CAPABLE OF MODIFICATION, THEREBY AIDING BOTH SUBSEQUENT OPTIMISATION AND MAINTENANCE. EACH OF THE MAIN FUNCTIONAL MODULES ARE FURTHER EXPLODED INTO SUB MODULES BEFORE STRUCTURED PROGRAMMING IS APPLIED TO BUILD THE CODE SECTIONS. 38
FIGURE 25 THE FLOW CHART DEMONSTRATES THE SEQUENTIAL ORDER FOLLOWED BY THE PROGRAM TO OPERATE THE MICROCONTROLLER AND FORMS THE BASIS OF THE INITIALISATION MODULE OF CODE. 39
FIGURE 26 THE ADC TRANSFORMS THE OUTPUT FROM THE SENSOR CIRCUITS INTO A DIGITAL REPRESENTATION OF THE VOLTAGE SO THAT IT CAN BE STORED IN THE FLASH MEMORY FOR LATER RETRIEVAL. 40
FIGURE 27 THE WRITING OF DATA TO EXTERNAL MEMORY REQUIRES PRECISE SEQUENTIAL STEPS INDICATED IN THE FLOW CHART. 41
FIGURE 28 THE DECISION TO CONTINUE RECORDING DATA IS CRITICAL TO PREVENT OVERWRITING EARLIER DATA SHOULD THE MEMORY ADDRESS EXCEED 3F FF FF. 42
FIGURE 29 PCB DESIGN OF INSTRUMENT USING A TWO LAYER BOARD. TOP LAYER COPPER TRACKS AND PADS ARE PRESENTED IN BLACK, BOTTOM LAYER IN RED, VIAS AND THROUGH HOLES IN GREY. THE ACTUAL DIMENSION OF THE BOARD IS 77MM X 50MM. 46
FIGURE 30 PCB DESIGN OF COMMUNICATIONS INTERFACE BOARD USING A TWO LAYER BOARD. THE DIMENSION OF THE BOARD IS 90MM X 33MM. 47
FIGURE 31 PROTOTYPE NO.1. USING SURFACE MOUNTED COMPONENTS IN THE DESIGN MADE THE INSTRUMENT COMPACT. TO FURTHER MINIATURISE THE DEVICE USING DECREASED TRACK WIDTHS AND CLEARANCES, COMMERCIAL PCB MANUFACTURING WOULD BE REQUIRED. SEVERAL FOOTPRINTS ARE UNPOPULATED AS THE COMPONENTS WERE ROBBED FOR THE CONSTRUCTION OF THE SECOND PROTOTYPE. 49
FIGURE 32 COMMUNICATIONS BOARD NO.1. ONLY A HANDFUL OF COMPONENTS ARE NECESSARY TO PROVIDE THE LEVEL SWITCHING TO ENABLE A PC TO COMMUNICATE WITH THE MICROCONTROLLER EFFECTIVELY. 49
FIGURE 33 SINGLE POLE LOW PASS FILTER USED TO REMOVE SWITCHED CAPACITOR NOISE COMPONENTS FROM ACCELEROMETER. FREQUENCY COMPONENTS OF NOISE ABOVE THE CORNER FREQUENCY OF 1600HZ ARE ATTENUATED BY THE FILTER AT A RATE OF –20DB/DECADE. 56

FIGURE 34 PROTOTYPE NO.2 THE GROUND PLANE IS VISIBLE BETWEEN THE UPPER DATA LOGGER AND THE LOWER SENSOR BOARD IS CONSTRUCTED OF UNETCHED COPPER PCB CUT TO SIZE. 59
FIGURE 35 INSTRUMENT PROTOTYPE NO.2. THE SECOND PROTOTYPE IS CONSTRUCTED OF TWO PCBS CONNECTED BY A PIN HEADER. TO REDUCE NOISE A GROUND PLANE IS ALSO INSERTED BETWEEN UPPER AND LOWER BOARDS. 63
FIGURE 36 COMMUNICATIONS BOARD, SECOND PROTOTYPE. THE COMMUNICATIONS BOARD IS A SIMPLE ARRANGEMENT USING DB9 CONNECTORS AT EITHER END OF THE BOARD. THE CONNECTORS ARE POLARISED TO PREVENT INCORRECT CONNECTION. 63
FIGURE 37 THE BASIC CONCEPT OF A FACTORIAL DESIGN, IN THIS CASE THE SYSTEM IS REDUCED TO ONE FACTOR AND FIVE RESPONSE VARIABLES. THE ASSUMPTION MADE UNDER THIS DESIGN IS THAT THE FACTORS AND RESPONSE VARIABLES ARE INDEPENDENT OF EACH OTHER. 73
FIGURE 38 ATTACHING THE INSTRUMENT TO THE SURVEYORS SIGHT PERMITTED ACCURATE ROTATION, STRENGTHENING THE REPEATABILITY OF THE EXPERIMENTAL METHOD. THE GRADUATION RING SEEN AT THE BOTTOM OF THE SIGHT IS MARKED WITH 1˚ INCREMENTS WITH EXPERIMENTAL MEASUREMENTS TAKEN AT 10˚ INTERVALS. 74
FIGURE 39 MAGNETIC SENSOR OUTPUT FROM *X, Y* AND *Z* SENSORS WITH MID RAIL INCLUDED. THE GRAPH SHOWS SUBSTANTIAL OFFSET IN THE *Y* SENSOR OUTPUT WITH THE *Z* SENSOR RESPONSE = 0. THE EXPERIMENT WAS CONDUCTED TWICE HENCE THE DATA ARE LABELLED '1' AND '2'. THE DIFFERENCE BETWEEN READINGS INDICATES THE PRESENCE OF NOISE IN THE CIRCUIT ..75
FIGURE 40 THE VARIABILITY BETWEEN *X* AXIS TRIALS IS SUBSTANTIAL, THE AVERAGE VARIATION IS 5.8 ADC STEPS, THIS REPRESENTS A VOLTAGE DIFFERENCE OF APPROXIMATELY 20MV AND THE WORST CASE IS 15 ADC STEPS WHICH IS EQUIVALENT TO AROUND 52MV. 77
FIGURE 41 VARIATION BETWEEN THREE EXPERIMENTAL RUNS OF X^* AND Y^* MAGNETIC ADC READINGS. THE GENERAL SHAPE IS SIMILAR TO FIGURE 13 SHOWING THE 90˚ PHASE DIFFERENCE BETWEEN X^* AND Y^* MAGNETIC READINGS AND THE GENERAL SINUSOIDAL WAVEFORM IN QUADRATURE AS EXPECTED. 78
FIGURE 42 EACH POINT REPRESENTS THE STANDARD DEVIATION OF THREE *X* AXIS READINGS X^* TAKEN AT 10˚ INCREMENTS OVER A FULL 360˚ ROTATION. 79
FIGURE 43 EACH POINT REPRESENTS THE STANDARD DEVIATION OF THREE *Y* AXIS READINGS Y^* TAKEN AT 10˚ INCREMENTS OVER A FULL 360˚ ROTATION. 79
FIGURE 44 DATA OBTAINED BY THE INSTRUMENT WITH EXTERNAL SOURCES OF NOISE REMOVED. THE READINGS DEMONSTRATE THE QUALITY OF DATA OBTAINABLE AND OFFER AN INSIGHT INTO THE REPEATABILITY OF THE INSTRUMENT. THE IMPROVEMENT IN DATA QUALITY IS EVIDENT WHEN COMPARED WITH FIGURE 41. 81
FIGURE 45 COLLATING ADC INPUTS GRAPHICALLY DEMONSTRATES THE EFFECTIVENESS OF THE DESIGN. OFFSET IS EVIDENT IN ALL SENSORS, PROVIDED THE SENSORS DO NOT MAKE EXCURSIONS TOO CLOSE TO THE TOP OR BOTTOM RAIL CLIPPING WILL NOT OCCUR AND THE DATA WILL BE COMPLETE. 83
FIGURE 46 DIAGRAMMATIC REPRESENTATION OF THE COMPONENTS OF MAGNETIC FIELD DETECTED BY THE INSTRUMENT AND THE RELATIONSHIP TO THE HORIZONTAL PLANE. AN200 (1996) 84
FIGURE 47 THE ERROR IN PITCH AND ROLL CLEARLY SHOWS THE DEVICE IS MORE ACCURATE FOR SMALL VALUES OF TILT AND INCREASES TO A MAXIMUM AT ±90˚ TILT. 90

FIGURE E. 1 TOPCON SURVEYORS LEVEL WITH INSTRUMENT IN POSITION PRIOR TO SECURING USING CABLE TIES AND INSULATING TAPE. 124

List of Tables

TABLE 1 A WIDE RANGE OF BATTERY CHEMISTRIES ARE AVAILABLE IN THE LITHIUM RANGE, EACH CHEMISTRY HAS IT'S OWN ADVANTAGES AND DISADVANTAGES FOR APPLICATIONS. SONNENSCHEIN LBT BROCHURE (2003) 13
TABLE 2 ABBREVIATED SPECIFICATION OF HONEYWELL DIGITAL COMPASS MODULE. *HMR3000 DCM (2004)* 19
TABLE 3 A LIST OF FUNDAMENTAL COMPONENTS SATISFYING THE SPECIFICATION IS LISTED, THE COMPONENTS ARE ALL CAPABLE OF OPERATING BELOW 3.6V AND AT TEMPERATURES BELOW 0°C. 24
TABLE 4 ALLOCATION OF ADDRESS BUS LINES TO MICROCONTROLLER PORT BITS. 28
TABLE 5 ALLOCATION OF DATA BUS LINES TO MICROCONTROLLER PORT BITS. 28
TABLE 6 ALLOCATION OF CONTROL BUS LINES TO MICROCONTROLLER PORT BITS. 29
TABLE 7 ALLOCATION OF ANALOGUE TO DIGITAL INPUT PORTS TO SENSOR OUTPUTS. 29
TABLE 8 LEVELS REQUIRED TO TRIGGER MONITOR MODE DURING POR. 29
TABLE 9 DIP SWITCH SETTINGS PROVIDED TO SELECT NECESSARY OPERATING FREQUENCIES AND VOLTAGES TO PROGRAM MICROCONTROLLER 36
TABLE 10 CONFIGURATION REGISTER 1 43
TABLE 11 CONFIGURATION REGISTER 2 43
TABLE 12 CHIP ERASE ADDRESS HEX 555 COMMAND DEFINITION IN BINARY FORM. 44
TABLE 13 PORT OUTPUTS OF C, D AND F 44
TABLE 14 CHIP ERASE ADDRESS HEX AAA COMMAND DEFINITION IN BINARY FORM. 44
TABLE 15 REQUIRED PORT OUTPUTS OF C, D AND F 44
TABLE 16 PCB CONSTRUCTION LIMITATIONS FOR *FOES* WORKSHOP ASSISTANCE AND SPECIFICATION REQUIRED BY PROJECT. 45
TABLE 17 SOLDERING METHODS FOUND SUCCESSFUL ON REJECT BOARD AND ADOPTED DURING THE PLACEMENT OF COMPONENTS ON THE PROTOTYPE BOARDS. 47
TABLE 18 THERE ARE EIGHT MAJOR FUNCTIONS REQUIRED FOR THE COMMUNICATIONS BOARD TO INTERROGATE, DOWNLOAD DATA AND PROGRAM THE MICROCONTROLLER IN ACCORDANCE WITH THE SPECIFICATION. 52
TABLE 19. STATIC TESTING RESULTS OF THE ACCELEROMETER REFLECT THE MANUFACTURERS SPECIFICATIONS. 55
TABLE 20 THE RESULTS OF STATIC TESTING OF THE MMA6260 66
TABLE 21 LOW PASS FILTER COMBINATIONS AND RESPONSE TO DYNAMIC TESTING OF ACCELEROMETER. 67
TABLE 22 VOLTAGE MEASUREMENTS OF THE MAGNETIC FIELD SENSING CIRCUIT. THE APPLIED VOLTAGE WAS 3.4V AND THE MID RAIL VOLTAGE WAS 1.7V. 68
TABLE 23 EXPERIMENTS TO DETERMINE FACTORS CONTRIBUTING TO VARIATION IN RESPONSE. 80
TABLE 24 COMPASSING ERROR RESULTS. THE TOTAL ERROR INDICATES THE DIFFERENCE BETWEEN THE INSTRUMENTS READING AND MAGNETIC NORTH. 89

TABLE E. 1 SAMPLE A RAW DATA. CONDITIONS: NO SET/RESET, 3.5V REGULATED SUPPLY, 9MHZ OSCILLATOR IN CIRCUIT 125
TABLE E. 2 SAMPLE A NORMALISED DATA. (OFFSET REMOVED.) 126
TABLE E. 3 SAMPLE B RAW DATA. CONDITIONS: NO SET/RESET, 3.5V REGULATED SUPPLY, 9MHZ OSCILLATOR IN CIRCUIT 127
TABLE E. 4 SAMPLE B NORMALISED DATA. (OFFSET REMOVED.) 128
TABLE E. 5 SAMPLE A RAW DATA. CONDITIONS: NO SET/RESET, 3.5V REGULATED SUPPLY, 9MHZ OSCILLATOR IN CIRCUIT 129
TABLE E. 6 SAMPLE A NORMALISED DATA. (OFFSET REMOVED.) 130
TABLE E. 7 SAMPLE B RAW DATA. CONDITIONS: NO SET/RESET, 3.5V REGULATED SUPPLY, 9MHZ OSCILLATOR IN CIRCUIT. 131
TABLE E. 8 SAMPLE B NORMALISED DATA. (OFFSET REMOVED.) 132
TABLE E. 9 SAMPLE C RAW DATA. CONDITIONS: NO SET/RESET, 3.5V REGULATED SUPPLY, 9MHZ OSCILLATOR IN CIRCUIT 133
TABLE E. 10 SAMPLE C NORMALISED DATA. (OFFSET REMOVED.) 134
TABLE E. 11 SAMPLE A RAW DATA. CONDITIONS: SET/RESET EMPLOYED, 3.5V REGULATED SUPPLY, 9MHZ OSCILLATOR IN CIRCUIT. 135
TABLE E. 12 SAMPLE A NORMALISED DATA. (OFFSET REMOVED.) 136

TABLE E. 13 SAMPLE B RAW DATA. CONDITIONS: SET/RESET EMPLOYED, 3.5V REGULATED SUPPLY, 9MHZ OSCILLATOR IN CIRCUIT. 137
TABLE E. 14 SAMPLE B NORMALISED DATA. (OFFSET REMOVED.)....138
TABLE E. 15 SAMPLE C RAW DATA. CONDITIONS: SET/RESET EMPLOYED, 3.5V REGULATED SUPPLY, 9MHZ OSCILLATOR IN CIRCUIT. 139
TABLE E. 16 SAMPLE C NORMALISED DATA. (OFFSET REMOVED.)....140
TABLE E. 17 SAMPLE A RAW DATA. CONDITIONS: SET/RESET EMPLOYED, 3.5V REGULATED SUPPLY, 9MHZ OSCILLATOR DISCONNECTED FROM CIRCUIT....141
TABLE E. 18 SAMPLE A NORMALISED DATA. (OFFSET REMOVED.) 142
TABLE E. 19 SAMPLE B RAW DATA. CONDITIONS: SET/RESET EMPLOYED, 3.5V REGULATED SUPPLY, 9MHZ OSCILLATOR DISCONNECTED FROM CIRCUIT....143
TABLE E. 20. SAMPLE B NORMALISED DATA. (OFFSET REMOVED.) 144
TABLE E. 21 SAMPLE C RAW DATA. CONDITIONS: SET/RESET EMPLOYED, 3.5V REGULATED SUPPLY, 9MHZ OSCILLATOR DISCONNECTED FROM CIRCUIT....145
TABLE E. 22 SAMPLE C NORMALISED DATA. (OFFSET REMOVED.) 146
TABLE E. 23 SAMPLE A RAW DATA. CONDITIONS: SET EMPLOYED, 3.5V REGULATED SUPPLY, 9MHZ OSCILLATOR DISCONNECTED FROM CIRCUIT....147
TABLE E. 24 SAMPLE A NORMALISED DATA. (OFFSET REMOVED.) 148
TABLE E. 25 SAMPLE A RAW DATA. CONDITIONS: SET/RESET EMPLOYED, 3.6V LITHIUM BATTERY, 9MHZ OSCILLATOR DISCONNECTED FROM CIRCUIT....149
TABLE E. 26. SAMPLE A NORMALISED DATA. (OFFSET REMOVED.) 150
TABLE E. 27 SAMPLE B RAW DATA. CONDITIONS: SET/RESET EMPLOYED, 3.6V LITHIUM BATTERY, 9MHZ OSCILLATOR DISCONNECTED FROM CIRCUIT....151
TABLE E. 28. SAMPLE B NORMALISED DATA. (OFFSET REMOVED.) 152
TABLE E. 29 SAMPLE C RAW DATA. CONDITIONS: SET/RESET EMPLOYED, 3.6V LITHIUM BATTERY, 9MHZ OSCILLATOR DISCONNECTED FROM CIRCUIT....153
TABLE E. 30. SAMPLE C NORMALISED DATA. (OFFSET REMOVED.) 154
TABLE E. 31. SAMPLE A RAW DATA. CONDITIONS: SET/RESET EMPLOYED, 3.6V LITHIUM BATTERY, 9MHZ OSCILLATOR DISCONNECTED FROM CIRCUIT....155
TABLE E. 32 SAMPLE A NORMALISED DATA. (OFFSET REMOVED.) 156
TABLE E. 33. SAMPLE A RAW DATA. CONDITIONS: SET/RESET EMPLOYED, 3.6V LITHIUM BATTERY, 9MHZ OSCILLATOR DISCONNECTED FROM CIRCUIT....157
TABLE E. 34 SAMPLE A NORMALISED DATA. (OFFSET REMOVED.) 158
TABLE E. 35 SAMPLE A RAW DATA. CONDITIONS: SET/RESET EMPLOYED, 3.6V LITHIUM BATTERY, 9MHZ OSCILLATOR DISCONNECTED FROM CIRCUIT....159
TABLE E. 36. SAMPLE A NORMALISED DATA. (OFFSET REMOVED.) 160
TABLE E. 37. SAMPLE A RAW DATA. CONDITIONS: SET/RESET EMPLOYED, 3.6V LITHIUM BATTERY, 9MHZ OSCILLATOR DISCONNECTED FROM CIRCUIT....161
TABLE E. 38. SAMPLE A NORMALISED DATA. (OFFSET REMOVED.) 162

TABLE F 1 BATTERY BUDGET BY FUNCTIONAL MODULES. 163

Chapter 1 Introduction

1.1 Project Aim

This project set out to design an instrument that marine mammal researchers can attach to a living elephant seal in order to monitor its physical position in the water column whilst on an extended foraging trip at sea. The device needs to be small, battery operated and able to survive submersion up to 2km in depth.

The instrument is required to act as a companion device to existing Velocity Time Depth Recorders (VTDRs) and Satellite Linked Time Depth Recorders (SLTDRs) that researchers use to gather variables of an elephant seal excursion to sea such as dive depth, duration, water temperature and light levels. The linking mechanism between the existing instruments and the positional device relies on accurate time keeping built around a precision oscillator. In order to establish the position of the animal, a reference point is required, in this case the device uses the earth's magnetic field to provide a compass bearing and an accelerometer to determine the angle of roll and pitch based on a measure of gravity. The overall control of the instrument is the responsibility of a microcontroller and the storage of data provided by a 32Mbit flash memory IC.

1.2 Specific Project Objectives

To achieve the aim of the project a research design was developed based on identifying a number of research objectives, the sum of which satisfy the overall project aim.

The objectives identified are

- To research available literature and engage in personal communication with seal researchers to develop an insight into the biological aspects of the southern elephant seal.
- To examine the nature of data already being obtained via trackers to permit seamless integration of positional data.

- To investigate compassing technologies especially with respect to magneto-resistive devices.
- To consider microcontrollers and non volatile memory to form the foundation of a data recording device.
- To design circuit schematics and create PCB design.
- To explore and develop a microcontroller operating programme.
- To construct prototype board and evaluate, debug and refine hardware design.
- To load microcontroller program, debug and refine.
- To develop a non-aquatic test regime to evaluate the positional discrimination achieved.

These objectives provide the foundation of the project and constitute the Project Specification (Appendix A).

1.3 Chapter Overview

Chapter 2 The Southern Elephant Seal. Provides the biological background to the project and investigates the use of existing electronic instrumentation used by marine mammal scientists. The chapter also uncovers the need for a new instrument and forms the basis of this project.

Chapter 3 Hardware Development. Justifies the selection of magnetism and gravity as the fundamental measurands and chooses a list of candidate components to construct the instrument.

Chapter 4 Circuit Schematic Design. Integrates the components into a working electronic circuit based on a modular design.

Chapter 5 Software Design Requirements. Forms the framework for developing the software necessary to run and test the microcontroller and instrument in general.

Chapter 6 Prototype No.1 Construction. Converts the schematic diagrams developed in Chapter 4 into a printed circuit board design. The printed circuit board is then produced and populated with components to form a working instrument.

Chapter 7 Prototype No.1 Evaluation. Looks at the prototype to determine its overall functionality and seeks areas within the design where improvements can be made for implementation in a following prototype.

Chapter 8 Prototype No.2 Construction. Implementing the design improvements derived from Chapter 7 and producing the final prototype for further evaluation.

Chapter 9 Prototype No.2 Evaluation. Examines the electrical characteristics of the instrument against the schematics and determines the fitness of the device for further hardware development or if the device can proceed to performance evaluation.

Chapter 10 Instrument Performance. This chapter uses an experimental approach to investigate the performance of the instrument. Data obtained from the instrument is analysed to determine the discrimination achieved in the design.

Chapter 11 Interpreting the Data. This chapter examines the output of the instrument and develops the mathematical models used to deliver the required magnetic bearing, roll and pitch angles with a stated degree of accuracy.

Chapter 12 Conclusion. Provides the concluding discussion and identifies the objectives successfully achieved before considering future work required.

Chapter 2 The Southern Elephant Seal

2.1 The impetus for research

Each year around the 14th October scientists on Macquarie Island in conjunction with support staff from the Australian Antarctic Division Research Station perform an around island census of the Southern Elephant Seal, *Mirounga Leonina*. The island, with 90 kilometers of coast line, is traversed by small teams of people and a count of bulls, cows and pups is recorded. The long term census data has uncovered a marked decline in the overall population and more importantly female seals as indicated in Figure 1. This unexplained decline has contributed to the Commonwealth Government listing the Southern Elephant Seal as *vulnerable* under the *Environment Protection and Biodiversity Conservation Act 1999* and for the Tasmanian State Government to award the classification of *endangered* under the *Threatened Species Protection Act 1995*.

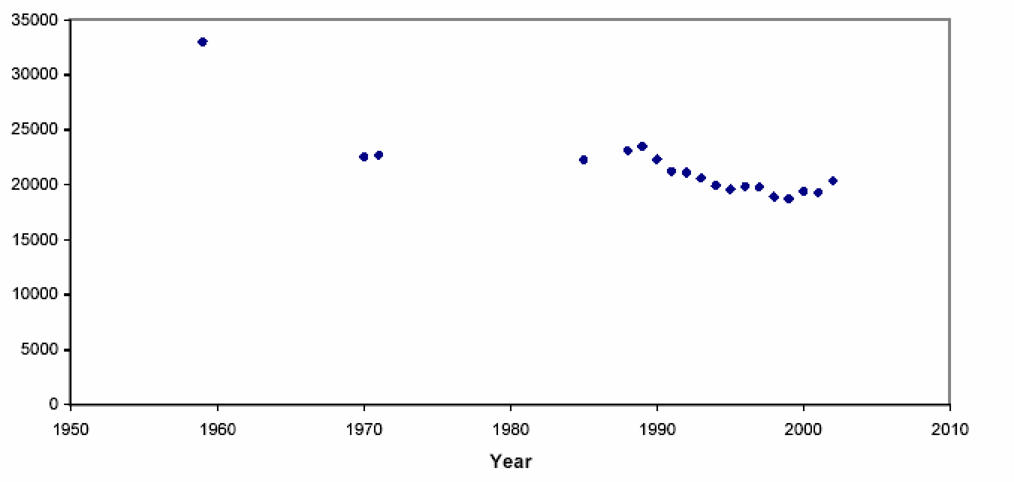

Figure 1 Annual census results shows clearly the long term decline in the female elephant seal population. The female population numbers are a crucial reflection of the species ability to regenerate. http://www.dpiwe.tas.gov.au

The Macquarie Island southern elephant seal (*Mirounga leonina*) population has been steadily declining in numbers at an estimated rate of 2.1 % pa since1949, which is when detailed population studies were started by the Australian Antarctic Division (AAD).
In 1959 the total Macquarie Island population was estimated to be 156,000, whilst the current population is estimated in the vicinity of 70,000, a reduction of approximately 45 % Laws (1994).Concern over the fate of the population, and the implications for the rest of the Southern Ocean ecosystem has stimulated a considerable body of research into the potential causes for this unexplained decline. Although Figure 1 indicates a recent reversal, this is not considered sufficient evidence within the scientific community to remove the mammal from either the endangered or vulnerable lists.

2.2 Biological Research Direction.

Extensive demographic studies have identified a number of possible causes of the population decline, most notably the drop in first year survival in the 1960s, but no ultimate cause has yet been identified. However, there is a strong relationship between the size of pups at weaning and their ultimate survival, and pup size is strongly related to the size and condition of the mother, therefore it is a reasonable hypothesis that first year survival is related to the foraging performance of the mothers.
In order to test this hypothesis researchers at the University of Tasmania have been quantifying the links between the foraging performance and behaviour of adult female southern elephant seals with a range of oceanographic parameters, including primary productivity, sea surface temperature and bathymetry. These data serve to determine how southern elephant seals will respond to changes in the distribution of marine resources as a result of global climate change and/or commercial fisheries activities. In order to gather this data during the extended periods southern elephant seals spend at sea (up to 8 months of the year, only hauling out twice, to breed and to moult), seals are fitted with velocity time depth recorders (VTDRs) and satellite linked time depth recorders (SLTDRs), instruments known less formally as ‘trackers’ or ‘tags’.

2.3 Existing Trackers and Tags.

Both VTDR and SLTDR units measure a number of oceanographic variables such as light intensity, water temperature and conductivity as well as behavioural variables including swim velocity, dive depth and duration. The fundamental difference between VTDRs and SLTDRs is the VTDR archives the data for retrieval when the animal returns to the island, whereas the SLTDR transmits data via satellite allowing GPS positioning for real time mapping to within an accuracy of 1 km. When either tracker is deployed a small VHF locating beacon is also attached to the animal allowing researchers to more easily locate both the animal and the payload when it returns to the island. Figures 2, 3 and 4 demonstrate the physical size of the trackers employed and the universal use of resin in their construction.

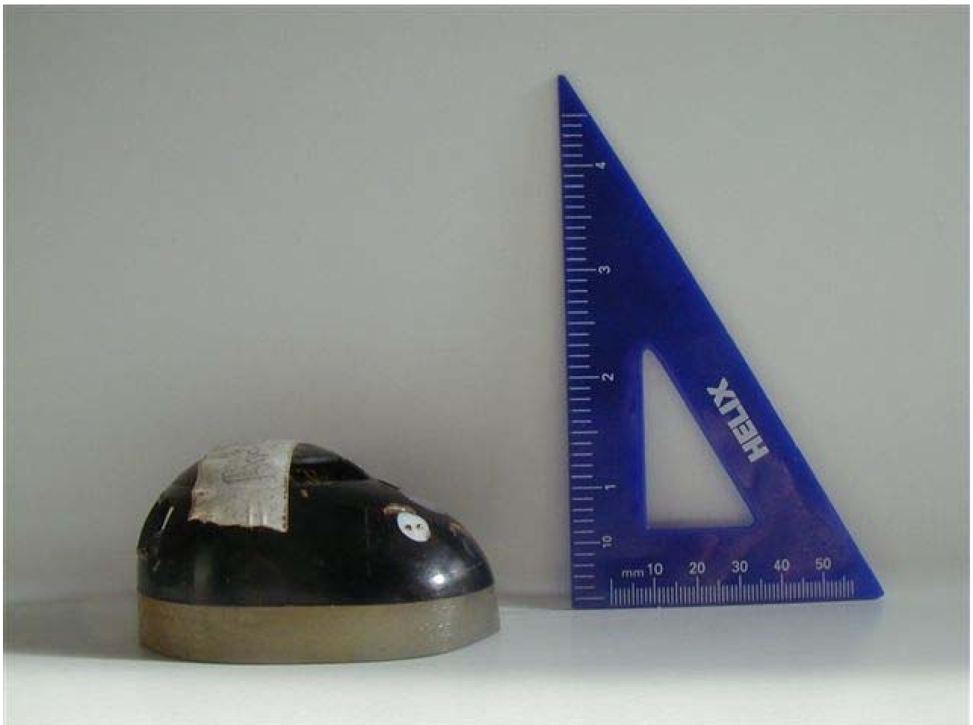

Figure 2. The Wildlife Computers MK8 VTDR is configured to record depth, light level, temperature and velocity at 30 second intervals and stores the information using 16MB of memory for later retrieval.

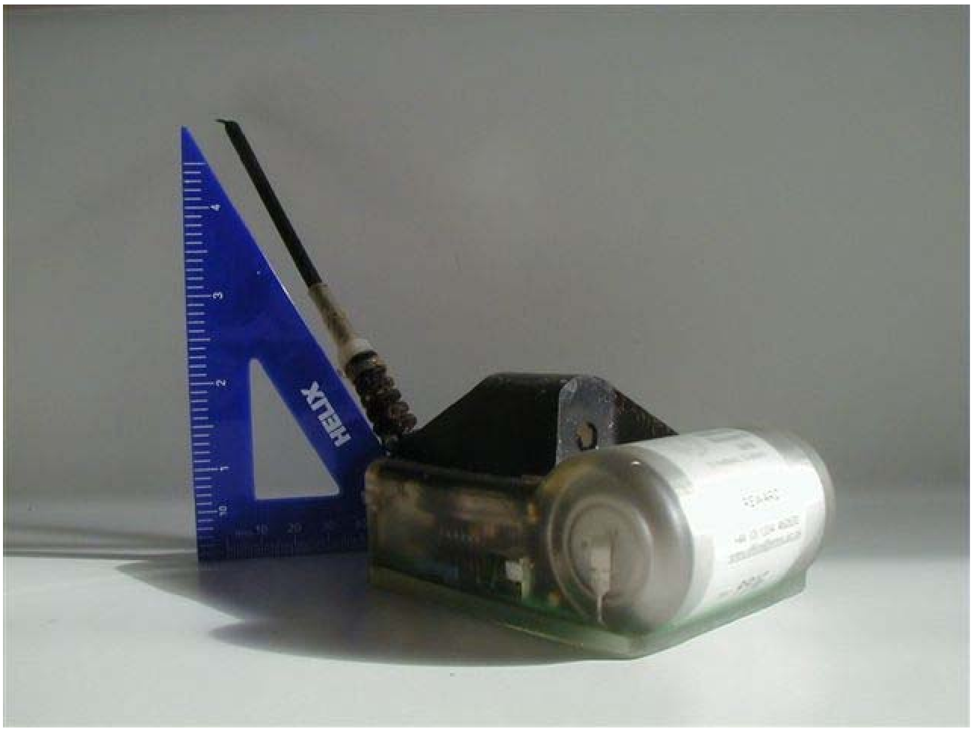

Figure 3 The Series 7000 SLTDR uses the Argos satellite system to relay data from a surfaced seal and provides researchers with close to real time geographical positioning via a secure web address generated at the Sea Mammal Research Unit at the University of StAndrews, Scotland. Time, depth and velocity is also recorded on board and downloaded when the unit is recovered.

Figure 4 SLTDR (L), VTDR (R) and VHF locator beacon (top R). The scientific payloads attached to seals are small in comparison to the target animal, an adult cow being in the order of 300kg and 2.5m in length.

2.4 Velocity Time Depth Recorder (VTDR) data.

VTDR trackers are capable of providing researchers with variables such as depth, temperature, light level, velocity, sea water conductivity and time which can yield an extraordinary amount of information.

Data recovered by VTDR trackers permits accurate dive profiles to be generated, which in turn provides clues as to how the animals behave and what strategies are adopted for successful foraging. A screenshot of an actual dive profile is given in Figure 5, with depth on the vertical axis and time on the horizontal axis. Data were recorded at 30 second intervals. The data do not however indicate the hunting pattern used by the seal, methods of navigation, course correction techniques or positional information (yaw, pitch and roll) of the seal in the water column.

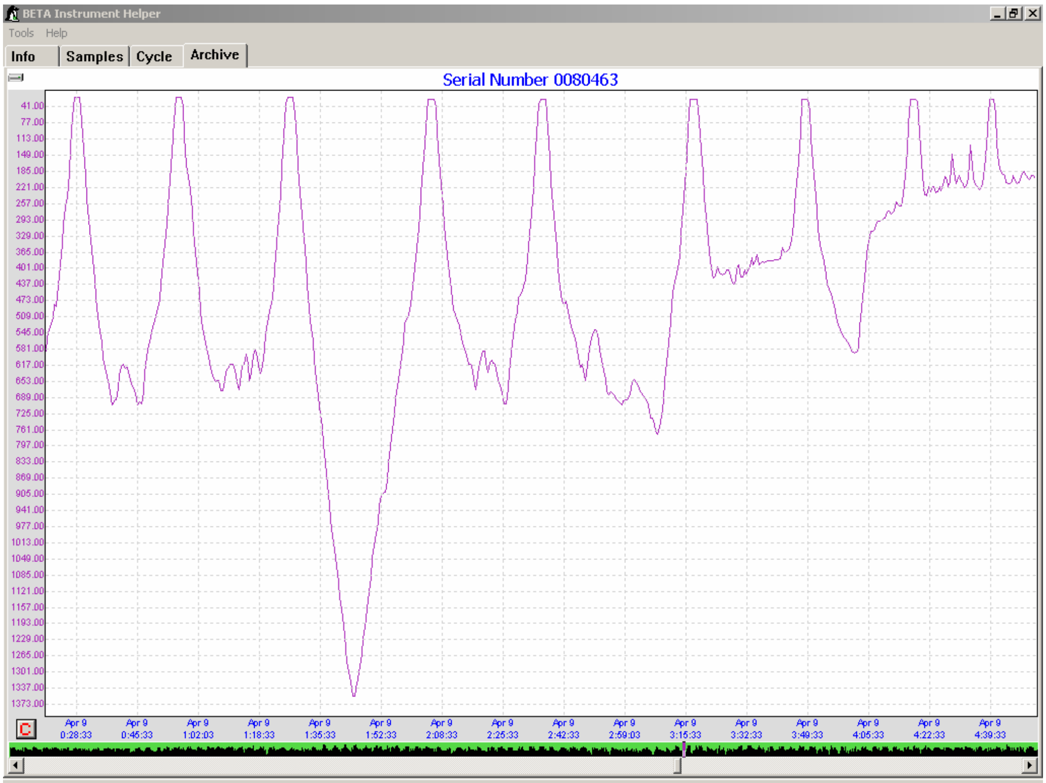

Figure 5 VTDR data. The screenshot frame represents eight dives, the deepest being approximately 1350 meters of 37 minute duration recorded on April 9th 2004 at 1.45am. The seal providing this data was B836, a mature female. Data courtesy of Dr M Hindell.

The relationship between temperature and depth during a dive sequence is explored in Figure 6. By overlaying the depth profile (upper curve) on the same plot as the temperature data (lower curve) the relationship between depth and temperature can be evaluated.

Combinations of data can also be used to provide an approximate global position of the animal based on hours of day light received and the time of day.

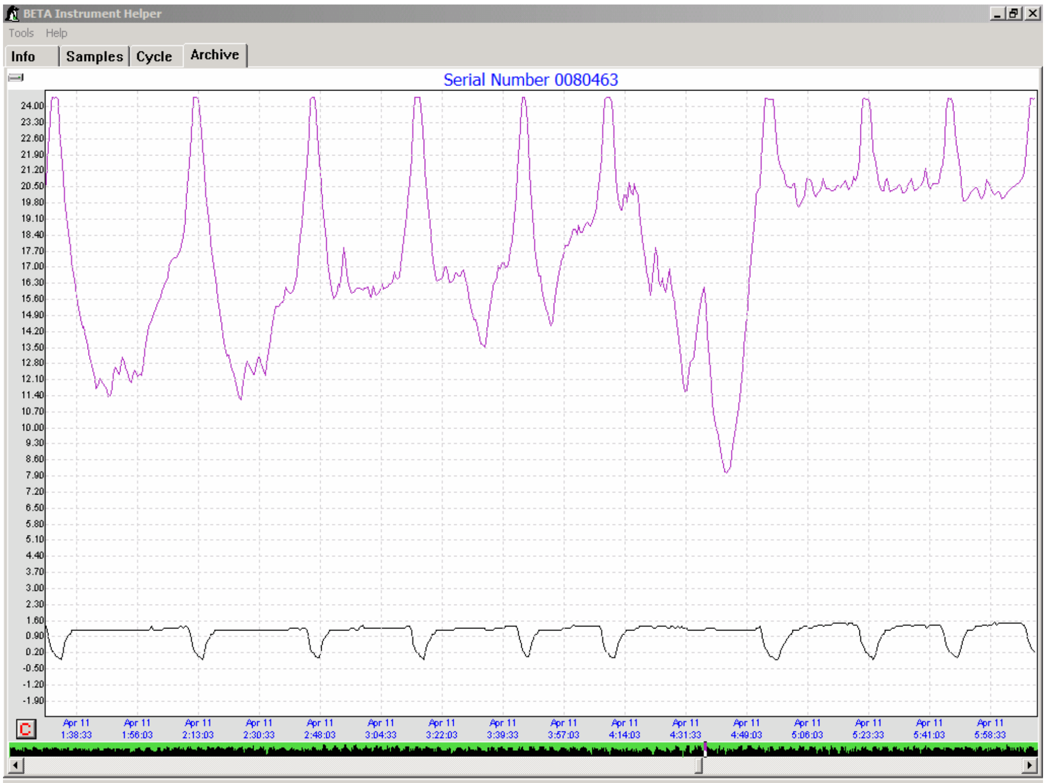

Figure 6 VTDR data. The screenshot frame represents 9 dives on the 11th April 2004 at 4am. The water temperature is plotted as the lower curve towards the bottom of the frame. By superimposing the dive profile, upper curve, on the same frame, the relationship between depth and temperature can be explored. Data courtesy of Dr M Hindell.

2.5 Satellite Linked Time Depth Recorder (SLTDR).

The deployment of satellite trackers assists marine mammal researchers in determining where seals go during their extended time at sea. Until very recently this has been a mystery. The SLTDR instrument relays the position of a surfaced animal via satellite, permitting the animals progress to be plotted in near to real time. This data exposes what sector of the Southern Ocean the animals traverse and the time spent in each area. An example of this mapping is given in Figure 7. At the centre of the figure, where the satellite tracks originate, is Macquarie Island, a small Sub-Antarctic Island approximately 35km long and 5km wide. It is not fully appreciated how seals manage to navigate these extraordinary courses and return each year to the same small island to breed or moult. The latest data indicate some seals travel from Macquarie Island to the

Antarctic ice edge some 1800km to the south before returning to the island in September to breed.

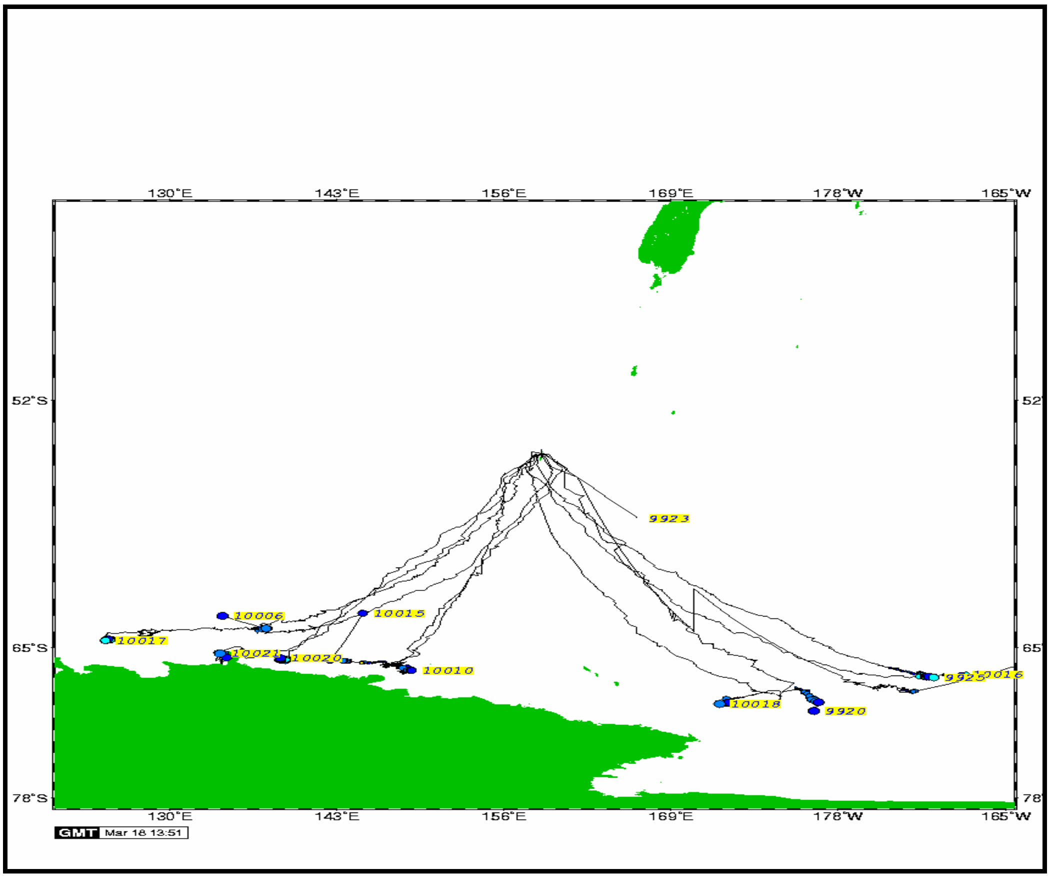

Figure 7 Satellite tracks of deployed SLTDR units on 18 March 2005. Eleven tracks are recorded emanating from Macquarie Island (centre) extending well south towards Antarctica, a distance travelled of 2000km. New Zealand is visible at the top, Antarctica at the bottom of the frame with latitude and longitude inscribed on the boarders. Image courtesy of S. Wall.

2.6 Limitations of current trackers.

One of the limitations of the current data is its two dimensional nature. Elephant seals are capable of diving to depths in excess of 1800 m for periods of up to 2 hours submerged. Researchers can only map their behaviours in terms of changes in depth and changes in speed and geographical position can only be fixed from surface positions. For broad scale oceanic patterns this information is adequate; however fine-scale habitat use and behaviour may be important factors in the foraging performance of southern elephant seals. Research has shown that within a marine environment biologically important features of prey patchiness cannot be addressed in a 2-dimentional analysis Zamon et al. (1996). Hindell et al. (2002) who have tracked Weddell seals under sea ice are the only researchers to successfully quantify true 3-dimensional diving behaviour of a seal. They used a triangular array of 3 omni-directional hydrophones. However this approach is not applicable for southern elephant seals in thousands of kilometres of open ocean. True 3-dimentional data are those where the horizontal and the vertical coordinates, *x y* and *z* are collected simultaneously while the animal is swimming. This information may reveal important behavioural clues in determining foraging performance and is a data set not currently collected by existing trackers.

2.7 Demand from the Scientific Community.

The scientific community have looked towards technology in the pursuit of data pertaining to the southern elephant seal, an animal that spends two thirds of its life at sea. Commercial interests have responded to that demand and a niche market has evolved to develop and supply the trackers and tags that exist today, namely the VTDR and SLTDR. Elephant seal researchers experienced in the successful deployment of these trackers have recognised the benefits of applying high-tech solutions to their research and are again looking towards technology to provide *x y* and *z* coordinate data of an animal whilst at sea.

The head of the Marine Mammal Research Unit at the University of Tasmania, Dr Mark Hindell, strongly supports development of a new tracker capable of delivering positional and course data to address the fine scale limitations imposed by currently employed trackers. The challenge is now handed over to the engineering community to develop an instrument that can provide the data the researchers need.

Chapter 3 Hardware Development.

3.1 Introduction-The Component Selection Process

The engineering specification generically identifies major functional sections such as power supply, microcontroller and memory. During hardware development those sections are investigated further and candidate components identified that satisfy the specification. A list of candidate components permits the development of circuit stages and subsequent PCB construction. The entire process is aimed at producing a prototype instrument capable of integration with the developed software for evaluation. The process is one of continual revision and improvement, comparing components and specifications to produce a list of components for further development.

3.2 Candidate Component Selection Criteria.

Universal selection criteria for all components nominated in the construction of the instrument are, reliable operation at low temperature (in the order of -1.7°C), low power operation and must be rugged in construction.

3.2.1 Battery Operated Power Supply

The need for a stable, high capacity power supply, with good discharge curves and capable of withstanding low temperatures is recognised as being crucial to the instruments operation. Literature from battery manufactures, Panasonic, GM Batteries and Sonnenschein indicates a battery in the lithium family as the most likely solution. An extensive range of battery chemistries are available within the lithium genre, examples produced by Sonnenschein are listed in Table 1 with associated discharge and voltage curves explored in Figure 8.

Table 1 A wide range of battery chemistries are available in the Lithium range, each chemistry has it's own advantages and disadvantages for applications. Sonnenschein LBT Brochure (2003)

Battery Curve	Chemistry	Energy Density Wh/dm^3	Sealing Method
1	$Li/SOCL_2$	1280	Hermetically Welded
2	Li/SO_2	430	Hermetically Welded
3	Li/CF_x	550	Crimped Elastomer
4	Li/MnO_2	580	Crimped Elastomer
5	Li/FeS_2	450	Crimped Elastomer
6	Alkaline	280	Crimped Elastomer

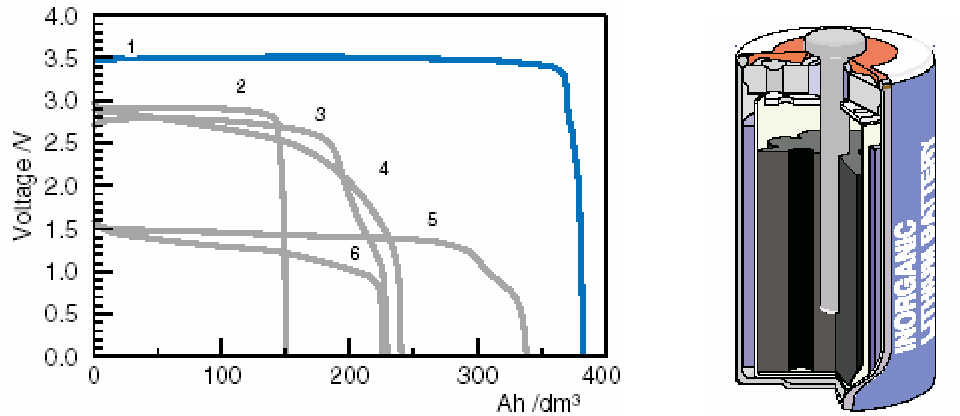

Figure 8 Discharge curves of different battery chemistries listed in Table 3. The curves are recorded at 25°C at the 1000 hour rate. A cut away diagram of a lithium battery shows the structural elements. Data Sheet: Sonnenschein LBT Brochure (2003)

Examining Table 1 and Figure 8 from Sonnenschein exposes range of lithium batteries of varying capacities and offers a promising battery in the $Li/SoCl_2$ chemistry range. The selection of a primary cell in this chemistry is supported in TCL Battery (2004) and satisfies the requirements of the instrument. A suitable Sonnenschein battery of this chemistry is the SL-700 and has an open circuit voltage of 3.67V with an operating voltage of 3.6 V making this a plausible choice of power supply.

3.2.2 Micro-Controller Selection.

Considerations foremost in the selection of a microcontroller was the availability of a real time clock (RTC), Analogue to digital converters (ADC), a high pin count for addressing storage memory without buffers, support from the vendor, capable of running on battery supply voltages, contain non-volatile memory and have power saving features. After examining many microcontroller data sheets by Phillips, Microchip and

Freescale, a controller was found that satisfied these basic requirements, the MC68HC908LJ24 from Freescale Semiconductor, Inc.[1] The specification sheet provided by Freescale, *MC68HC908LJ24 Data Sheet (2004)* comprehensively describes the device.

Relevant features of the LJ microcontroller in the design of the instrument are

- High performance M68HC908 architecture
- Upward compatible code with M6805, M68HC05
- 4MHz at 3.3 V operating voltage
- 32.768kHz crystal clock input with 32MHz internal PLL
- Continuous crystal oscillator in stop mode.
- 24K-bytes user programmable FLASH memory
- 768 bytes on-chip RAM
- 40 general purpose input/output pins
- High Current 15mA sink on 22 pins
- Real time clock with clock, alarm and chronograph
- RTC interrupts
- 6 channel, 10 bit successive approximation analogue to digital converter ADC
- In circuit programming
- Low power design with wait and stop modes
- Master Reset pin
- 80 pin Low Profile Quad Flat Pack (80LQFP)

Although the MC68HC908LJ24 has inbuilt features and functions in excess of what is required for this project, information gained from *CPU08 Reference Manual (2001)* indicates those modules not required can be disabled and impose no limitation or negative effects on the power consumption of the controller overall.

[1] Freescale Semiconductors were contacted via their web page and three sample controllers obtained at no cost. Samples are issued conditionally for the expressed purpose of evaluation only. The full agreement is available at http://www.freescale.com

3.2.3 Non-volatile memory selection.

The instrument is a battery operated device that requires solid state memory to store the data for later retrieval. In order to mitigate against a flat battery the memory should be non-volatile and robust. Many memory vendors produce non-volatile memory that would be fit for this task. Atmel® produces a 32-megabit 3-Volt Flash Memory component that is small in size and suitable for this application. A full description is given in the data sheet, 32Mbit Flash Memory (2004).

The main features of the AT49BV322AT are

- Single voltage Read/Write Operation: 2.65V to 3.6V
- Access time- 70ns
- Sector erase architecture
- Fast word program time -12us
- Low power operation- 12mA active – 13uA Standby
- VPP pin for write protection
- TSOP package option
- Minimum 100 000 erase cycles
- 4,194,304 bytes of 8 bits each

The memory capacity of the AT49BV322AT provides approximately 97 days of data recording according to equation 3.1

Given, Sampling period = Ts = 10 seconds
Magnetic Data = Md = 3 bytes
Accelerometer = Ad = 2 bytes
Total Bytes = Bt = 4,194,304 bytes

$$Days = \frac{Bt \times Ts}{(Md + Ad) \times 3600 \times 24} \tag{3.1}$$

Data storage calculations allow for sensor sampling at 10 seconds intervals, three bytes for storing the magnetoresistive ADC data (*x,y,z*), two bytes for the storage of the accelerometer (*x,y*), plus some time stamping overheads.

3.2.4 Oscillator

According to the microcontroller data sheet MC68HC908LJ24 Data Sheet (2004), the accuracy of the Real Time Clock (RTC) Module is dependant on the properties of the oscillator. The instrument is required to operate accurately over a temperature range of 20°C down to -1.7°C. In order to achieve accuracy over a range of operating temperatures a temperature compensated oscillator is required. There are many oscillator designs using discrete components available, however they all require additional circuitry to attain temperature compensation. Dallas Semiconductors produce a 32.768 kHz oscillator in an IC package the DS32kHz that performs compensation within two temperature error bands of ±1 min/yr down to 0° C and ±4 min/yr below 0°C as shown in Figure 9 reproduced from DS32Khz TCXO (2004). The microcontroller internal clocking options are determined by code and explained in TIM08 Timer Interface Module (1996). Dallas Semiconductors were contacted and two sample precision oscillators in DIP packages obtained at no cost. [2]

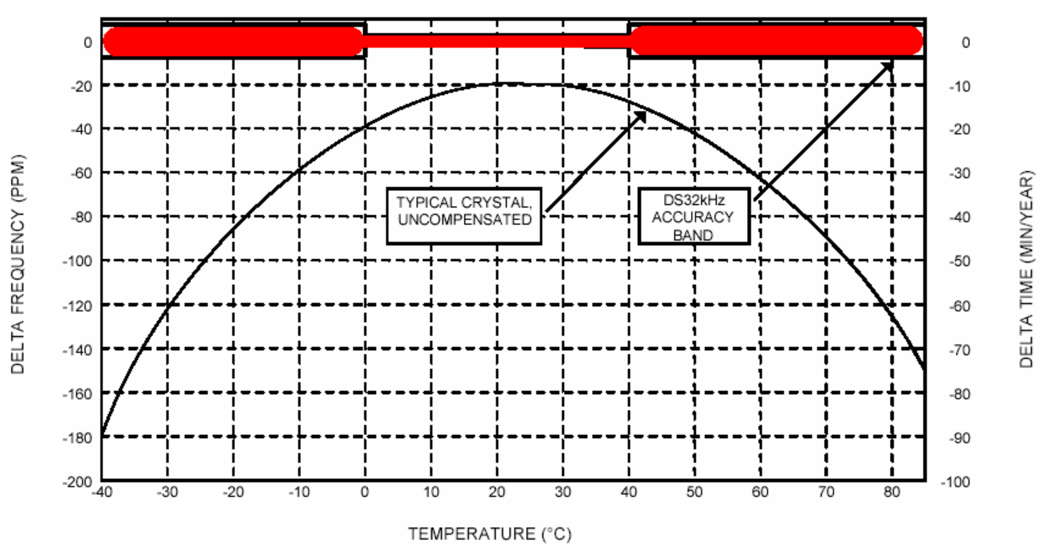

Figure 9 The DS32kHz produces a temperature compensated output of 32.768kz. The oscillator corresponds with the specified frequency needed for the RTC in the selected MC68HC908LJ24 microcontroller. DS32Khz TCXO (2004).

[2] Sample components are available by request from Dallas Semiconductors via their web address http://www.maxim-ic.com , all costs including freight are covered by Dallas Semiconductors. The issuing of samples is conditional; the full agreement is available from the web site.

3.2.5 Communications Interface

Communications software written specifically for the MC68HC908 microcontroller relies on the RS232 standard to provided communication between a PC and the controller. Examination of MC68HC908LJ24 Data Sheet (2004) also promotes the RS232 standard as the most usual communications interface. As the microcontroller is battery powered by a 3.6V source a low voltage RS232 integrated circuit was sought. Maxim produce a new generation low power/ low voltage IC the MAX3232ECPE which is capable of operating at 3.6V. Application notes *RS232 Drivers/Receivers (2004)* in conjunction with +5V RS232 Drivers/Receivers (2004) outline biasing requirements. Most other RS232 ICs require a 5V rail, choosing the MAX3232E extinguishes the requirement for a separate 5V supply and simplifies the circuit design. Dallas Semiconductors were contacted and provided two MAX3232ECPE components as samples at no cost.[3]

3.3 Sensors.

Lengthy discussions with marine mammal researchers from the University of Tasmania has indicated strong support and encouragement for the development of an instrument to measure both position and direction of an elephant seal swimming, those discussions framed using biological expressions and terms. By removing the biological emphasis and reducing the problem down to fundamental concepts a powerful analogy can be drawn between an elephant seal swimming and an aircraft in flight as illustrated by Caruso (2004) reproduced in Figure 10. Adopting aviation terminology used to detail the flight of an aircraft describes position, in terms of pitch and roll, and direction in terms of magnetic bearing. Pitch and roll are quantities taken with respect to the vertical axis and detected using gravity, whereas magnetic bearing uses the earth's magnetic field and magnetic north as the reference. Gravity and the earth's magnetic field are universal quantities and measurable irrespective of location on earth. The sensing of these quantities is seen in compassing, navigation, pointing and tilt measurement applications which are commercially well developed areas.

[3] Sample components are available by request from Dallas Semiconductors via their web address http://www.maxim-ic.com , all costs including freight are covered by Dallas Semiconductors. The issuing of samples is conditional; the full agreement is available from the web site.

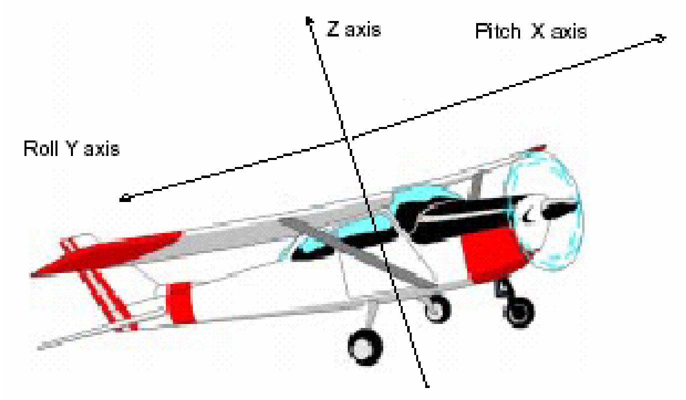

Figure 10 The position of an aircraft can be described by roll and pitch combined with a compass bearing. Pitch is the position of the nose, either up or down, roll is the amount of tilt with respect to the wings, either left or right and is most commonly represented in the cockpit by a gimballed instrument. Course is derived from a magnetic compass and displayed with respect to magnetic north. Caruso (2004)

3.3.1 Exploring existing compassing solutions.

Honeywell produce a digital compass module HMR3000 , the protective enclosure and circuit board shown in Figure 11, which provides a useful learning tool for developers exploring compassing and tilt measurement.[4] The HMR3000 outputs heading, pitch and roll information to the specifications listed in Table 2 and communicated to a PC via either RS232 or RS485 in half duplex mode.

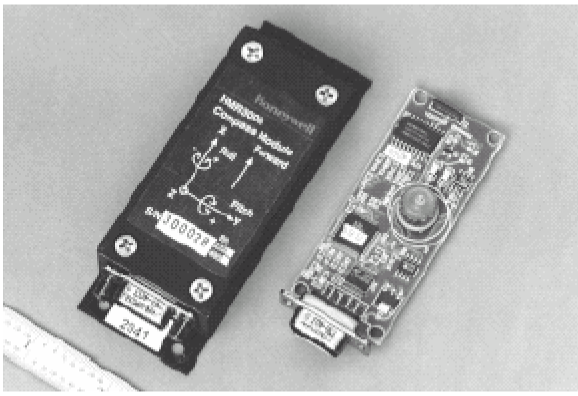

Figure 11 The HMR3000 provides compassing information by combining a two axis magnetoresistive sensor in conjunction with a two axis electrolytic tilt sensor. Honeywell Australia provided a demonstration unit for evaluation purposes. HMR3000 DCM (2004).

[4] Mr Mark Leo, Victorian Sales Representative for Honeywell Australia, was contacted and a demonstration HMR3000 obtained for evaluation.

Table 2 Abbreviated specification of Honeywell digital compass module. *HMR3000 DCM (2004)*

Parameter	**Value**	**Comments**
Heading Accuracy	< 0.5° RMS	Dip < 50°, Tilt < 20°
	< 1.5° RMS	Dip < 75°, Tilt < 20°
Heading Resolution	0.1°	
Pitch and Roll Accuracy	0.4°	Tilt < 20°
	0.6°	Tilt ≥ 20°
Pitch and Roll Range	± 40°	(Electrolytic Tilt Sensor)
Magnetic Field Resolution	1 mGauss	
Electrical	35mA @ 6Vdc	

Evaluating the HMR3000 began with construction of a RS232 cable approximately one meter in length as no cable was supplied with the demonstration unit. The cable carries communication signals and provides power to the module in accordance with Figure 12. After installing the new cable, proprietary software *PCdemo Interface*© (by True North Technologies) was loaded, the HMR3000 module turned on and communications established. *PCdemo Interface*© provides the user with a rich graphical interface, the primary display offers a real time gimballed indicator to represent roll and pitch with a compass to indicate bearing.

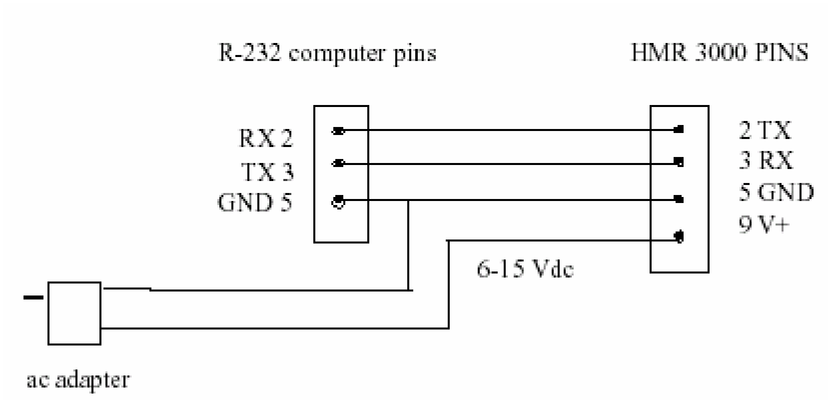

Figure 12 Schematic of connecting cable to provide power and communications lines between the HMR3000 and a PC. *DCM Users Guide (2004)*

A simple experimental procedure was developed to test the operation of the HMR3000 and show the compassing and tilt measurement functions.

To evaluate the compassing function of the HMR3000 the device was placed on a level board next to a hand held compass and both turned through 360° to permit a comparison

between the electronic bearing and handheld compass. The resulting observations demonstrated the operation of the magnetoresistive components and indicated their satisfactory operation with zero pitch and roll indicated on the gimballed display.
To explore the tilt measurement capabilities of the HMR3000, three timber blocks were cut at 15°, 30° and 45°, the device was then place on the blocks and the display observed. The resulting display demonstrated accurate measurement of 15° and 30° with out of range indicated when placed on the 45° block as expected.
The evaluation uncovered a limitation in the design of the unit, a maximum of ±40° pitch and roll caused by the use of an electrolytic tilt sensor. In general the HMR3000 supports the use of a magnetoresistive sensor for bearing but indicates the use of an accelerometer to increase the tilt range for the project to produce an electronically gimballed compass.

3.3.2 Magnetic Sensing.

The earth's magnetic field is approximately 0.6 Gauss and can be detected using solid state magnetoresistive components. The principle of operation for these components exploits the properties of a nickel-iron alloy (Permalloy), applied as a thin-film to a silicon wafter in a resistive strip pattern. The strips are arranged in a Wheatstone bridge circuit. As the magnetic field direction relative to the sensitive axis of the bridge circuit changes, the resistance of the magnetoresistive elements also change, which is converted to a voltage output. The expected output from a two axis sensor is illustrated in Figure 13 from *Compass Heading using Magnetometers AN203* (2004). These linear devices are used extensively in compassing and navigation systems and provide a low cost solution where high reliability, sensitivity and fine resolution are required. Honeywell manufacture a wide selection of magnetoresistive devices that are suitable for compassing, the HCM1053 is a three axis device described in *1,2 and 3 Axis Magnetic Sensors (2004)* with the following features

- Miniature Surface-Mount packages
- Wide Field Range of ±6 Gauss
- 1.0mV/V/Gauss Sensitivity
- 120 micro-Gauss maximum sensitivity
- Low power operation down to 1.8V

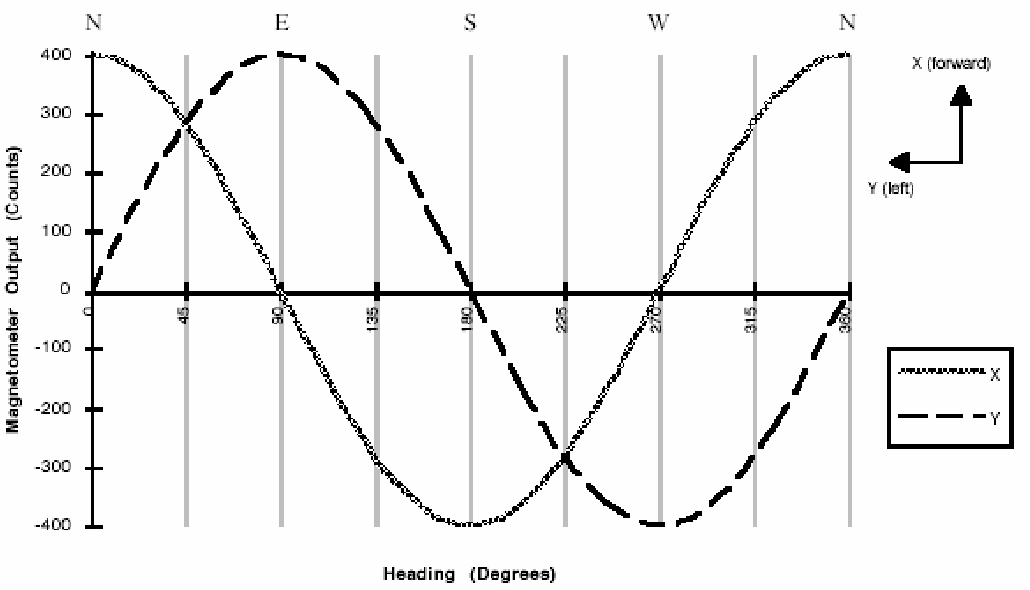

Figure 13 Hx and Hy Magnetometer readings for different compass headings. A full explanation is provided in *Compass Heading using Magnetometers AN203 (2004).*

3.3.3 Gravitational Sensing.

There are several devices that could be employed to provide useful sensing of the earth's gravitational forces in order to produce a quantifiable measure of tilt and pitch.

Two such devices are the electrolytic tilt sensor and an accelerometer.

- An Electrolytic Tilt Sensor (ETS) uses an electrolytic fluid of known viscosity in conjunction with electrodes that measure the resistivity between the electrodes. As the device is tilted the contact between the electrolytic and the electrodes changes and this is converted to an angle of tilt or pitch.
- An Accelerometer uses micro-machined elements constructed at the wafer level producing a varying capacitance depending on the position of the movable capacitive plate.

A limiting factor applied to all ETSs is the angle of detection, as the angle of detection increases so to does the length of the electrodes and overall size of the component. This results in maximum usable angles of detection of around 60 degrees. The ruggedness of the devices and the inclusion of an air gap at the top of the electrodes provide a source of concern when considering the device may be required to operate at depths of 2000m or 200 atmospheres.

Accelerometers on the other hand are effectively solid state devices as indicated in Figure 14 and can sense over a full ±180 degrees of rotation as illustrated in Figure 15.

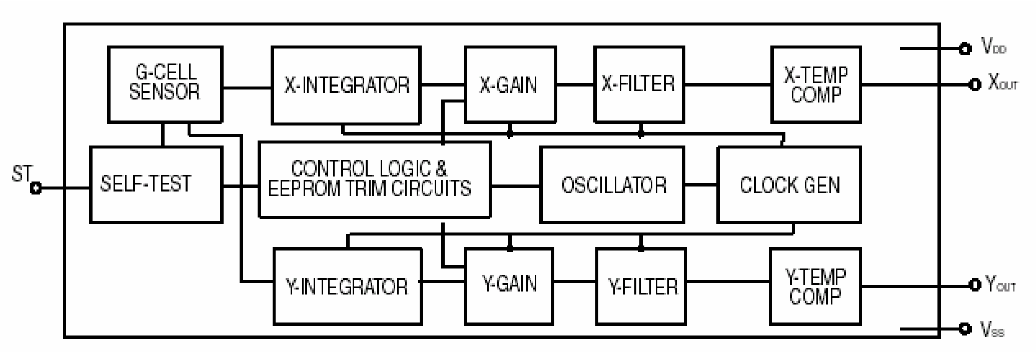

Figure 14 Functional block diagram of accelerometer showing the complex stages within the integrated circuit which result in compact sensing solutions requiring little external biasing circuitry. ±10g Duel Axis Micromachined Accelerometer (2004).

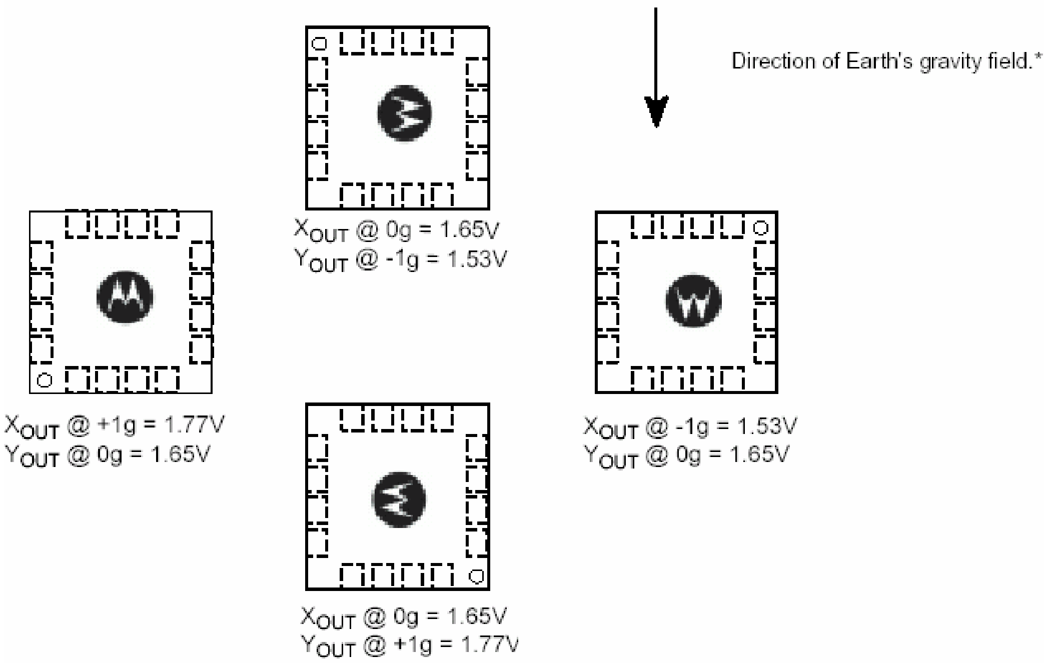

Figure 15 Anticipated output of accelerometer to the effect of gravity in a static application. When the component is positioned as shown the X and Y output voltages represent a 1g output. *±10g Duel Axis Micromachined Accelerometer (2004).*

Freescale Semiconductors (previously Motorola) offer a Micromachined Accelerometer the MMA6233Q which is suitable for position and motion sensing.[5]
The main features of the device are

- Low - Noise, Cost and Power
- 2.7-3.6V operation
- 6mm x 6mm QFN
- Integral signal conditioning with Low-pass filter
- Ratio metric Performance
- Robust design, high shock survivability.
- ±10g acceleration range.

Micromachined components, accelerometers, offer a compact and robust method of sensing roll and pitch by using gravity as the reference and delivering a voltage output indicating the position. This is stable in a static model however difficulties may surface using accelerometers in a dynamic model as other forms of acceleration such as centripetal, linear or a combination of these will affect results.

3.4 Component Selection - an iterative process

The components selected were chosen from amongst hundreds of possible devices using a literature review of data sheets and other relevant documents. The selected devices represent one step in a highly iterative process of selection, design and evaluation. The next stage, schematic design, investigates integrating the devices together to achieve the specification. During schematic design, compatibility between devices is further explored which may revise the component selection. Schematic design leads directly to prototype construction and evaluation where component selection is again scrutinized against the specification.

---

[5] Freescale Semiconductors provided two sample accelerometers at no cost and were contacted via their web address http://www.freescale.com. Conditions apply to the issuing of sample components.

Chapter 4 Circuit Schematic Design.

4.1 Schematic Design Methodology

The result of the literature review of manufacturer data sheets has culminated in a provisional component list upon which the next stage of circuit development was based. Each component in Table 3 has been viewed as a fundamental building block within an electronic circuit. Each circuit also has its own specification determining biasing conditions, interfacing and electromagnetic interference considerations.

Table 3 A list of fundamental components satisfying the specification is listed, the components are all capable of operating below 3.6V and at temperatures below 0°C.

Functional Circuit	Major Component	Manufacturer
Power Supply	SL-700 Lithium Battery	Sonnenschein
Microcontroller	MC68HC908LJ24	Freescale
Memory	AT49BV322AT	Atmel
Oscillator	DS32kHz	Dallas Semiconductor
Magnetic Sensor	HMC1053	Honeywell
Accelerometer	MMA6233Q	Freescale
Communications Interface	MAX3232ECPE	Maxim

The circuit schematics were developed using data sheets in conjunction with manufacturer application notes. Circuits were drawn using Protel 99SE and later transferred to Protel DXP2004 prior to routing. The breaking down of a complex design into smaller electronic circuits has many advantages and has been adopted in the design of this instrument. Easily distinguishable functional circuits listed in Table 3 assist with overall circuit design, development, fault finding, calibration, testing and repair by providing simplified circuit schematics which are easier to read and understand.

4.2 Power Supply

The power supply uses a Sonnenschein SL-700 lithium battery with a terminal voltage V_{bat} of 3.6V to power the instrument during its deployment for periods of up to 8 months at sea. Because the instrument is exposed to extremes of both pressure and temperature, the likelihood of battery failure or exhaustion needs to be considered. The approach taken in this example is to provide an alternate method of powering the instrument when it is recovered to permit downloading of data stored prior to any failure. A simple arrangement of diodes permits external supply to bring the system on line. The forward voltage drop across a diode V_F does influence the output voltage V_{CC} of this stage, as such a diode with a low forward voltage specification was chosen a 1PS74SB23.

V_{CC} is calculated in accordance with equation 4.1.

Given $V_{bat} = 3.6V$ and $V_F = 0.3V$

$$\begin{aligned} V_{CC} &= V_{bat} - V_F \\ &= 3.3V \end{aligned} \tag{4.1}$$

All other stages in the instrument are required to operate at 3.3V or less to comply with the power supply specification.

4.3 Microcontroller

The MC68HC908LJ24 microcontroller from Freescale has been specifically designed to operate with a minimum of external biasing components. Most biasing conditions are specified in MC68HC908LJ24 Data Sheet (2004).

To ensure stable internal phase locked loop (PLL) operation a choice of oscillator components is provided in the data sheet as shown in Figure 16. Option (a) was selected to ensure stable PLL operation, this assists in ensuring accurate internal clocking and timing.

To provide microcontroller power supply noise immunity the data sheet recommends using capacitors across the supply to provide frequency bypassing of noise components as explained in Fitchen and Motchenbacher (1973). If employed, the capacitors are placed as close as possible to the controller as shown in Figure 17. However as the controller is battery operated (ripple free), will be deployed in a noise free environment and each sensor circuit has dedicated output filtering, the recommended filtering requirements have been relaxed to reduce component count and increase circuit reliability.

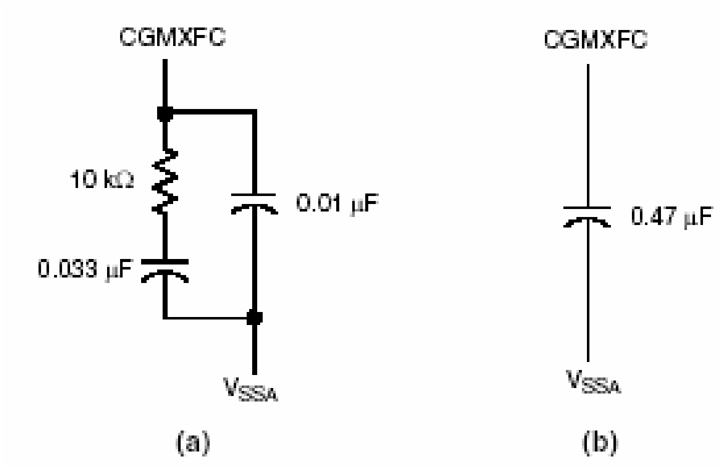

Figure 16 Two options for external filtering was provided in data sheets, option (a) is for applications where stable PLL operation is important and option (b) is suggested for applications where stability is not critical as described in *MC68HC908LJ24 Data Sheet (2004).*

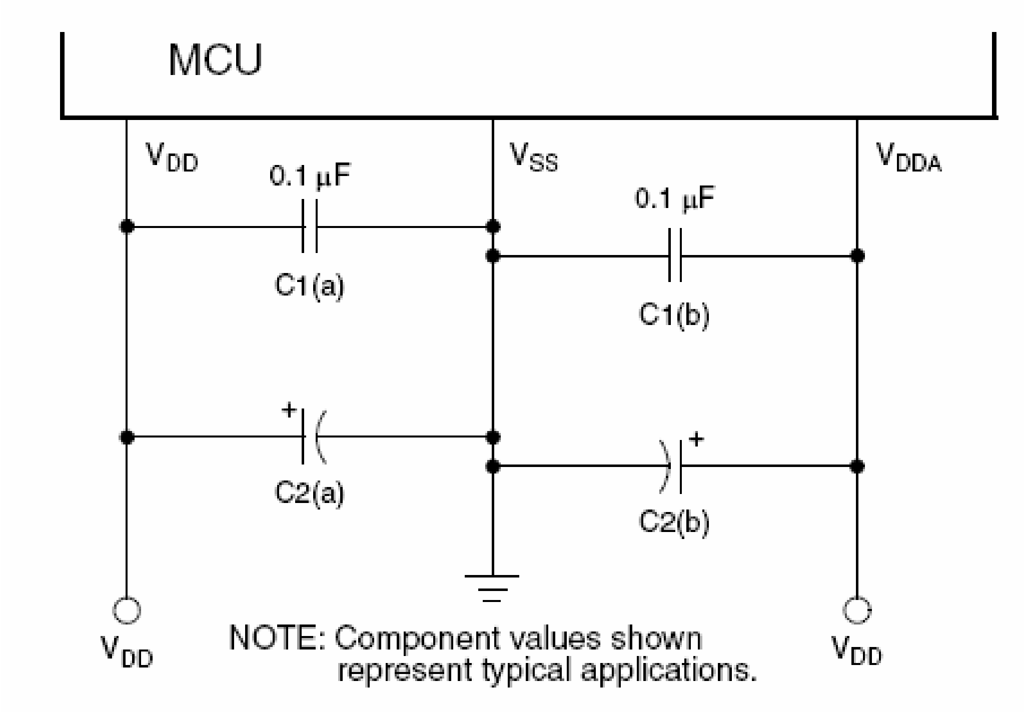

Figure 17 Power supply bypassing recommended to reduce noise effects on the microcontroller. MC68HC908LJ24 Data Sheet (2004). Copyright material owned by Freescale Semiconductor, Inc. used with permission, 2005

The input/output pins are arranged as ports with registers correspondingly assigned and shown in Figure 18.

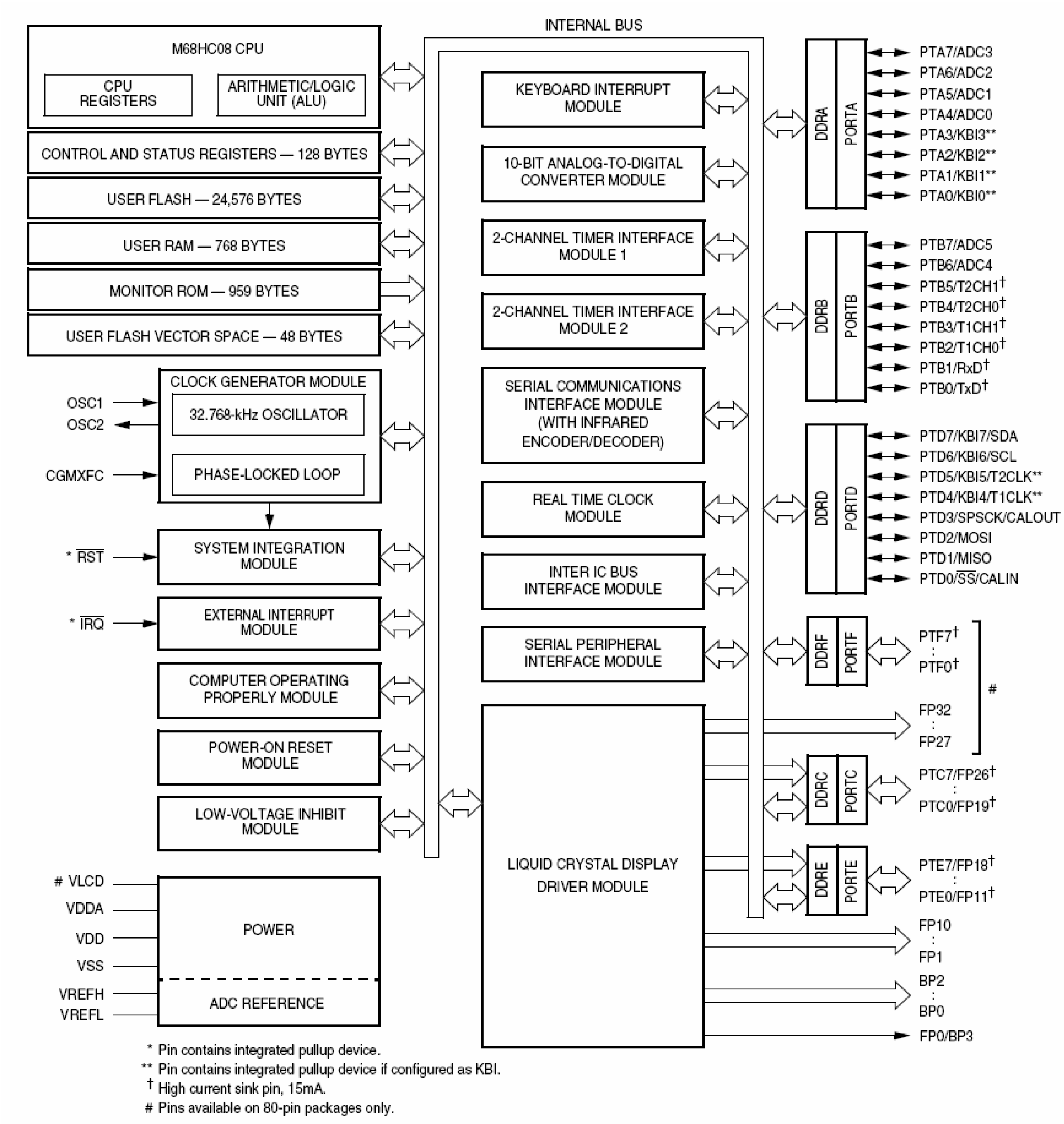

Figure 18 Mc68HC908LJ24 Block Diagram showing port usage and functional blocks. This controller was specifically designed by Freescale to control LCD displays and adapted for this project. Copyright material owned by Freescale Semiconductor, Inc. used with permission, 2005

The large number of ports on the controller has been fully utilised to satisfy the data and address bus requirements of the instrument in order to interface with the flash memory. By having plenty of ports and corresponding pins the reliance on external latching components to control address and data bus lines is alleviated. The elimination of latching components reduces component count, PCB real estate and routing complexity resulting in a more reliable instrument.

The port structure provides a simple method of connecting to the data, address and control buses required to interface the flash memory stage. Port bits have been assigned to bus lines in accordance with Tables 4, 5 and 6. Examination of port and address bus bits reveals an apparent random allocation; this allocation is the product of assigning priority to routing of the copper tracks between components resulting in a simpler routing solution on the final printed circuit board. The disadvantage of using the pin allocation in Table 4 is that the flash memory is viewed by the microcontroller as a homogenous storage element and memory locations are filled in a non sequential way. This effectively disallows sector protection of written data, a function available in the AT49BV322 flash memory component. Sector protection permits areas of memory to be "locked down" once written to and provides a method of protecting the stored data from inadvertent overwriting.

Table 4 Allocation of address bus lines to microcontroller port bits.

Port C BIT	**C0**	**C1**	**C2**	**C3**	**C4**	**C5**	**C6**	**C7**
Address BIT	A11	A17	A7	A6	A5	A2	A3	A4
Port D BIT	D0	D1	D2	D3	D4	D5	D6	D7
Address BIT	A1	A19	A8	A0	A15	A14	A13	A12
Port F BIT	F0	F1	F2	F3	F4	F5		
Address BIT	A18	A20	A9	A10	A-1	A16		

Table 5 Allocation of data bus lines to microcontroller port bits.

Port BIT	**E0**	**E1**	**E2**	**E3**	**E4**	**E5**	**E6**	**E7**
DATA BIT	IO 0	IO 1	IO 2	IO 3	IO 4	IO 5	IO 6	IO 7

Table 6 Allocation of control bus lines to microcontroller port bits.

Port BIT	F6	F7	B3
Control BIT	OE	CE	WE

Analogue to digital conversions are performed by the controller to read the magnetoresistive sensor and the accelerometer outputs. The pin allocations are described in Table 7.

Table 7 Allocation of analogue to digital input ports to sensor outputs.

Port BIT	A4 /ADC0	A5/ADC1	A6/ADC2	A7/ADC3	B6/ADC4	B7/ADC5
Input	X MAGNETIC	VSW/2	Y MAGNETIC	Z MAGNETIC	X ACCELER	Y ACCELER

Communication is necessary between the controller and a PC in order to program the controller and to access stored data. To enter the Monitor mode pins on the controller must be held at specific logic or voltage levels on a power on reset (POR) as shown in Table 6. To achieve these conditions, weak pullup and pulldown resistors (10kΩ) are included in the circuit and access via a physical interface socket to permit monitor mode is provided.

Table 8 Levels required to trigger Monitor mode during POR.

Port/Pin	A1	A2	C1	A0	IRQ	RST
Level	H	H	L	I/O	>7V dc	H

4.4 Memory.

The selected AT49BV322 flash memory component from Atmel can either be written one word at a time (16 bits) or one byte at a time (8bits). For this design the 8 bit mode has been selected demanding a one byte data bus (8 lines). To access over 4 million bytes a 22 bit wide address bus is required. Three control lines, WE, CE and OE perform all reading and writing control functions on the device. No other components are required to bias the memory chip and the functional block diagram is provided in Figure 19 Reproduced from the device data sheet 32Mbit Flash Memory (2004).

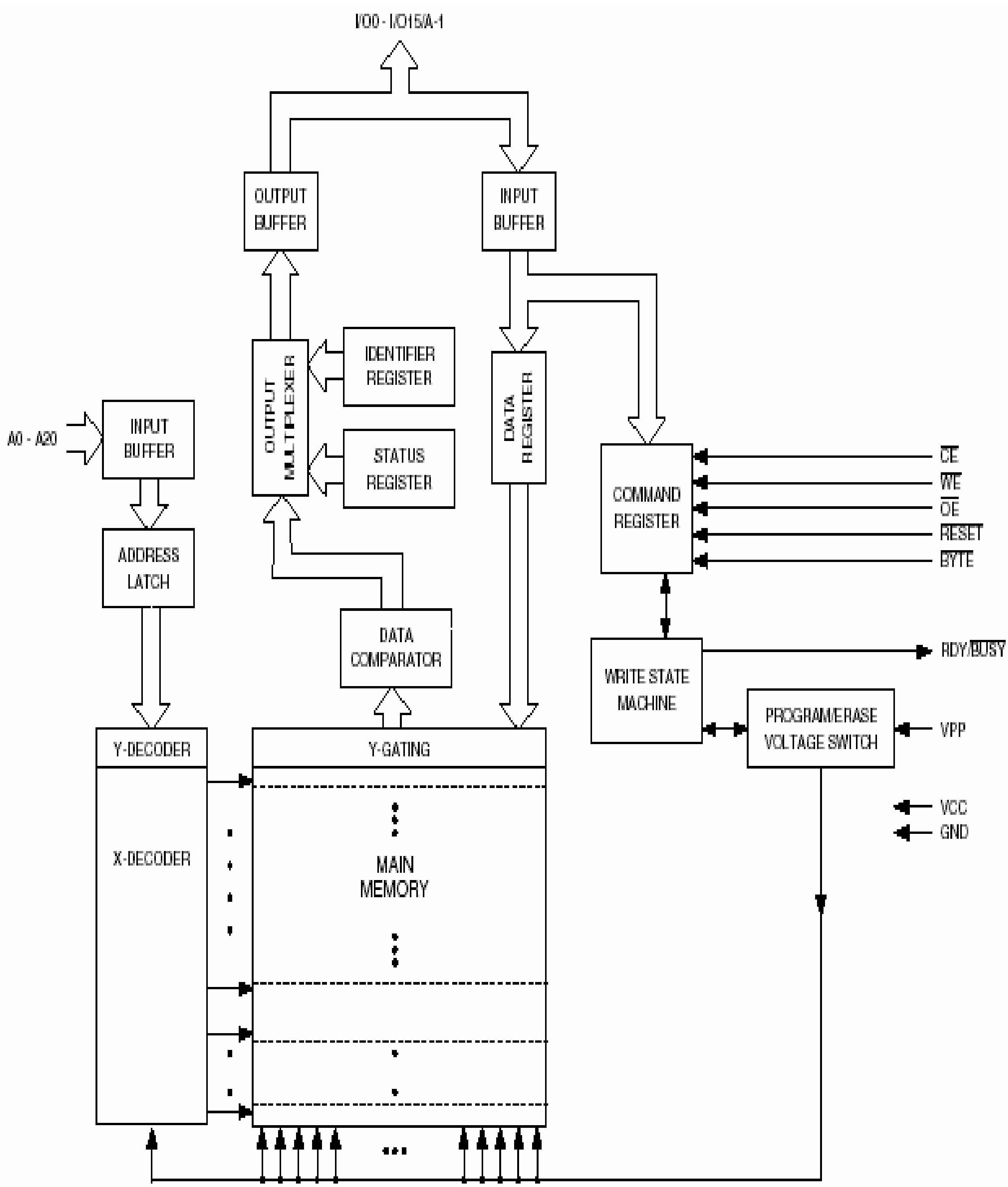

Figure 19 The AT49BV322AT provides a choice of 16bit word or 8 bit byte data bus width, for this application the 8 bit byte option was selected. *32Mbit Flash Memory (2004).*

4.5 Precision Oscillator

In accordance with the specification accurate time keeping is necessary to permit the overlaying of positional data with the data from existing trackers. The DS32kHz from Dallas Semiconductors requires no additional components to function and is connected in the 'battery supply' configuration described in the data sheet *32.768kHz Temperature Compensated Crystal Oscillator (2004)*. The output from the oscillator is connected to the microcontroller OSC1 pin. When programming the microcontroller, the 32kHz oscillator is disconnected from the microcontroller and replaced with an external 9MHz clocking source (in the Communication Stage) necessary for RS232 communication at 9600 baud. The clocking of the microcontroller is explained in Arendarik (2003).

4.6 Magnetic Sensor

The selection of a HMC1053 sensor to detect the earth's magnetic field requires a more substantial biasing network of components in order to provide a usable output for the microcontroller analogue to digital converter. The magnetic sensing elements within the HMC1053 are simply resistors that vary according to their alignment with a magnetic field. They are arranged in a Wheatstone bridge configuration which provides a standard differential voltage output as shown in Figure 20 and described in 1,2 and 3 Axis Magnetic Sensors (2004). The application notes provide Figure 20 as an example circuit when using the HMC1053 magnetic sensor in a three axis compassing solution. The circuit was adopted as a starting point in the design with the output from each bridge being amplified using an operational amplifier stage with a gain of 100. The suggested LMV324 operational amplifiers were not available so an equivalent LMV358 amplifier was obtained instead. The LMV358/324 amplifiers are general purpose devices with relatively poor specifications compared with more expensive instrument amplifier grade amplifiers. However as a starting point they were retained in the design and their suitability left for the later stage of evaluation to address.

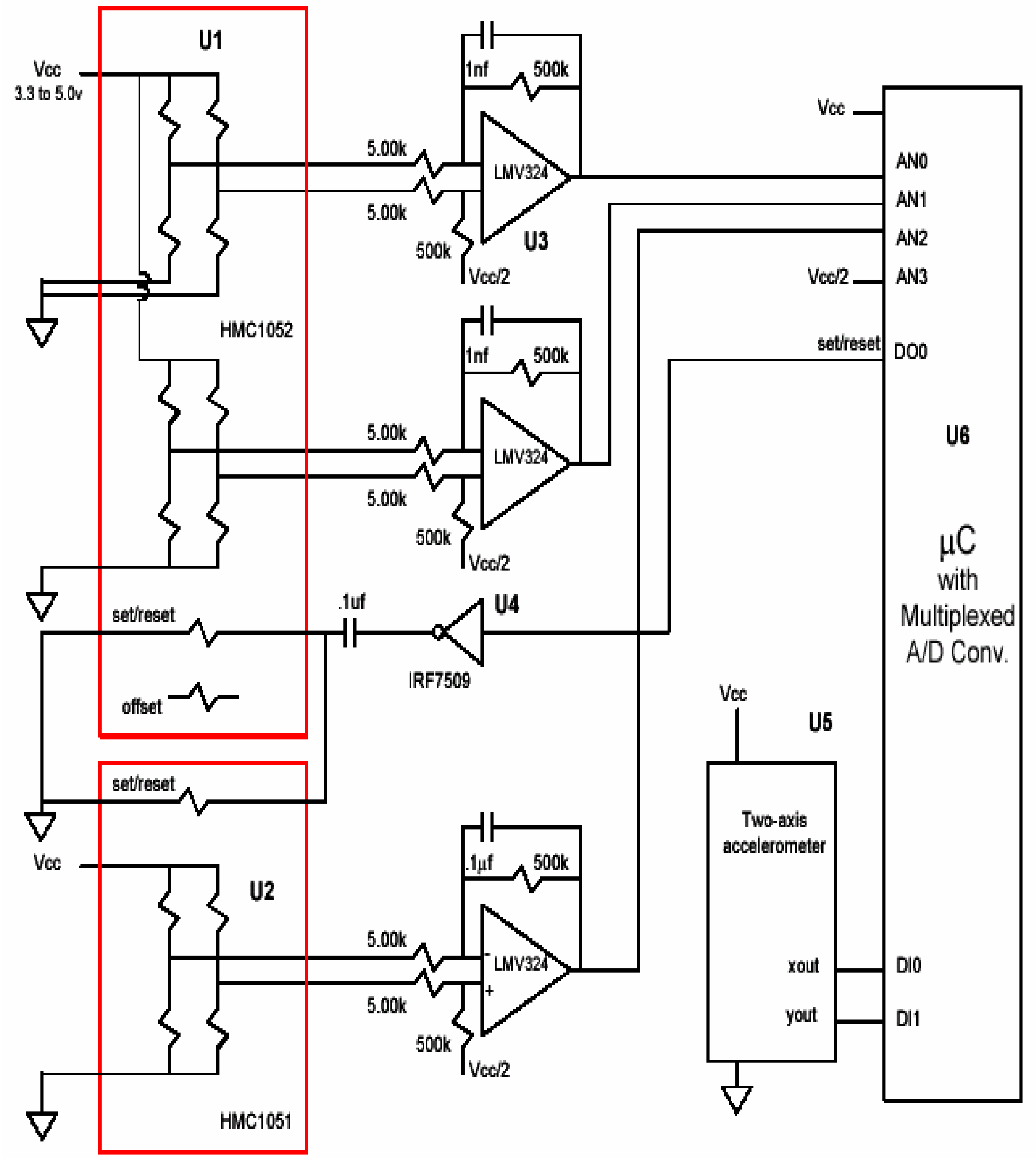

Figure 20 Each of the bridge networks is arranged to represent one axis of magnetic detection, either *x,y* or *z*. The output of the bridge provides the input to the operational amplifier stage then directly into an analogue to digital converter. *1,2 and 3 Axis Magnetic Sensors (2004)*

The circuit uses low voltage LMV358 operational amplifiers to increase the output from the magnetoresistive device as seen in Figure 21.

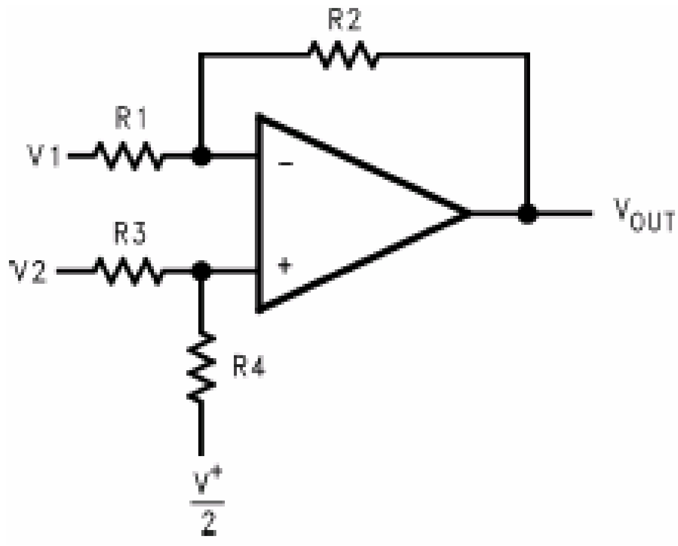

Figure 21 Operational amplifier used as a difference amplifier to increase the output of the magnetoresistive bridge circuit. In this application R1=R3=4.7k and R2=R4=470k. *1,2 and 3 Axis Magnetic Sensors (2004).*

The gain of the amplifiers is set by the biasing network of resistors according to the formula 4.2 producing a gain of approximately 100.

$$V_{Out} = \frac{R_2}{R_1}(V2 - V1) + \frac{V^+}{2} \qquad (4.2)$$

To refresh the magnetic detection elements a Set/Reset circuit is included in the design. The circuit charges a capacitor and then quickly switches the charged capacitor using a duel MOSFET through the set/reset straps to produce a pulsed current through the device in one direction for a *set* and in the reversed direction for the compliment *reset.* The average current consumed by the refresh circuit is around 2 microamperes when pulsed at a rate of 1Hz. The advantage of using this circuit is to reduce offset in the bridge circuit. The *set/reset* input to the FET is toggled on and off by the microcontroller. 1,2 and 3 Axis Magnetic Sensors (2004)

4.7 The Accelerometer

The accelerometer stage is very simple and requires only 5 external components as shown in Figure 22 to bias the device with output directly to the microcontroller ADC. The combination RC network produces a low pass filter with a corner frequency of 1.6kHz to attenuate noise generated within the device. The effects of a varying power supply voltage is discussed in Schultz (2004) in terms of Power Supply rejection Ratio (PSRR) but is of little effect in this design where the supply is stable and produced by a lithium battery with a flat discharge curve as shown in Figure 8.

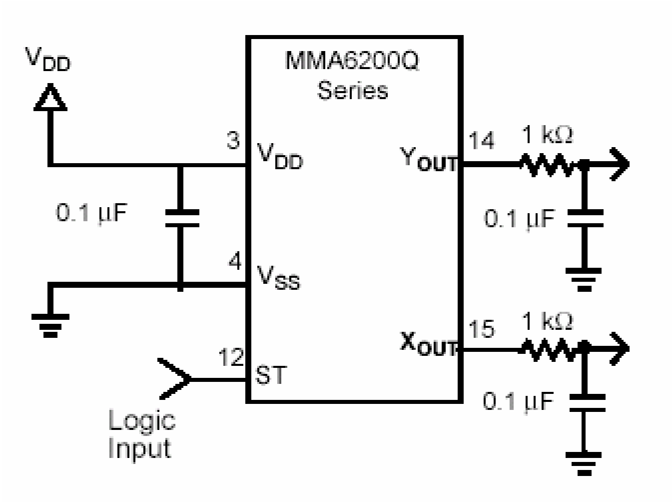

Figure 22 The accelerometer IC samples the internal micro machined sensors at a rate of 52kHz. The output filter circuit of 1kΩ and 0.1uF removes the noise generated from the internal switched capacitor filter circuit. *±10g Duel Axis Micromachined Accelerometer (2004)*

4.8 The Communications Interface

The communications interface stage provides level shifting between RS232 standard from a PC to the board levels around 3V DC. In addition the design allows the user to switch power, adjust logic levels on specific pins and select the oscillator frequency to permit entering the monitor mode on the controller for programming and monitoring in accordance with Figure 23, MC68HC908LJ24 Data Sheet (2004). At the heart of the design is a Maxim MAX3232ECPE IC a special low voltage RS232 IC which functions from battery supply voltages around 3 V, RS232 Drivers/Receivers (2004). The inclusion of this component eliminates the requirement for a 5V supply. The communications stage is a stand alone circuit on a separate board and is disconnected from the instrument at the completion of programming or interrogation. An 8 way DIP switch allows the programmer to select a variety of operating conditions for programming or monitoring according to Table 7.

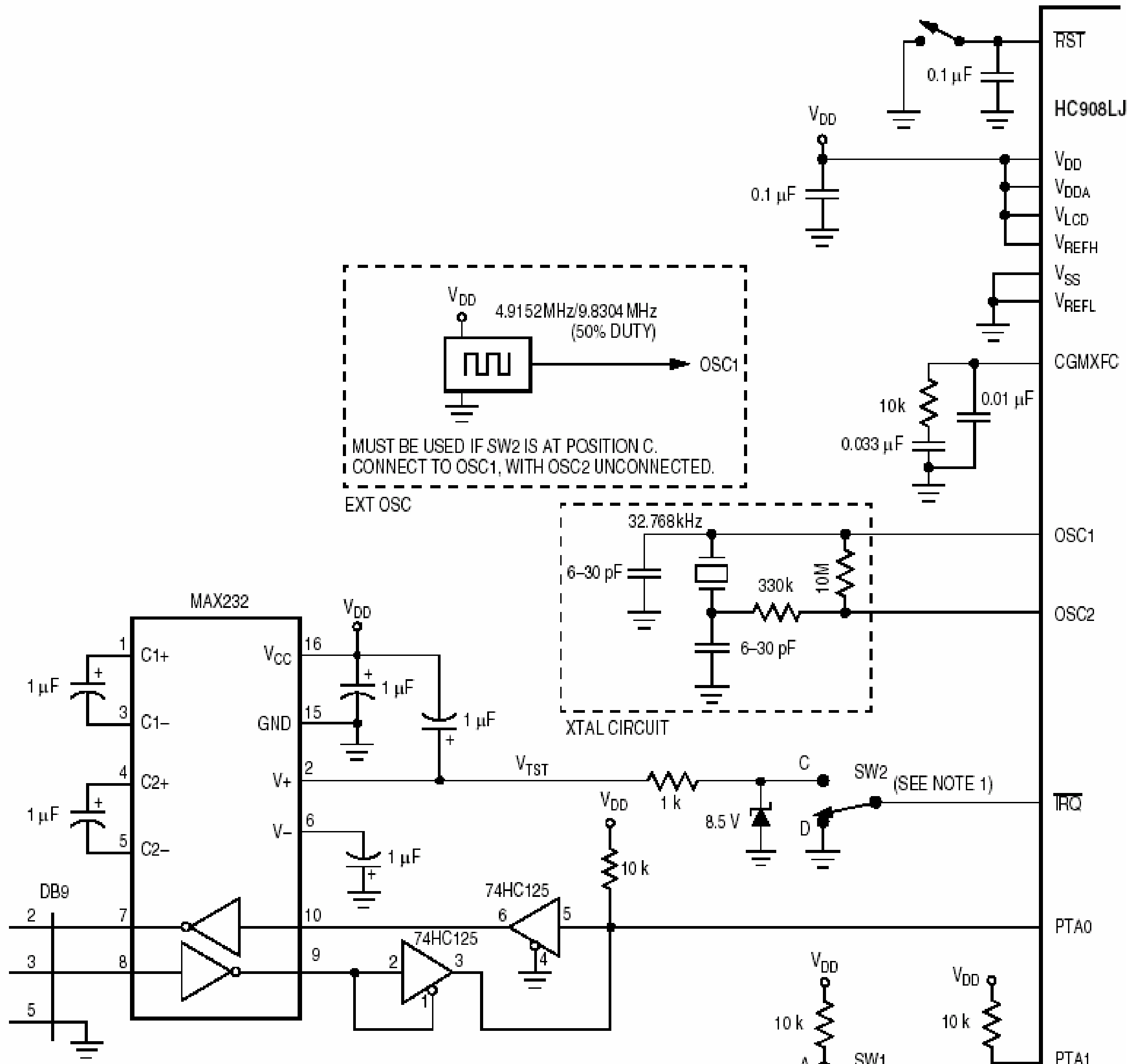

NOTES:
1. Monitor mode entry method:
SW2: Position C — High voltage entry (V_{TST}); must use external OSC
Bus clock depends on SW1 (note 2).
SW2: Position D — Reset vector must be blank ($FFFE:$FFFF = $FF)
Bus clock = 2.4576MHz.
2. Affects high voltage entry to monitor mode only (SW2 at position C):
SW1: Position A — Bus clock = OSC1 ÷ 4
SW1: Position B — Bus clock = OSC1 ÷ 2
5. See Table 24-4 for V_{TST} voltage level requirements.

Figure 23 Conditions required to enter Monitor Mode as outlined in MC68HC908LJ24 Data Sheet (2004). Copyright material owned by Freescale Semiconductor, Inc. used with permission, 2005.

Table 9 DIP switch settings provided to select necessary operating frequencies and voltages to program microcontroller.

DIP Switch	**1 On/Off**	**2 On/Off**	**3 On/Off**	**4 On/Off**	**5 On/Off**	**6 On/Off**	**7 On/Off**	**8 On/Off**
Function	External Power	7V IRQ Pulse	Port A0 Data	9MHz Osc	32kHz Osc	32kHz Osc	GND RST	POR Power On/Off

The communications interface also contains a programmable oscillator with an output frequency of 9.8304MHz necessary to permit 9600 baud transmission *HE-TXO-10C1 Temperature Compensated Oscillator (2004)*. The interface is connected to a PC via a standard 9pin DB connector and to the target board via a 16 pin DIP socket.

Chapter 5 Software Design Requirements.

5.1 Software Specification.

The primary function of the direction and positional tracker is to be a companion instrument to the existing velocity time depth recorders (VTDRs) and satellite linked time depth recorders (SLTDRs) in use today. In ensure the data is in phase, so that the positional information can be overlayed with the dive profile, accurate independent clocking is required between the units as no physical connection is possible. A software specification has been drawn from the information offered by scientists outlining the functions required of the device to provide useful data for their purpose.
The software specification

- Accurate time keeping over an extended period to permit overlaying with data from other trackers
- The positional information recorded from 1 second intervals to 30 second intervals.
- As many recordings taken as memory and power permits
- Able to retrieved saved data from memory when the instrument is recovered.

Accepting a microcontroller is the most logical method of controlling an instrument to achieve the scientist specification the data sheets and instruction set can be explored to achieve the program necessary to achieve the desired results.
The aim is to design software in a modular form to effectively test the instrument and thereby proving the overall design concept. Having the software in modular form also assists future development of the instrument by producing basic functional building blocks of code, as stand alone as possible. The selected MC68HC908LJ24 microcontroller is programmed *in circuit* via the monitor mode using the general methods described by Airaudi (2000) and Fan (2000) using the hardware suggested in MC68HC908LJ24 Data Sheet (2004).

5.2 Software Approach.

The adoption of a top down design with structured sub modules, as advocated by Miller (1999), forms the design methodology used in the development of the microcontroller program using sub modules. Figure 24 demonstrates the top down design architecture using a flow chart to represent the main functional modules.

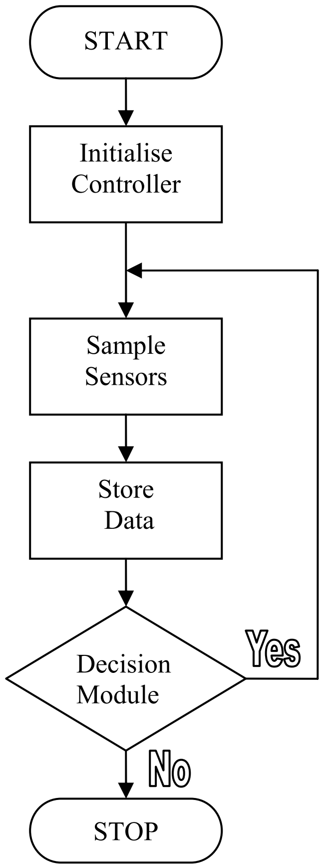

Figure 24 The top down approach promotes a modular design capable of modification, thereby aiding both subsequent optimisation and maintenance. Each of the main functional modules are further exploded into sub modules before structured programming is applied to build the code sections.

Following Figure 24 each module was explored in conjunction with the microcontroller instruction set and comprehensive reference manual. The first step taken was to determine the status of registers and internal settings needed to produce a working microcontroller capable of executing instructions and performing the needed tasks.

5.2.1 Initialisation Module.

Initialisation provides a blank processor with a beginning point and sets the stage for all of the functions inherent in the processor that will be drawn on to achieve the software specification. Figure 25 demonstrates the process of initialising the processor for operation. The order of initialising a microcontroller is specified in the programming reference manual for the microcontroller, *Technical Data M68HC08 Microcontrollers (2002)*.

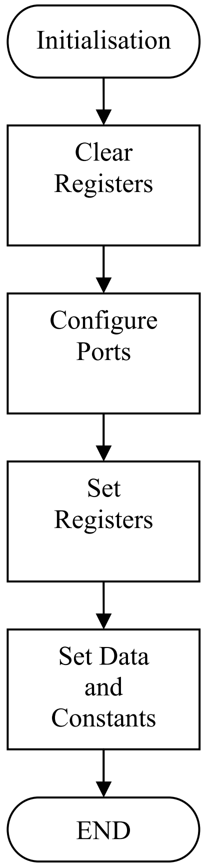

Figure 25 The flow chart demonstrates the sequential order followed by the program to operate the microcontroller and forms the basis of the initialisation module of code.

5.2.2 Sample Sensors Module

Analogue inputs to the microprocessor are required to be sampled and converted into a digital value. The MC68HC908 processor has 6 ADC channels however only one can be read at any one time. Figure 26 shows the process of analogue to digital conversion and is a core operation of the controller. Although the ADC is capable of 10 bit resolution an 8 bit lesser resolution satisfies the requirements of the specification and reduces the number of bytes required to store the information.

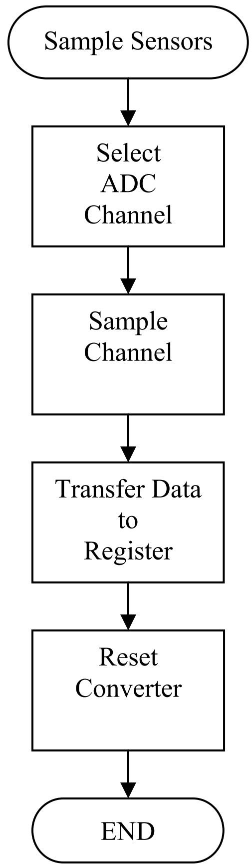

Figure 26 The ADC transforms the output from the sensor circuits into a digital representation of the voltage so that it can be stored in the flash memory for later retrieval.

5.2.3 Store Data Module

In order to store data on the external memory device the microcontroller puts data on the Address, Data and Control in accordance with the flow chart given in Figure 27 and following the procedures outlined in *Recommended Reprogramming Procedure for Atmels's Flash Memories* (*2000)*.

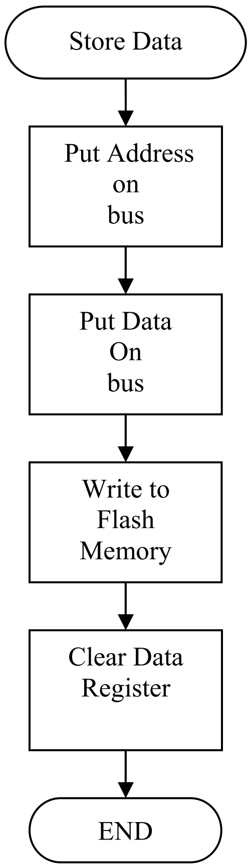

Figure 27 The writing of data to external memory requires precise sequential steps indicated in the flow chart.

5.2.4 Decision Module

The Decision Module is at the heart of the program and controls which sub modules are called at the overall timing of the device. The decision module is activated using an interrupt routine from the microcontroller real time clock to bring the device out of sleep mode. This is necessary to minimise the power consumption of the device between sensor readings to prolong the battery life. The module checks the availability of external memory prior to writing, increments counters, registers and places the device in sleep mode at the completion of a round of sampling as shown in Figure 28. The writing of this section of code is highly dependant of discussions with research biologists as the microcontroller has an inbuilt calendar that can generate interrupts on specific days, weeks or months. This factor in the code design process was not expanded on, instead the programming was restricted to code elements that evaluated the operation of the instrument and written in a modular form to facilitate this requirement at a later date.

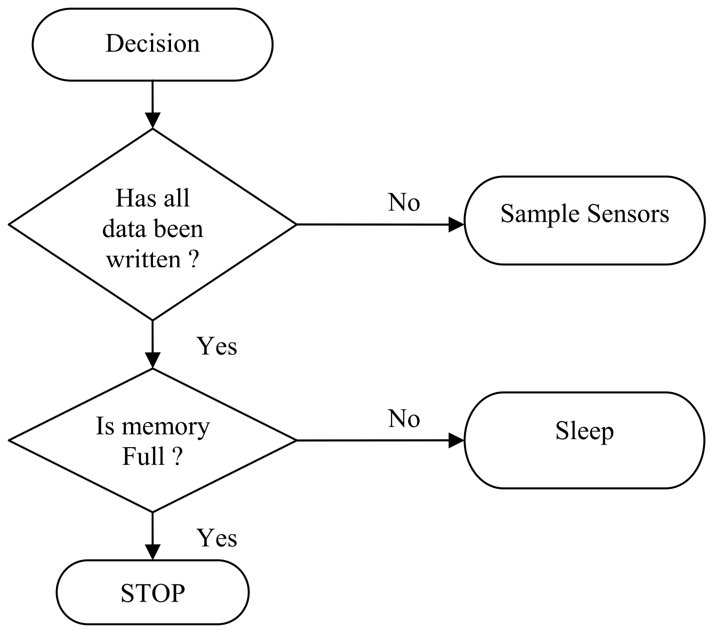

Figure 28 The decision to continue recording data is critical to prevent overwriting earlier data should the memory address exceed 3F FF FF.

5.3 Structured Programming.

Having developed the outlines of the program modules the task of writing the necessary code began in accordance with the principles of structured programming. Miller (1999) suggests when adopting structured programming that an initial program be developed as soon as possible and tested; then build the program in increments with constant testing using the debugging methods described by Suchyta (2002). An example of modular code used for evaluation is provided in Appendix D.

5.3.1 Initialisation

Following the CPU08 Reference Manual (2001) it is recommended to set the CONFIG registers immediately after a reset (POR). In order to permit termination of the program if external memory is exhausted the STOP instruction must be enabled by setting to 1. The required register contents are given in Table 10.

Table 10 Configuration Register 1

	COP	LVIST	LVIR	LVIPW	UNIM	SSRE	STOP	COPD
Bit	7	6	5	4	3	2	1	0
Default	0	0	0	0	0	0	0	0
Required	0	0	0	0	0	0	1	0

The STOP_XCLKEN bit needs to be set to 1 to permit the RTC to continue to run during stop mode and is altered by changing the Configuration Register 2 contents according to Table 11.

Table 11 Configuration Register 2

	PEE	STOPIRCDIS	STOPXCLOCKEN	DIV2CLK	PCEH	PCEL	LVISEL1	LVISEL0
Bit	7	6	5	4	3	2	1	0
Default	0	0	0	0	0	0	0	1
Required	0	0	1	0	0	0	0	1

ATMEL memory requires words to be written to the device in order to invoke chip functions such as read, write and erase, Atmel AT29 Flash Memories (1998). The printed circuit board design was developed with efficient of routing as a priority so microcontroller ports do not sequentially connect to the flash memory. Therefore a conversion process is required to determine the microcontroller port output register words necessary to interface with the memory chip. Rearranging Table 4 produces Table 12. The conversion from Flash HEX555 to microcontroller port words is given in Table 13. The conversion from Flash HexAAA to microcontroller port words is given in Table 14 and 15.

Basically the significance of this is best described by the following small example.

Example 1. Flash memory requires hexadecimal 555 to be impressed on the flash IC address pins, A0 to A10 to begin a write sequence. In order to achieve this, the microcontroller port registers must be loaded with hexadecimal words Port C = A8, Port D = 0C and Port F = 08.

Table 12 Chip erase Address hex 555 Command Definition in binary form.

MEMORY ADDRESS	A10	A9	A8	A7	A6	A5	A4	A3	A2	A1	A0
PORT C, D AND F BITS	F 3	F2	D2	C2	C3	C4	C7	C6	C5	D0	D3
HEX 555	1	0	1	0	1	0	1	0	1	0	1

Table 13 Port outputs of C, D and F

Port	Binary	Hexidecimal
Port C	1010 10xx	#$A8
Port D	xxxx 11x0	#$0C
Port F	xxxx 10xx	#$08

Table 14 Chip erase Address hex AAA Command Definition in binary form.

MEMORY ADDRESS	A10	A9	A8	A7	A6	A5	A4	A3	A2	A1	A0
PORT C, D AND F BITS	F 3	F2	D2	C2	C3	C4	C7	C6	C5	D0	D3
HEX AAA	0	1	0	1	0	1	0	1	0	1	0

Table 15 Required port outputs of C, D and F

Port	Binary	Hexidecimal
Port C	0101 01xx	#$54
Port D	xxxx 00x1	#$01
Port F	xxxx 01xx	#$04

Chapter 6 Prototype No.1 Construction.

6.1 PCB Layout and Construction

To achieve successful PCB layout and construction, the circuit schematics were developed using an integrated software package by Altium, Protel DXP2004. Protel DXP2004 includes a schematic editor, component placement tool, routing tool and produces output files necessary for PCB manufacture. Before routing commenced FoES were contacted and guidance received concerning the capability of the faculty to manufacture PCBs in accordance with Table 16. The selection of fine pitch components infringed the FoES specification and negotiations to overcome those limitations were pursued. The workshop was able to successfully produce a prototype board of high quality and to the project specification.

Table 16 PCB construction limitations for *FoES* workshop assistance and specification required by project.

Specification	FOENS Limitation	Project Requirement	Compliance
Track width	≥ 0.3mm	0.25	NO
Dist Between Tracks	≥ 0.5mm	0.25	NO
Minimum Component Size	≥ 806	1206	Yes
Minimum Hole Size	≥ 0.8mm	0.8	Yes
Between Components	≥ 1.5mm	2mm	Yes
Minimum Board Size	≥ 50mm x 50mm	75mm x 50mm	Yes

6.2 PCB Layout

Before circuit schematics can be transferred onto a PCB design each component has to be assigned a footprint. Protel DXP2004 is equipped with extensive component footprint libraries however footprints for the accelerometer, magnetoresistive and microcontroller components were not available and were manually developed using the Protel footprint design tool. After footprints were assigned, components were placed manually within the PCB design area; this ensured the circuit stages remained as physically definable groups. Routing was then performed with Data, Address and Control busses laid manually to minimise vias. The DXP routing tool *Situs* was employed to complete the routing operation on both the tracker and communications boards. The result of this process is shown in Figure 29 and the communications interface board displayed in Figure 30. At the completion of PCB design all intended components were ordered and when received their footprints checked with vernier callipers. After confirming footprint dimensions PCB construction was initiated with FoES. Routing underneath the magnetoresistive component is permissible under Mounting Tips for LCC Magnetic Sensors (2004).

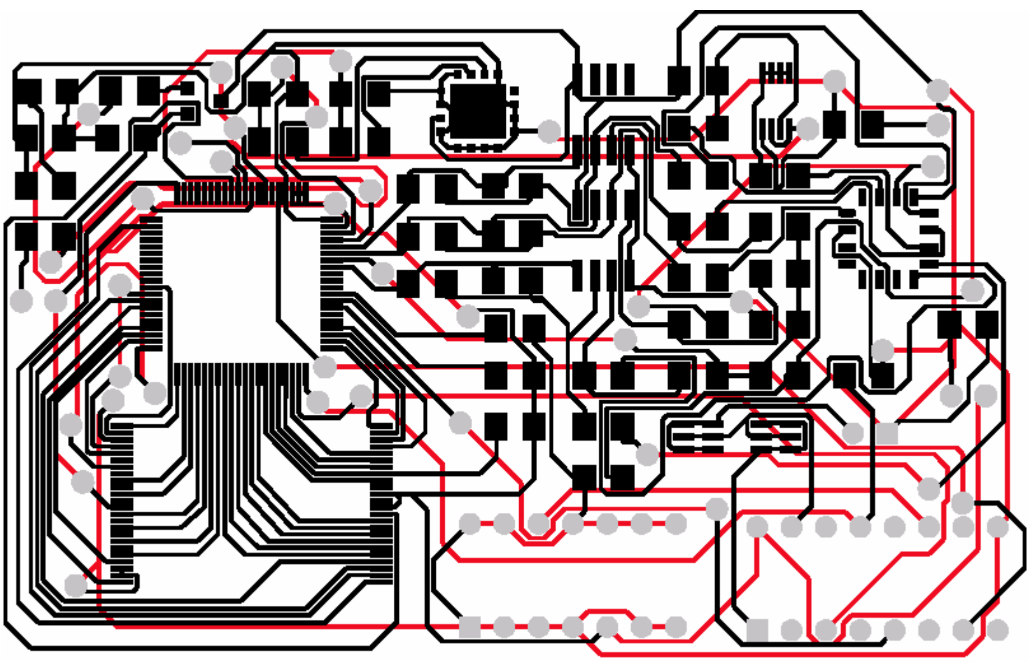

Figure 29 PCB design of instrument using a two layer board. Top layer copper tracks and pads are presented in black, bottom layer in red, vias and through holes in grey. The actual dimension of the board is 77mm X 50mm.

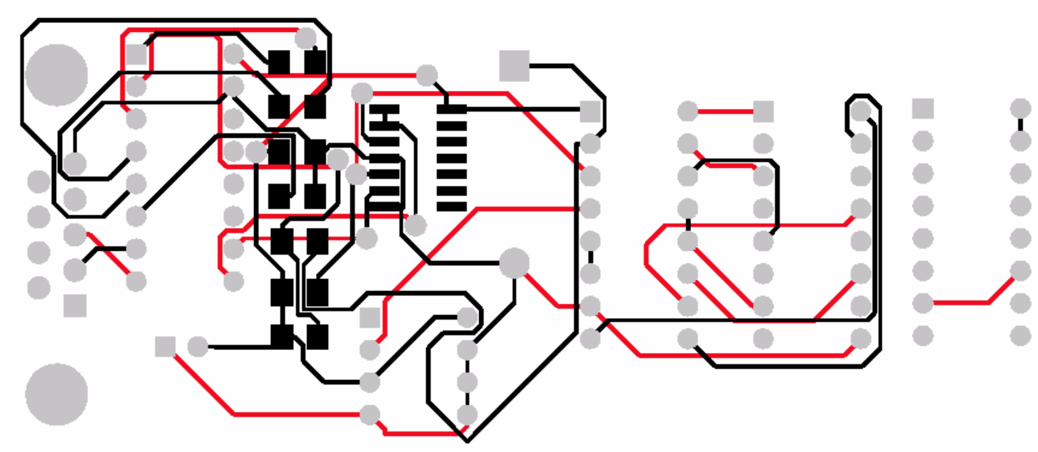

Figure 30 PCB design of Communications Interface board using a two layer board. The dimension of the board is 90mm X 33mm.

6.3 PCB Construction.

The Protel files necessary to construct the printed circuit boards were generated and forwarded to the Faculty of Engineering and Surveying for manufacture. Due to the fine pitch of some components (0.5mm) and the board being two layered, careful attention was required during the manufacturing process. In addition to the prototype boards, a defective tracker board produced by FoES was also supplied enabling experimental and practice soldering to be conducted. As the design had both surface mounted and through hole components, several methods of soldering components were required in the construction as described in Table 17.

Table 17 Soldering methods found successful on reject board and adopted during the placement of components on the prototype boards.

Solder Method	Components	Comment
Conductive Tool, (temp controlled soldering iron).	Through hole and SMDs.	Both solder paste and flux cored solder used
Convective Tool, (Sunbeam domestic oven)	Accelerometer (LCC) and Magnetoresistive device.	Solder paste with flux

Successful component attachment using the methods given Table 17 was observed. As SMD components are hydroscopic all SMD components were baked for 8 hours at 100°C in a domestic oven prior to placement to reduce the likelihood of "pop corning" during the solder reflow process. The attachment of components to the prototype boards was carried out in the following order

1. Convection method used to attach leadless chip carrier components, (accelerometer and magnetoresistive device) and other surface mounted devices.
2. Conductive method used to attach through-hole devices.

A solder reflow curve was provided by Honeywell in the document *Mounting Tips for LCC Magnetic Sensors* (2004), for the attachment of the HMC1053 magnetoresistive component. The profile was also suitable for the attachment of the accelerometer and was used as a guide in convection soldering. Without having access to a professional reflow oven, a domestic *Sunbeam* oven was employed for this task. The temperature curve could only be approximated using this method but with care resulted in a satisfactory result using Loctite Solder Paste with an alloy constitution of SN62Pb36Ag02 combined with a no clean type flux. The use of a 4X binocular microscope was instrumental in ensuring the fine pitch components were soldered satisfactorily and for general inspection.

6.4 Completion of Prototype No.1

The first prototype shown in Figure 31 demonstrates a monolithic design and closely resembles the layout desired in a final product. The construction of the communications board shown in Figure 32 was relatively simple compared with the complexities of the instrument tracker.

Having successfully constructed prototypes the next phase was to test each electronically for correct operation and determine if all circuits interact according to the overall design specification. Any hardware deficiencies detected can be addressed and incorporated in the design of a second prototype to become the subject of a second round of evaluation. Following successful electronic testing the software written to control the microprocessor can be loaded. The unit can then be evaluated as an operational prototype and an assessment made to determine the overall functionality of the design.

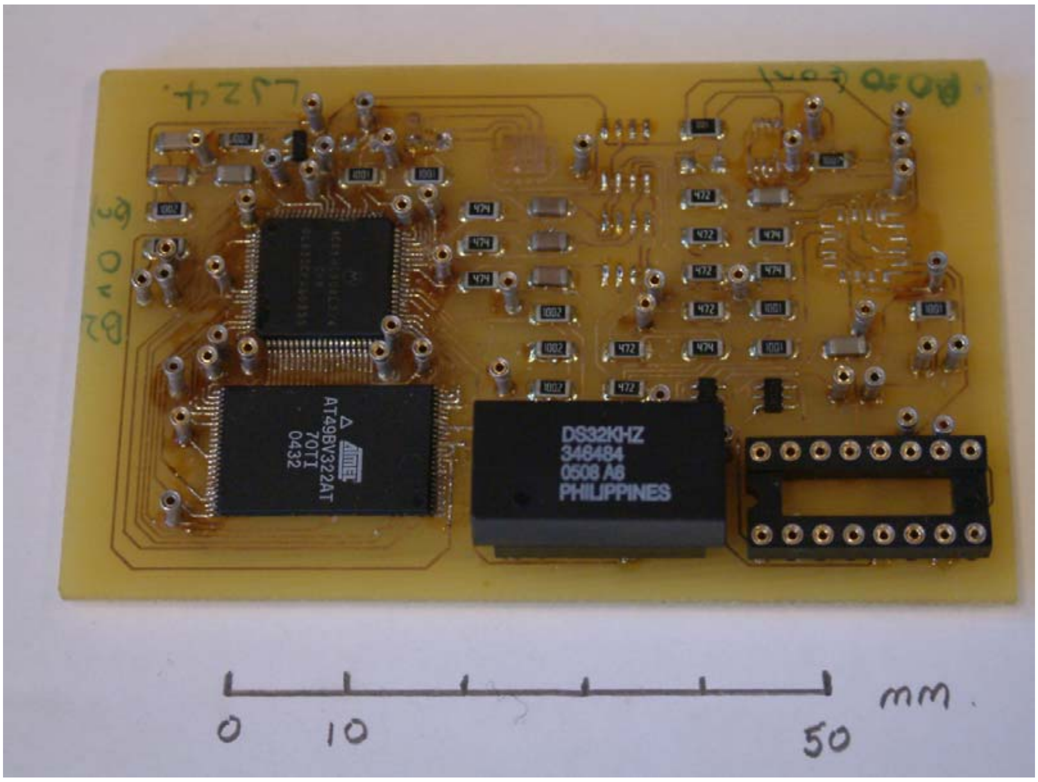

Figure 31 Prototype No.1. Using surface mounted components in the design made the instrument compact. To further miniaturise the device using decreased track widths and clearances, commercial PCB manufacturing would be required. Several footprints are unpopulated as the components were robbed for the construction of the second prototype.

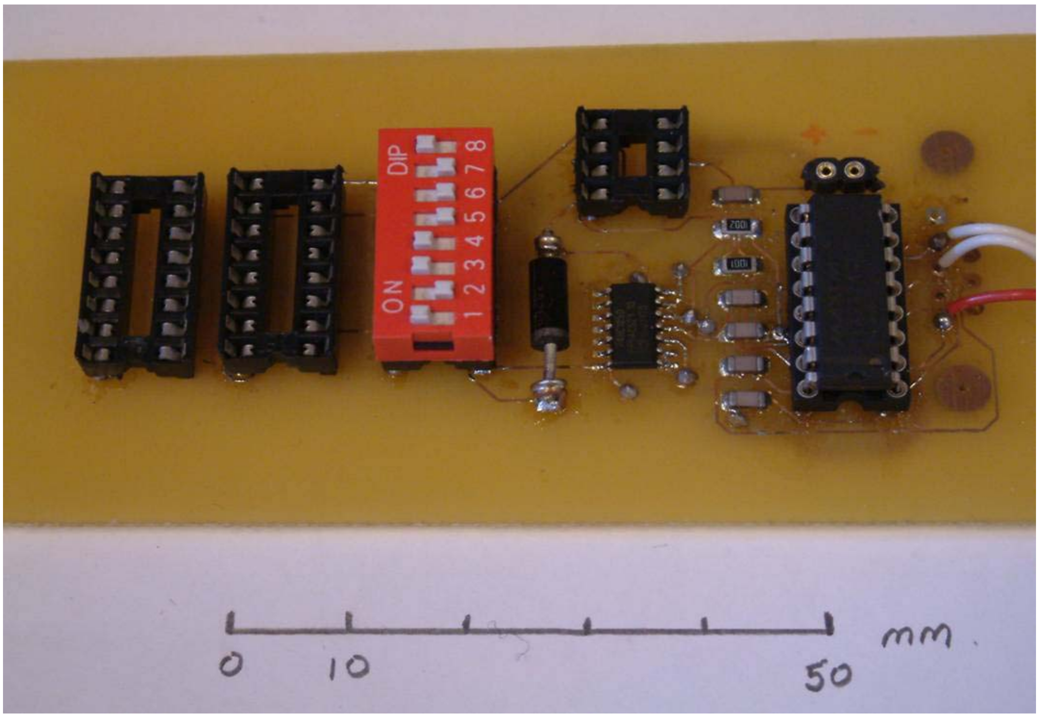

Figure 32 Communications Board No.1. Only a handful of components are necessary to provide the level switching to enable a PC to communicate with the microcontroller effectively.

Chapter 7 Prototype No.1 Evaluation

7.1 Prototype Evaluation Methodology.

The development of hardware and software has been presented previous chapters separate tasks, developed using a modular approach. The early adoption of this modular design assists evaluation by providing small sections of circuit or code that can be examined in near isolation for compliance and finally against the overall project specification.

The aim of evaluation is to compare the unit under test with the technical specifications and determine limits, uncover strengths and weaknesses in the design and provide a clear determination of the fitness of the device for the intended application, in this case the deployment of the instrument on a living animal, a southern elephant seal.

The evaluation of the first prototype began by assessing the physical attributes and then proceeding to examine the electrical performance against the design schematics before moving on to examine functionality of the devices.

Evaluation is also critical in uncovering improvements to the design permitting a structured way to develop further prototypes using an iterative method to reach a reliable end product.

7.2 Physical Inspection

Having successfully placed and soldered the components onto the printed circuit boards the next stage was to perform a visual inspection aimed at checking the following areas for accuracy and compliance against the circuit design

- ✓ Component values
- ✓ Component placement
- ✓ Soldering integrity
- ✓ Track integrity
- ✓ Overall arrangement of components

The visual examination indicated the construction was sound and reflected the overall design parameters. The quality of the solder joints on surface mounted components was satisfactory but varied in fillet thickness due to manual application of solder paste. The inclusion of IC sockets increases the vertical dimensions of both boards and introduces contact reliability problems in the design. The mixture of through hole and SMDs complicated the assembly of the boards requires multiple of methods to achieve soldering and placement. SMDs are more reliable and robust than through hole. The connection method between the communications board and instrument board is awkward to use and the pins on the connectors are sharp and dangerous.

Improvements incorporated in second prototype:

- Eliminate IC sockets.
- Select SMD components where possible.
- Improve the connection method between boards with emphasis to develop a robust, safe and effective form of connection.

7.3 Electrical Modules

Having established the integrity of construction the next step in the process, testing the electrical modules began.
The areas singled out for testing are

- Communications Board
- Power Supply
- Microcontroller Stage
- Memory Stage
- Oscillator
- Accelerometer
- Magnetoresistive

The basic electrical evaluation was conducted by applying 3.6V d.c. onto the circuit boards and measuring the response compared with expected values calculated from the circuit schematics.

7.3.1 Communication Board.

The communications board is a critical component in the project overall. It facilitates communications between the microcontroller and PC for programming and interrogation and provided voltage signals to specific controller pins to enter Monitor mode or User mode. Voltage was applied to the PCB and selected test points checked to verify the anticipated voltages in conjunction with the design parameters. The inputs and outputs of the communications board were examined and the results recorded in Table 18. Although the generation of V_{Test} by the Maxim RS232 IC is satisfactory, the possibility of V_{Test} inadvertently being pulled low due to the switching arrangement may load the component and effect RS232 transmission parameters.

Table 18 There are eight major functions required for the communications board to interrogate, download data and program the microcontroller in accordance with the specification.

Parameter	Expected Result	Result on Test
RS232 Communications	Loop back to PC	✓ Loop back confirmed
External Power	3.6V DC to all components	✓ 3.6V DC confirmed
Port A IO data	Changing logic levels H to L	✓ Measured by CRO
9MHz Oscillator	9.8304MHz oscillation	✓ Measured by CRO
32 kHz	Square wave 32.768kHz	✓ Measured by CRO
Ground Reset	Switch output pin L	✓ Switched L
High Voltage Interrupt V_{Test}	> 7 V DC	✓ 8.2V DC
Power-On-Reset	Interrupt supply to target	✓ Supply interrupted.

Improvements incorporated in second prototype:

- Provide external V_{Test} via a standard 9V battery and zenner diode circuit to reduce IC loading and improve circuit reliability.
- Reduce circuit complexity by amalgamating the Power-On-Reset function with External Power function.

7.3.2 Power Supply

The target board has duel supply capability with automatic current direction determined by a simple network of low forward voltage drop (V_F) diodes. The input voltage from the lithium battery is measured at 3.65 volts and V_F is a very low 0.2 volts, producing by simple subtraction a voltage supply of 3.45V. The sensor circuits are supplied via a switched PNP transistor, the V_F was measured at 0.2 volts producing a sensor circuit supply voltage of 3.25 volts. The resulting voltages comply with component specifications given in data sheets for predictable and reliable operation. Another important aspect of the power supply circuit is the power interruption switch which is located on the communication printed circuit board. The operation of the switch is essential in providing the Power-On-Reset required by the microcontroller.

Improvements incorporated in second prototype:

- Relocate the power interruption switch onto the tracker board.

7.3.3 Microcontroller

Functional evaluation of the microcontroller began by establishing communications between the controller and a PC via the RS232 communication interface. Contact was acheived using the *WinIDE Development Environment* software suit, freely available from P&E Micro (http//:www.pemicro.com).
The functional evaluation of the microcontroller was achieved by programming the device with small sections of code and observing the status of internal registers and input/output voltage levels. Examples of code written to evaluate the microcontroller is provided in Appendix D.
Testing proved the correct operation of the following functions,

- Analogue to digital converter,
- Real Time Clock
- Input ports
- Output ports.

7.3.4 Memory

The flash memory was tested by instructing the microcontroller to read addresses 0000 hex and 3FFF hex which returned in both cases hexadecimal FF, indicating an erased memory IC as expected. By reading the max and minimum address range the integrity of the address, data and control busses is confirmed. The next step was to program the device with data and check the integrity of the data stored, this process was repeated several times and proved the device was operating correctly and writing the data to memory. The memory device was successfully accessed, read and written.

7.3.5 Oscillator.

The DS32kHz oscillator provides the clock input to the microcontroller and is specified to maintain accuracy over one year to within ±1 minute. Testing of the device to that degree of accuracy was not possible; however the output waveform was examined by oscilloscope and found to be a well formed square wave which agreed with the published data sheet specifications. The oscillator also successfully operated the microcontroller's real time clock by pulsing a LED with a periodicity of 1 second. The oscillator was connected to the PCB by a DIP socket.

Improvements incorporated in second prototype:

- Change oscillator package from DIP to Ball Grid Array to produce a physically low profile and eliminate the socket arrangement.

7.3.6 Accelerometer

The MMA6233Q accelerometer is capable of measuring ±10G in both the X and Y axis and delivering a proportional voltage at the outputs. To evaluate the accelerometer two fundamental sets of conditions were applied and the results recorded

1. The device in a static environment
2. The device in a dynamic environment

7.3.6.1 'Static Testing' Regime

'Static testing' refers to recording the output of the accelerometer whilst stationary; this focuses attention on the ability of the device to measure acceleration due to gravity alone without other sources of acceleration. A static test of the accelerometer was conducted by attaching the device to a solid table using Blue Tac® then attaching an oscilloscope to the X and Y outputs of the device. The instrument accelerometer was then positioned in the horizontal plane, where the force on the accelerometer elements is regarded as 0g with the response observed on the oscilloscope recorded. The device was then rotated ±90° in both the X and Y planes as shown if Figure 15 which represents the maximum expected output under the influence of gravity (±1g) and the observed voltage on the oscilloscope again recorded. The results are provided in Table 19. The voltages were checked with a DMM to verify the oscilloscope readings.

Table 19. Static testing results of the accelerometer reflect the manufacturers specifications.

	X Output	Y Output	Expected	Difference
+90° rotation	1.77	1.77	1.77	0
0° rotation	1.65V	1.65V	1.65V	0
-90° rotation	1.53	1.53	1.53	0
Sensor Range ΔV_{Sensor}	±120mV	±120mV	±120mV	0

7.3.6.2 Accelerometer Static Resolution

The output of the accelerometer produces a sinusoidal response trace similar to that of magnetoresistive device shown in Figure 13. Accordingly, the resolution or accuracy of the response is not linear. The greatest error $R_{\pm 90}$ occurs when the accelerometer is required to measure angles close to ±90˚ and is calculated using equation (7.1).

Given

$R_{\pm 0}$ = Angular Resolution in degrees near ±0˚

$R_{\pm 90}$ = Angular Resolution in degrees near ±90˚

ΔR_{ADC} = 3.5mV (one ADC step)

ΔV_{Sensor} = ±120mV (Range of sensor voltage)

$$R_{\pm 90^\circ} = \arcsin\left(\frac{\Delta V_{Sensor}}{\Delta V_{Sensor}}\right) - \arcsin\left(1 - \frac{\Delta R_{ADC}}{\Delta V_{Sensor}}\right) \tag{7.1}$$

The least error $R_{\pm 0}$ occurs when the accelerometer is required to measure angles close to 0˚ and is calculated using equation (7.2)

$$R_{\pm 0^\circ} = \arcsin(0) - \arcsin\left(\frac{\Delta R_{ADC}}{\Delta V_{Sensor}}\right) \tag{7.2}$$

The best angular resolution obtainable near angles of tilt or roll of ±90˚ is 14° compared with 1.7˚ near 0˚.

Improvements incorporated in second prototype:

- Select a more sensitive accelerometer to increase the output resolution.

7.3.6.3 Accelerometer low pass filtering

Because the accelerometer uses an internal switched capacitor network operating at 52kHz the possibility of introducing noise at this frequency or a multiple of this frequency is worth considering. To eliminate noise at this frequency an external low pass RC network consisting of a 1kΩ resistor and 0.1μF capacitor has been included at the output of the accelerometer. The corner frequency f_c is calculated using equation 7.3 and provides a –20dB/decade response (roll off) for frequencies above 1600Hz , as shown in Figure 33.

$$f_C = \frac{1}{2\pi RC} \tag{7.3}$$

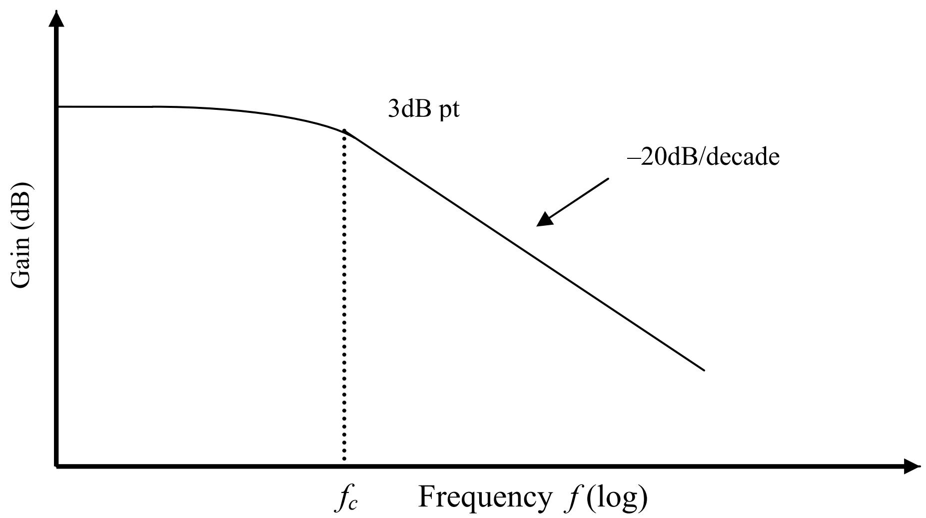

Figure 33 Single Pole low pass filter used to remove switched capacitor noise components from accelerometer. Frequency components of noise above the corner frequency of 1600Hz are attenuated by the filter at a rate of –20dB/decade.

Testing the accelerometer output by observing the oscilloscope set on 5 mV/div and varying the sweep rate from 500 to 10 μs/div failed to detected any noise from the internal switched capacitor circuit, indicating the signal from the accelerometer is clean.

7.3.6.4 'Dynamic Testing' Regime.

'Dynamic testing' refers to recording the output of the accelerometer whilst being hand held and moved about. Dynamic testing permits observation of the accelerometer response to accelerations other than gravity. Dynamic testing attempts to more closely reflect the conditions the instrument will endure during deployment on a living animal.
The assumption made here is an elephant seal swimming would cause acceleration no greater than that applied during the dynamic testing in the laboratory. An elephant seal, although capable of bursts of speed and no doubt swift changes in direction is still fundamentally a very large animal compared to a human hand holding the instrument and accelerating the device in different directions.
The hypothesis is, a hand can cause greater acceleration than an elephant seal, and therefore the acceleration generated by a seal resulting in accelerometer error would be somewhere less than that observed during the dynamic tests conducted by hand.
To examine the dynamic response of the accelerometer the X^* and Y^* outputs were connected to an oscilloscope and the instrument moved through a full range of motion by hand.
Rotating the device slowly revealed a smooth change in waveform on the oscilloscope when observed on a scale of 0.1V/div. With faster dynamic movement and sudden changes of direction the output waveform was noticeably affected producing overshoots in the order of 50mV. Allowing the overshoots to equal ΔR_{ADC} and substituting into equation 7.1 indicates errors due dynamic acceleration of approximately 36º and using equation 7.2 errors in the order of 24º.

Improvements incorporated in second prototype:

- To reduce the dynamic error caused by accelerations other than gravity an improved low pass filter was designed.

7.3.7 Magnetoresistive Stage.

To test the magnetometer an oscilloscope was attached to each amplifier output X^*, $Y^*$and Z^*. On examination there was no output from the amplifiers.
The circuit diagrams were traced and the fault was attributed to an incorrect component connection pin out. The pin out for a Honeywell HMC1023 was inadvertently used instead of the selected HMC1053 magnetoresistive device. This error prevented further analysis and evaluation of the magnetoresistive stage.

However the fault did highlight a problem with the design process, the system of checking and quality control was not developed enough to detect this error. To address this deficiency a system was developed of quality control and certification. The system involved XL spreadsheets with every component listed along with footprints and pin outs. This system required ticking off each component and cross referencing the Protel PCB design and schematic. Although the system took substantial time to develop had it been developed prior to the construction of the first prototype it would have prevented the necessity of constructing another prototype to continue the evaluation.

Improvements incorporated in second prototype:

- Implement a system of quality control.
- Update drawings and design to reflect component pin out of HMC1053 magnetoresistive sensor.

7.4 Conclusions: Prototype No.1

Bringing an instrument from a theoretical concept through the design process and finally producing a useable prototype for evaluation is part of an iterative process. By thoroughly evaluating the first prototype the number of iterations needed to develop a working design can be minimised. The evaluation of the first prototype uncovered opportunities for improvement in almost all major circuit modules. Accordingly any subsequent prototype stands to benefit substantially.

The integrity of the overall project was bolstered by the recognition that a structured quality control system was lacking in the design. This was detected when a critical component, the magnetoresistive sensor, was found to have been assigned an incorrect footprint. This recognition prompted the development of the quality control system used in the development of the second prototype.

Chapter 8 Prototype No.2 Construction

8.1 Adopting Recommendations from Prototype 1.

Having gained some useful experience in designing, constructing and evaluating the first prototype the task of building a second prototype was undertaken. The evaluation had uncovered flaws and scope for improvement in the design and the second prototype incorporated those points raised. The task of updating the circuit schematics was undertaken to reflect any design changes and are provided in Appendix C.

In addition to circuit enhancements another design change was to move away from the monolithic design and split the instrument into two separate boards, one board acting as purely the data logger consisting of microcontroller, flash memory and communications interface and the other board comprising the sensor circuits. This approach provides a more adaptable prototype where modifications can be made to one board without having to rebuild the entire tracker. The two boards are stacked together, one on top of the other and connected by a pin header and socket as shown in Figure 34. A ground plane was also inserted between the two boards to reduce interference.

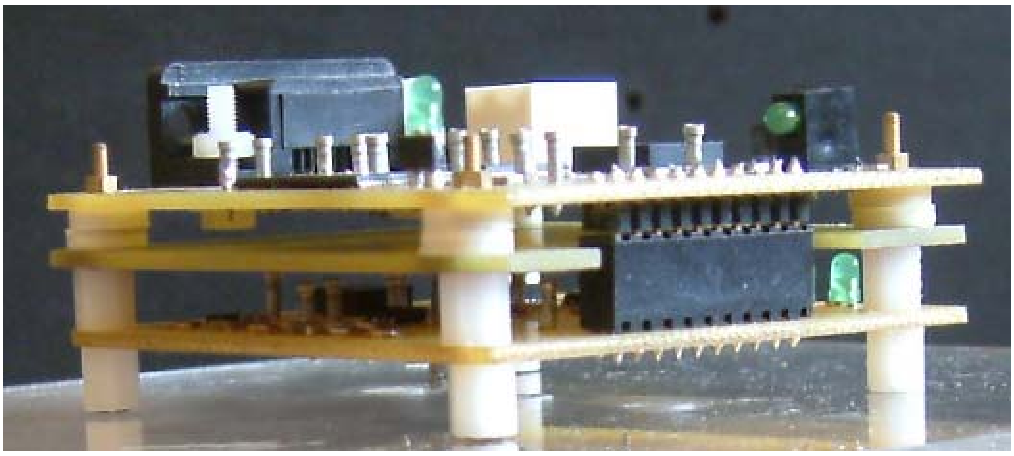

Figure 34 Prototype No.2 The ground plane is visible between the upper data logger and the lower sensor board and is constructed of unetched copper PCB cut to size.

8.2 Design Improvements Prototype No.2

A brief explanation of the design improvements undertaken is provided from subsection 8.2.1 to 8.2.8 and classified under the main circuit module headings.

8.2.1 Physical Inspection

- Improve the connection method between boards with emphasis to develop a robust, safe and effective form of connection.

To address this concern the 16 pin IC header was removed from the design and replaced with a standard DB9 connector. This design has no sharp points to cause personal injury and is an industry standard connector with proven reliability.

8.2.2 Communications

- Provide external V_{Test} via a standard 9V battery and zenner diode circuit to reduce IC loading and improve circuit reliability.
- Reduce circuit complexity by amalgamating the Power-On-Reset function with External Power function

Both of these suggestions are incorporated in the second prototype and provide a more user friendly prototype by reducing complexity and improving reliability.

8.2.3 Power Supply

- Relocate the power interruption switch onto the tracker board.

The original design required an external jumper to power the board. This design provides a hard wired switch and further simplifies the design.

8.2.4 Oscillator

- Change oscillator package from DIP to Ball Grid Array (BGA) to produce a physically low profile and eliminate the socket arrangement.

The adoption of this recommendation provides greater reliability for the device as the BGA is a surface mounted package. The elimination of a socket and the DIP package reduces the vertical dimension from 12mm to only 3mm. Again Dallas Semiconductors provided two precision oscillators in the BGA36 package at no cost[6].

---

[6] Dallas Semiconductors provide a limited number of components as samples for evaluation purposes only. Samples can be requested via their web site http:/www.maxim-ic.com.

8.2.5 Accelerometer

Two improvements were identified during the evaluation of the accelerometer circuit, the first to improve the static resolution and the second to improve the dynamic response.

- Select a more sensitive accelerometer to increase the output resolution.
- Provide a method to cancel the dynamic error caused by acceleration employing a hardware design feature such as an improved low pass filter.

8.2.5.1 Accelerometer resolution improvement

Investigations were conducted to replace the ±10G MMA6233Q two axis accelerometer with device capable of providing a higher resolution for the ADC. Freescale produce a range of accelerometers that are suitable for this purpose. A ±1.5g two axis accelerometer was selected, the MMA6260 which is available in the same footprint, package and pin out as the MMA6233Q making the utilisation of this device a straight forward replacement with no circuit modifications necessary. Freescale were again contacted and two sample MMA6260 accelerometers obtained at no cost[7].

8.2.5.2 Accelerometer improved low pass filter

Given the design already includes a low pass filter on the output the approach was to expand the properties of the filter to include unwanted acceleration disturbances, effectively damping the response. The unmodified corner frequency f_c calculated using equation 7.3 produced a response of 1600Hz. By adjusting the values of the capacitor and resistor network a damped response can be achieved. Values of 10KΩ and .1uF were selected as an initial starting point giving an expected corner frequency using equation 7.3 of 160Hz. By reducing the corner frequency the device will be less affected by sudden changes in acceleration by being effectively dampened, producing a smoother output response. The procedure of determining a suitable corner frequency will be through trial and error and using a degree of judgment in the selection. To assist in the selection the filtering components R70X, R70Y, C70X and C70Y are located on the edge of the PCB for ease of replacement.

[7] Freescale Semiconductors provide a limited number of sample components for evaluation purposes. The samples are requested on line at http:/www.freescale.com and are dispatched almost immediately, arriving from overseas within a week.

8.2.6 Magnetoresistive

- Update drawings and design to reflect component pin out of HMC1053 magnetoresistive sensor.

The circuit schematics were altered to reflect the correct pin configuration and the PCB updated with the new routing topology.

8.3 Construction of Prototype No.2

The improved schematics were again modified and processed using Protel 2004DXP to obtain PCB output files for manufacture. The construction process was very similar to that described in Chapter 6 for the first prototype. The three new boards were successfully etched by FoES workshop technicians and supplied predrilled and cut to shape.

- Communications Board
- Data logger and
- Sensor

The boards were once again populated using the techniques listed in Table 19. As the instrument is now constructed of multiple PCB layers some additional spacers and fine thread setscrews were used to assemble the unit. The assembled instrument and communication board is shown in Figure 35 and 36 respectively. The next phase was to repeat another round of electronic evaluation and determine the effectiveness of the modifications and overall function of the instrument and communications boards.

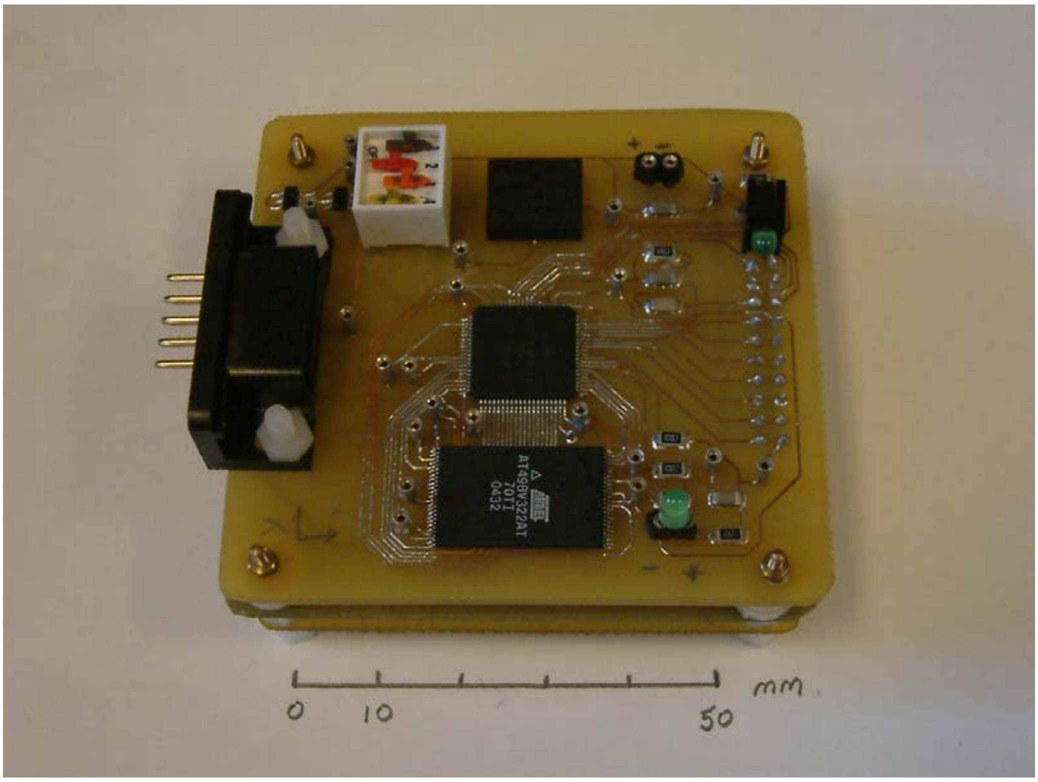

Figure 35 Instrument Prototype No.2. The second prototype is constructed of two PCBs connected by a pin header. To reduce noise a ground plane is also inserted between upper and lower boards.

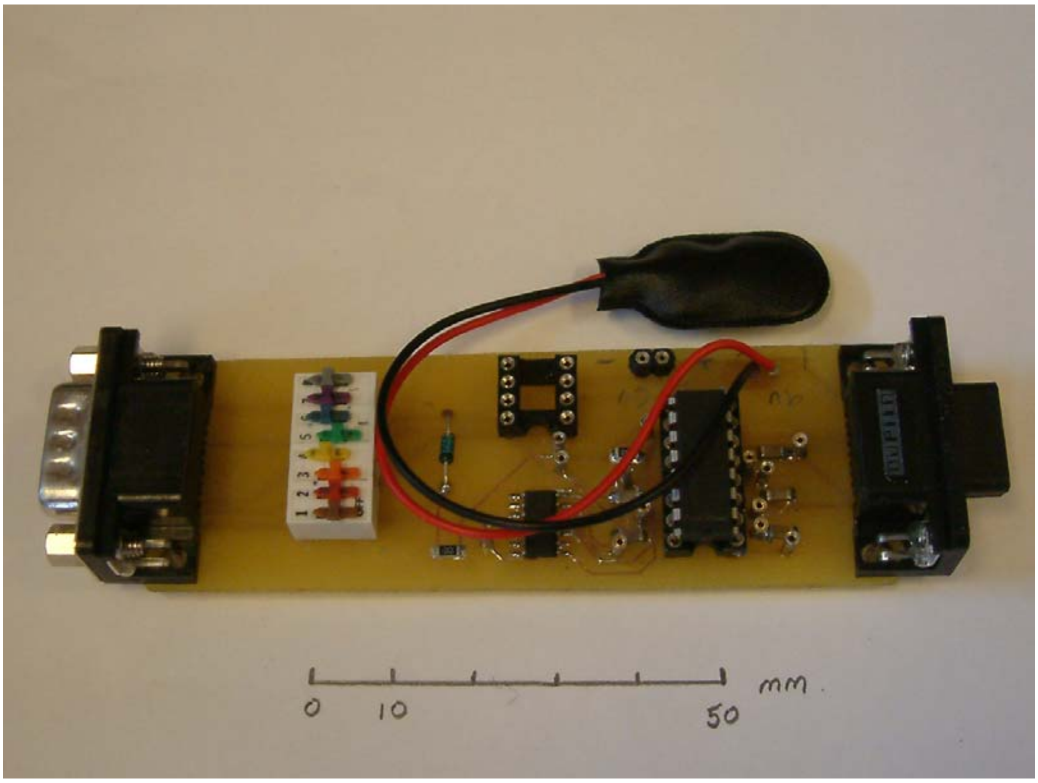

Figure 36 Communications Board, second prototype. The communications board is a simple arrangement using DB9 connectors at either end of the board. The connectors are polarised to prevent incorrect connection.

Chapter 9 Prototype No.2 Evaluation.

9.1 Prototype Evaluation Methodology.

The evaluation of the second prototype focussed on several areas

1. The electrical characteristics of the circuit modules compared with the circuit schematics
2. The effectiveness of any modifications made as improvements
3. The overall functionality of the circuit boards

In many respects the evaluation followed the procedure outlined in Chapter 7 and was conducted on a module by module basis beginning with an overall physical inspection.

9.2 Physical Inspection

The second prototype differs from the first in that it is not of monolithic construction. The inspection of the individual data logger, sensor and communications boards in conjunction with the objectives of section 7.2 raised no adverse findings. The fundamental construction of the prototype, using header pins and sockets to connect the data logging board with the sensor board, appears successful and a good connection appears to be achieved. Some force is required to mate the connector which indicates a solid connection. Having successfully passed the visual inspection the instrument was assembled as shown in Figure 35. The communications board was then connected to the instrument via a cable and also interfaced to a PC using an RS232 connection. A regulated 3.6V d.c was then applied to the communications board which in turn supplies the instrument.

9.3 Electrical Modules

Following on from the physical inspection each circuit module was tested electrically using a combination of oscilloscope and digital multimeter to assess the performance of the electronic components against the design schematics.

9.3.1 Communication Board

The communications board was inspected and voltages commensurate with the expected values derived from the circuit schematic observed. The 9MHz oscillator was examined by oscilloscope and found to be functioning in accordance with the data sheet specification. Communications was then established with the microcontroller indicating correct operation of the board.

9.3.2 Power Supply

Voltages were tested on the instrument and returned identical values recorded in section 7.3.2. The power supply interrupt switch on the instrument was tested and interrupt achieved.

9.3.3 Microcontroller

With communications established between the instrument and a PC the modules of testing code contained in Appendix D were again used to confirm the operation of the microcontroller. No problems were detected in the operation of the microcontroller.

9.3.3 Memory

The tests used in section 7.3.4 were again employed with success. The external Atmel flash memory was accessed by the microcontroller with read/write operations proven.

9.3.4 Oscillator.

The new ball grid array package provided by Dallas Semiconductors was tested by oscilloscope and complied with data sheet specifications. The low profile component represents a major improvement in reliability over the earlier design using a DIP socket and package.

9.3.5 Accelerometer

The evaluation the 1.5g accelerometer was approached in the same manner as the previous 10g device. The accelerometer was tested using the same principles of 'static' and 'dynamic' testing described in sections 7.3.6.1 and 7.3.6.4.

9.3.5.1 'Static Testing' Regime

The results of static testing are produced in Table 20 and reflect the anticipated design specification and that of the component data sheet.
A small offset voltage is observed in both the *x* and *y* axis responses.

Table 20 The results of Static testing of the MMA6260

	X Output	Y Output	Expected	Difference X/Y
+90° rotation	2.40	2.425	2.45	-0.05/-0.025
0° rotation	1.60V	1.625V	1.65V	-0.05/-0.025
-90° rotation	0.80	0.825	0.85	-0.05/-0.025

9.3.5.1 Static resolution

The expected output resolution of the MMA6260 with the application of ±1g (±90° rotation) is quoted as ±800mV compared with the MMA6233Q range of only ±120mv. Applying equation 7.1 produces an anticipated resolution of $R_{\pm 90} = 5.3°$ for angles near ±90° and using equation 7.2 errors in the order of $R_{\pm 0}$ = 0.25° for angles near 0°. Amalgamating equations 7.1 and 7.2 produces the general form of the static resolution equation for both pitch Φ and roll Θ the accelerometer, equations 9.1 and 9.2 respectively. (Φ and Θ are calculated later using the equations provided in section 11.3)

$$R_{\Phi S} = 5.3\sin(\Phi) \tag{9.1}$$

$$R_{\theta S} = 5.3\sin(\Theta) \tag{9.2}$$

9.3.5.2 'Dynamic Testing' Regime

'Dynamic testing' was again performed by holding the instrument by hand and moving the unit around whilst observing the accelerometer response on the oscilloscope.
The behaviour of the accelerometer response was immediately evident. The damping of the output using a corner frequency of 160Hz calculated in section 8.2.5.2 was not sufficient as the ±1.5g accelerometer is much more sensitive to vibration and movement (accelerations). A range of low pass filters were trialled and the responses recorded in Table 21 along with the expected static resolution calculated in section 9.3.5.1 allows a comparison of different filtering combinations. The dynamic errors are independent of the static errors.

Table 21 Low pass filter combinations and response to dynamic testing of accelerometer.

Trial No.	Resistor R kΩ	Capacitor C µF	Voltage ΔR_{ADC} V	f_c Hz	Time Constant RC s	Error Eq.7.1	Error Eq.7.2
1	10	0.1	0.1	160	.001	29°	7.2°
2	100	0.1	0.01	16	.01	**9°**	**0.7°**
3	100	1.0	0.001	1.6	.1	3°	0.07°
Static	-	-	-	-	-	**5.3°**	**0.25°**

Examining Table 21 indicates trial No.3 as being the best filtering solution providing the least error due to unwanted accelerations. However the time constant RC, for this combination is in the order of 100ms demanding the sensor circuit be allowed at least twice this long (rise time = 2.2RC) to stabilise before measurements can be made which increases instrument power consumption. To reduce the power consumption a compromise was achieved by adopting the filter used in Trial No.2 delivering a corner frequency of 16Hz and a time constant of 10ms. This level of filtering seems a reasonable figure for such a large marine mammal whilst reducing power consumption.

9.3.5.3 Dynamic Resolution

The dynamic resolution of the device is given by equations 9.3 and 9.4 and calculated using the same method to derive equations 9.1 and 9.2

$$R_{\Phi D} = 9\sin(\Phi) \tag{9.3}$$

$$R_{\theta D} = 9\sin(\Theta) \tag{9.4}$$

Variation due to noise can be further reduced by engaging sampling techniques (simple averaging) in software using a sampling frequency at least twice the corner frequency f_c. Digital sampling is used to reduce the interference and improve the overall resolution to the static resolution figures of $R_{\pm 90}$ = 5.3° for angles near ±90° and $R_{\pm 0}$ = 0.25° for angles near 0° as derived from subsection 9.3.5.1.

9.3.6 Magnetoresistive Stage

V_{CC} supply was provided to the magnetoresistive device and associated operational amplifier circuit. The sensor board was rotated by hand through the three axis sensed by the magnetoresistive device (*x,y,z*) to determine the limits of the operational amplifier outputs *Z*,X** and *Y**. The output from the operation amplifiers were recorded using a Fluke 77 Series II digital multimeter and are reproduced in Table 22.

Table 22 Voltage measurements of the magnetic field sensing circuit. The applied voltage was 3.4V and the mid rail voltage was 1.7V.

		Z*	X*	Y*
Maximum	V	1.85	1.78	1.55
Minimum	V	1.77	1.7	1.47
Range	V_{pp}	0.08	0.08	0.08
Voltage Offset	mV	115	40	-190

9.3.6.1 Offset Voltage Error

The results shown in Table 22 indicate the output offset voltages varied substantially from the biased mid-rail of 1.7V. In the magnetic sensing circuit there are two possible contributors to offset voltage

1. the characteristics of the operational amplifier
2. unbalanced magnetoresistive bridge circuit

The offset voltage specifications of the LMV358 operational amplifier ranges from 2 to 7mV, the error at the output terminal is calculated by the offset multiplied by the gain A_v, in this configuration A_v =100. The maximum offset permissible whilst remaining within specification is ± 700mV. To determine the component of the offset voltage attributable to the operational amplifiers the input terminals were tested by grounding and the output measured by oscilloscope. The testing revealed the offset from the *x* and *y* amplifiers were caused primarily by the offset error intrinsic to the LMV358 operational amplifier with some small variation attributable to *x* and *y* bridge element imbalance. The output offset of the *z* axis was found to be a mostly caused by unbalanced bridge impedance with a small component due to the LMV358.

9.3.6.2 Magnetic Resolution and Voltage Output.

To calculate the magnetic bearing Ψ in the horizontal plane the measured magnetic field strengths Y_h and X_h are substituted into equation 9.5.

$$\Psi = \arctan\left(\frac{Y_h}{X_h}\right) \qquad (9.5)$$

The instrument provides 80mV of change for 180° of rotation, dividing by the ADC step resolution of approximately 3.5mV results in approximately 22 ADC steps. The minimum ADC change is 1. This implies that the ratio of change is 1/22, substituting into equation 9.5 for Y_h/X_h produces a resolution of 2.6˚ according to the method used by Caruso (2004).

To improve the resolution of the device to better than 1˚ the gain of the amplifier circuit needs to be increased by a factor of 3. To increase the gain the ratio of resistors biasing the operational amplifiers needs to be modified. To increase the gain from 100 to 300, 6 matched resistors were changed in accordance with equation 4.2 and Figure 21. Accepting increased offset errors due to the increased gain would require further circuit modifications to correct; a more structured testing regime was embarked upon as described in Chapter 10 to define the extent of correction required.

9.4 Energy Budget

The instrument was calculated in subsection 3.2.3, as being able to record 4 million bytes of information. If calculated with a sampling period of 10 sec that produces approximately 2400 hours of positional data (100 days).

To determine the capacity of the lithium battery required the functional circuits were analysed and the results recorded in Appendix F. From that investigation the average current consumption of the instrument is 0.9mA. Even though this is a small supply figure there is still opportunity to reduce the current consumption by individual switching of the accelerometer and magnetoresistive circuits, reducing the voltage across the magnetoresistive bridge and refining the operating code to maximise savings.

The capacity of the battery required to supply the instrument is calculated by multiplying the average current in milliamperes by the time the instrument is required to operate for. In this case the minimum capacity required is 2100mAh. Lithium Thionyl Chloride batteries are available with a rating of 2300mAh in a AA size which would be sufficient. However to provide a measure of safety using the next size up, a C size cell which carries with it a rating of 8500mAh providing a four fold safety margin.

9.5 Conclusions: Prototype No.2

Having successfully designed and constructed a data logger capable of measuring and storing measurements of gravity and the earth’s magnetic field the attention now turns to discovering the quality of the data the device is producing. To achieve this goal a systematic progression of experiments was conducted and the data analysed.

Chapter 10 Instrument Performance

10.1 Why Performance Testing

The developed prototype No.2 is designed to measure the position of the device relative to the earth's magnetic field and the force of gravity. The instrument uses an accelerometer and a magnetoresistive sensor to detect those quantities and present the measurements as a voltage output. The voltage output in turn is read by the microcontroller via an analogue to digital converter and the result stored as data for later conversion into magnetic bearing Ψ and angles of roll Θ and pitch Φ.

How the device achieves this result is of little concern to the end user, the biologist. What is of concern to the biologist is the accuracy of the device, defined as a quantifiable measure of error so that data can be given some degree of significance. In addition to an estimate of error other factors influencing the quality of the retrieved data needs to stated clearly to provide a contextual framework for the appropriate use of the device.

10.2 Testing Methodology

The prototype having reached a stage where the electrical circuits are capable of producing data from all sensors allows the testing of the device to extend beyond the oscilloscope and digital multimeter into the realms of data recording and subsequent analysis. However a few important assumptions need to be stated when experiments in the laboratory are aimed at predicting the performance of an instrument in the field.

The first assumption made was the reference quantities of magnetic field strength and gravity are constants and the results of laboratory testing will be valid under deployment conditions.

This assumption recognises both quantities may vary depending on geographical location. Certainly considering the instrument may travel several thousand kilometres during the course of deployment it is reasonable that the magnitude of output from instrument sensors will vary over the course of deployment and may require treatment when analysed.

The second assumption was that 'static testing', taking measurements with the instrument stationary, provides a useful measure of the dynamic performance of the device.

This second assumption recognises the limitations in accurately recreating the environment of the device in actual service, on a moving platform, but is a reasonable assumption to make given damping of the accelerometer has been considered. Accepting these two assumptions, an experimental design was constructed to facilitate gathering data by adjusting the prototype relative to magnetic north and gravity in a controlled manner.

10.3 Experimental Design

A factorial design was chosen to explore the response variables and to confirm outputs of the instrument being sinusoidal waveforms of varying magnitude based on the factor of relative position of the instrument. The design identified factors and response variables in the system and accepted the coordinate system offered in Figure 10 to provide the three dimensional perspective and define the x, y and z planes.

The response variables were identified as voltage outputs from both

- The magnetoresistive device, X^*, Y^* and Z^* and
- The accelerometer, pitch X^{Φ} and roll Y^{Θ}.

The factors were classified into two main groups

1. Factors considered as constants. The magnetic field strength components relative to the (x,y,z) planes and the force of gravity in two axis (x,y).
2. Factors considered as being variable. In this case the angle of rotation ω of the instrument relative to the earth's magnetic field and gravity.

This resulted in an experimental design with only one factor, the angle of rotation of the instrument ω, with multiple response variables X^*,Y^*,Z^*, X^{Φ} and Y^{Θ}. This concept is shown graphically in Figure 37.

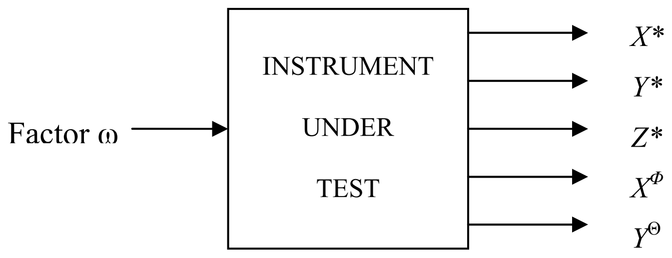

Figure 37 The basic concept of a factorial design, in this case the system is reduced to one factor and five response variables. The assumption made under this design is that the factors and response variables are independent of each other.

Using this design required careful consideration given Greenwood (2002) cautions the use of an experimental approach where only one factor is varied and the responses observed. The danger in this design is that possible interactions between factors and response variables may not be fully explored. To address this concern the schematics and data sheets were examined and indicated sensors act independently from each other but have common circuit connections such as power supply. Therefore additional experimental evaluation was required to ensure sensor independence. Experiment 9 and Experiment 10 permitted exploration of sensor independence by monitoring isolated variables whilst changing the independent variable. This confirmed the schematic analysis that sensors act independently and rejected interactions from other sensors. The principles of factorial design are described by Atkinson and Donev (1992) in Chapter 7, and the use of empirical methods when modelling discussed by Box et al. (1978) Chapter 10.

10.4 Testing Environment

The sensors employed by the tracker are sensitive to both acceleration and magnetic disturbances. In order to limit unwanted effects of these quantities and to lessen the effects of electromagnetic noise the following procedures were developed.

- Controlling the testing environment. All magnetic materials, ferrous tables, chairs and other equipment were excluded in a >1m radius from the instrument under test. Electrical equipment was distanced from the device with only essential power and communications cables permitted using screened cables where possible. To reduce any acceleration due to vibration the device was securely attached to the surveyor's sight using cable ties and insulation tape.
- An apparatus set up procedure was developed to provide a repeatable method of conducting experiments and is described in Appendix E.

At the completion of the set up procedure the surveyors' sight shown in Figure 38, was set at 0° on the incremental ring and the experiments conducted. Response variables were recorded manually by observing the microcontroller registers and entering the response in an XL spreadsheet.

After each recording was taken the surveyors sight was indexed 10° CW using a precision thumb wheel on the sight. The process continued until 350° was reached indicating a full set of observation of the selected response variable over a range of 360˚.

The orientation of the surveyors sight shown in Figure 38 permits the response variables of magnetic field strength X^* and Y^* to be explored, as the magnetic sensors for the *x* and *y* axis are sensitive to rotation in this configuration.

Figure 38 Attaching the instrument to the surveyors sight permitted accurate rotation, strengthening the repeatability of the experimental method. The graduation ring seen at the bottom of the sight is marked with 1˚ increments with experimental measurements taken at 10˚ intervals.

To explore the magnetic response Z^*, and the accelerometer responses to gravity X^{Φ} and Y^{θ} the surveyors' sight was placed horizontally to allow measurements of magnetic *z* axis and pitch and roll to be determined.

10.5 Experiment No.1.

The aim of Experiment 1 was to observe the magnetoresistive response variables X^*, Y^* and Z^* when the instrument was rotated in the horizontal plane and to explore the repeatability of the device using two identical trials (two rotations).

The two trials were conducted by rotating the instrument in 10˚ steps and the results graphed as illustrated in Figure 39.

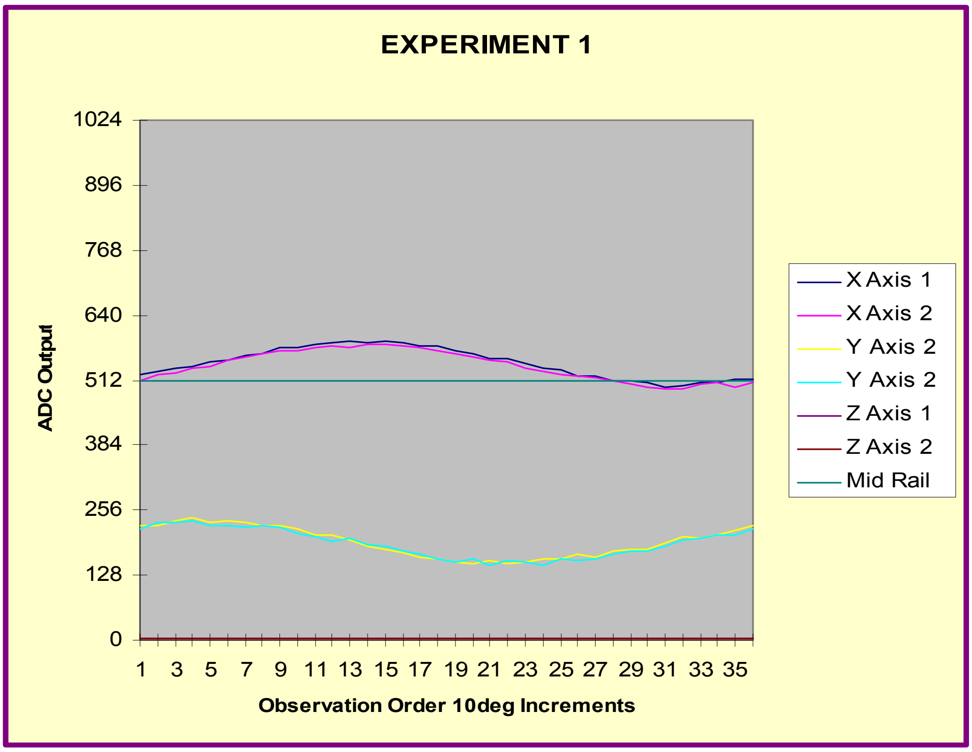

Figure 39 Magnetic sensor output from *x,y* and *z* sensors with mid rail included. The graph shows substantial offset in the *y* sensor output with the *z* sensor response = 0. The experiment was conducted twice hence the data are labelled '1' and '2'. The difference between readings indicates the presence of noise in the circuit.

The results of the exploratory experiment indicate two main areas of interest, namely:

1. The offset present in the output of the *x, y* and *z* axis amplifiers
2. Variation between experimental runs

10.5.1 Error due to amplifier offset

Amplifier offset error moves the waveform closer to the top or bottom rails where clipping can occur. To improve the operational amplifier offset and reduce the chance of clipping a precision amplifier was selected, the Maxim 478 Operational Amplifier in an identical package as the LMV358. With an input offset voltage specified as 40-70uV the maximum expected offset in the output with a gain of 300 is 12mV. Dallas Semiconductors were contacted and two MAX478 precision operational amplifiers obtained as samples and installed.[8]

10.5.2 Adjusting sensor offset

Figure 39 indicates no modulated output from the *z* axis amplifier. This was primarily due to resistive imbalance detected in one leg of the Wheatstone bridge sensor. This imbalance produced a sufficient magnitude of input offset voltage to the differential amplifier which has in turn driven the amplifier to the bottom rail (0V).

To correct bridge offset in the *z* axis sensor two methods were available,

1. resistance trimming of the Wheatstone bridge elements
2. applying offset nulling to the operational amplifier mid rail voltage

Offset nulling was selected due to component access for modification. To achieve offset nulling, the voltage divider circuit that provides the mid rail reference for the operational amplifiers was modified to change the reference voltage by just a few millivolts. This increase opposes the offset from the Z^* bridge cancelling the effect. The nulling was achieved by selecting voltage divider values of 1004Ω and 995Ω from amongst a selection of 1k Ω 1% resistors and brought the Z^* response within the detectable range of the ADC. This exercise highlights the need to have individual offset adjustment on all magnetic field sensing amplifiers.

10.6 Determining magnetic resolution

From the experiment No.1 data the response range of X^* and Y^* was determined to be approximately 80 ADC steps for 180˚ of rotation. Applying equation 9.5 with a ratio of

[8] Dallas Semiconductors provide a limited number of components as samples for evaluation purposes only. Samples can be requested via their web site http:/www.maxim-ic.com.

1/80 the expected bearing resolution of the instrument is found to be 0.71˚. This is compared with the resolution of 2.6˚ before the gain was increased from 100 to 300 as discussed in section 9.3.6.2.

10.7 Determining the variability in the responses

Data observed from Experiment No.1 and seen graphically in Figure 39 indicates unexplained variability. Where data variation exists John and Quenouille (1977) suggest applying experimental replication sooner rather than later to quantify and describe the variation. The importance of variation can not be overstated as it lies at the centre of determining repeatability, accuracy, discrimination and reliability of the gathered data.

Accordingly the data from Experiment No.1 was analysed to produce a simple stick histogram of the variability between trial readings and is shown in Figure 40. The data from Experiment No.1 suggests average variation between readings for both the *X** and *Y** readings is approximately 6 ADC steps and the most variation between readings was found to be 15 ADC steps.

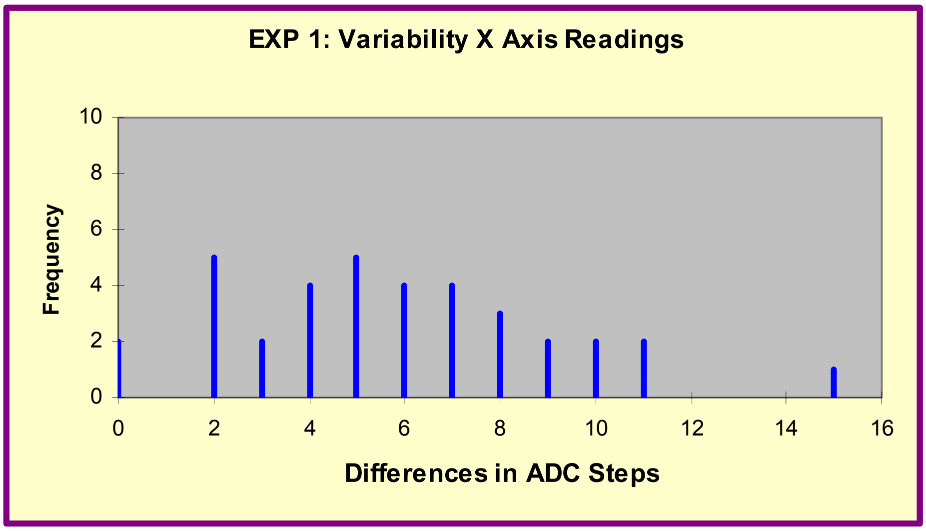

Figure 40 The variability between *x* axis trials is substantial, the average variation is 5.8 ADC steps, this represents a voltage difference of approximately 20mV and the worst case is 15 ADC steps which is equivalent to around 52mV.

Examining Figure 40 shows the variation between readings to be gross and of substantial magnitude. A series of experiments were then conducted to examine noise in the system and to monitor the effect of changing experimental conditions.

10.8 Experimental Investigation[9]

Experiment No.2 involved rotating the instrument through 360˚ in the horizontal plane using the apparatus shown in Figure 38 and the method described in Appendix E. Measurements were taken of the *X** and *Y** magnetic field strength using the microcontrollers ADC at 10˚ intervals. Hence a sinusoidal response was expected with *X** and *Y** in quadrature. The experiment was repeated 3 times and the results compiled to produce Figure 41 with offset removed for clarity and convenience

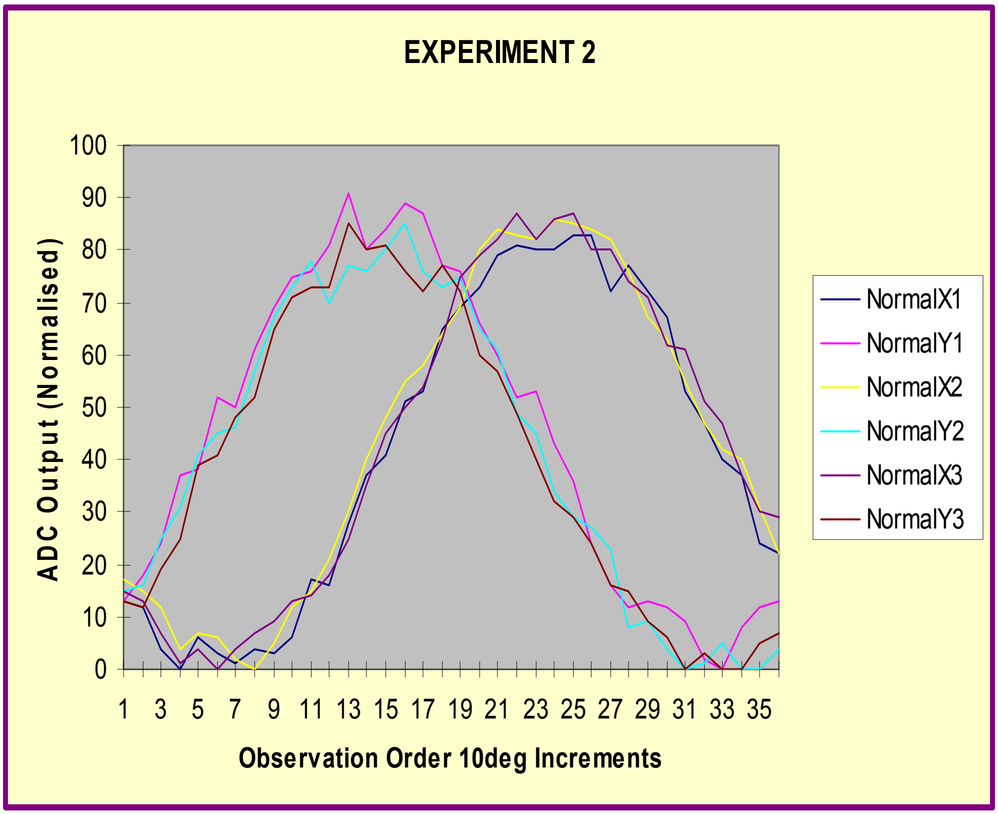

Figure 41 Variation between three experimental runs of *X** and *Y** magnetic ADC readings. The general shape is similar to Figure 13 showing the 90˚ phase difference between *X** and *Y** magnetic readings and the general sinusoidal waveform in quadrature as expected.

The variation between readings seen in Figure 41 is marked and from the graph there appears to be no obvious pattern to the variation. This is highly indicative of noise being injected in the system and has severely degraded the quality of the data. Applying a statistical treatment to quantify the variation produced plots of standard deviation for

[9] To be chronologically accurate, electrical testing was conducted next to determine the source of the variation in the *X** and *Y** response and is described in section 10.11

both X^* and Y^* readings as shown in Figures 42. and 43. The homogeneity of the variation is evident in the plots, there seems to be no systematic pattern to the noise. This suggests the noise is equally distributed across the full range of rotation and is therefore independent of device orientation.

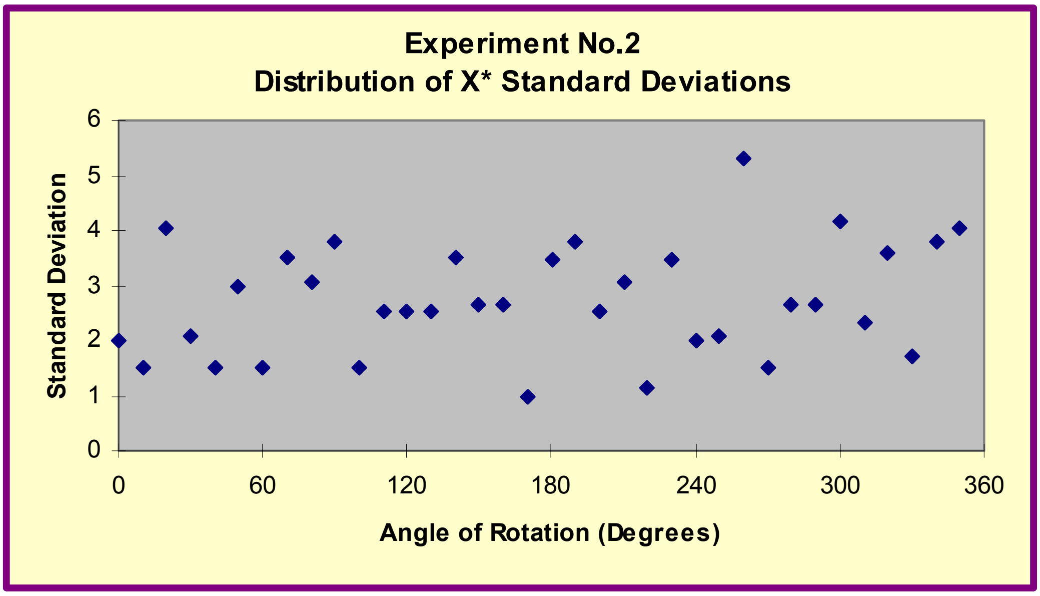

Figure 42 Each point represents the standard deviation of three x axis readings X^* taken at 10° increments over a full 360° rotation.

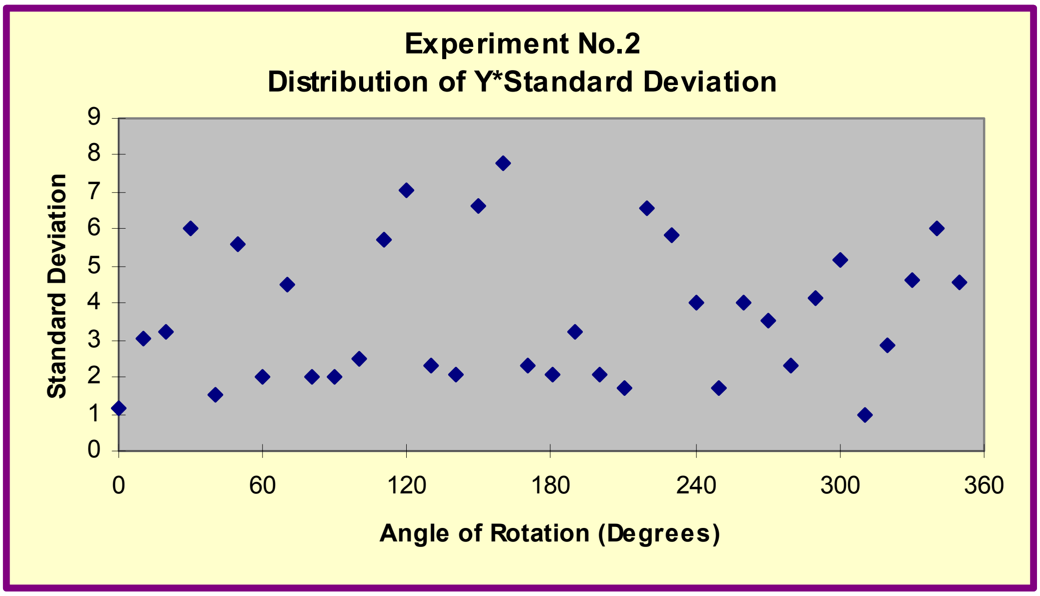

Figure 43 Each point represents the standard deviation of three y axis readings Y^* taken at 10° increments over a full 360° rotation.

10.9 Determining sources of variation

In an effort to define factors contributing to the noise a series of experiments were conducted. The experiments followed the form were suspected sources of noise were identified and then changed or removed whilst observing the response. The results of those experiments are given in Table 23 and the data recorded in Appendix E.

Table 23 Experiments to determine factors contributing to variation in response.

Experiment	No.1	No.2	No.3	No.4	No.5	No.6
3.5V Power Supply	✓	✓	✓	✓	✓	
9MHz Oscillator	✓	✓	✓			
3.6V Battery Operated						✓
Set/Reset Used.			✓	✓	Incomplete Set/Reset	✓
Max ADC Variation X, Y	11, 13	10, 15	9,8	6,9	NA	2,2

The results of experiments No.1 to No.6 indicate measurable sources of interference. Experiment No.5 involved applying only a Set pulse to the magnetoresistive device. This resulted in a severe degradation of the sensitivity of the device as evidenced by a reduction in output magnitude. The experiment indicated sensor conditioning should be done using both the Set and Reset pulse and reaffirms the importance of refreshing. Magnetic conditioning also reduces cross axis effect as described by Pant and Caruso (1996) which impacts as a minor error in magnetoresistive devices.

Experiment No.6 produced the best result when the device was battery operated and the magnetic sensors conditioned using the Set/Reset circuit. When deployed, the instrument will be in the lowest variation configuration, battery operated with regular conditioning of the magnetic sensors producing data quality as shown in Figure 44.

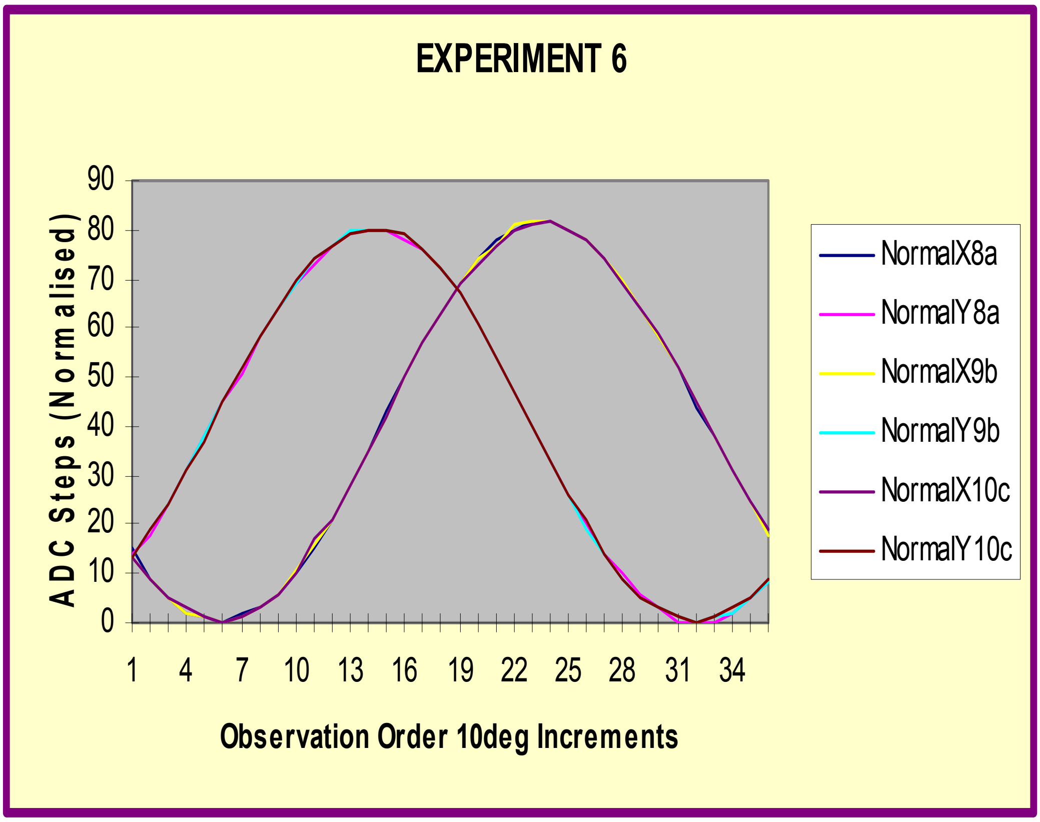

Figure 44 Data obtained by the instrument with external sources of noise removed. The readings demonstrate the quality of data obtainable and offer an insight into the repeatability of the instrument. The improvement in data quality is evident when compared with Figure 41.

10.10 Determining repeatability of readings

A quantification of the variation in the data was conducted by subjecting the instrument to four further experiments No.7, 8, 9 and 10. The results are tabularized in Appendix E. By examining the residual differences between measurements a statistical treatment can be applied to quantify the variation and results in the following standard deviations. The units of standard deviation are ADC steps derived from a sample size of $n = 36$.

- Accelerometer X^{θ} SDs = 0.63
- Accelerometer Y^{Φ} SDs = 0.38
- Magnetoresistive X* SDs = 0.61
- Magnetoresistive Y* SDs = 0.56
- Magnetoresistive Z* SDs = 1.61

The results indicate the repeatability of the device is similar with the exception of *Z** which is elevated due to the lower magnitude of that magnetic component.

10.11 Electrical Investigation into Noise

The usual expression describing variation in an electronic system is noise and described by Ott (1988) as being unwanted signal components. When looking for sources of noise in an instrument that principally relies on amplification of small signals the usual response is to examine the sensitive input side of the amplifiers. Taking the greatest output variation between readings from Figure 40 of 52mV (15 ADC steps at 3.5mV/step), then dividing by the gain factor of 300, results in noise referred to the amplifier inputs in the order of 173µV. This calculation provides the order of the noise and a starting point for investigation. An examination of the power supply circuit discovered approximately 10mV_{pp} of high frequency noise emanating from the bench top power supply. As the bridge circuit is ratio metric by design this could equate to, at most, a change in the differential voltage of 2µV_{pp}, compared with the required 173µV of noise. This eliminates the likelihood of noise being introduced from the effects of power supply ripple on the magnetic sensor elements. Considering the effects of power supply ripple on the operational amplifiers was the next step. Applying 10mVpp to the operational amplifier, given a Power Supply Rejection Ratio (PSRR) of around 20dB for high frequency components arrives at an error of 1mVpp at the output, still only around 1/3 of an ADC step. So the variation exhibited in experiment is unlikely to be caused by the power supply ripple.

However when the communications module was included in the tests a voltage of 0.4Vpp at high frequency was detected by the oscilloscope on the power supply to the tracker. This magnitude of interference when applied to the amplifiers, and considering PSRR, would produce an error of approximately 40mV in the output response. This is commensurate with the variation observed in Experiment No.1 and seen in Figure 40. This assessment is also confirmed by results given in Table 23.

Chapter 11 Interpreting the Data

11.1 Output from instrument

Combining the raw ADC sensor data from the experiments produces Figure 45 and clearly shows the offsets present in the design. Ideally all sensor data would be symmetrical about the mid rail voltage which coincides with midpoint of the ADC range.

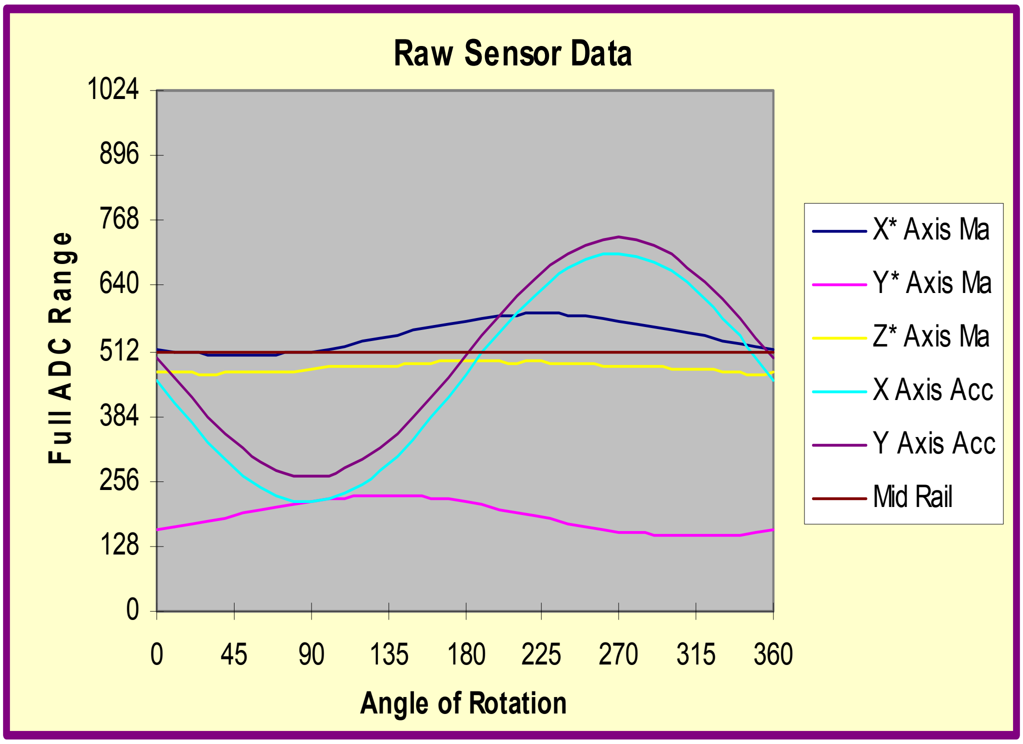

Figure 45 Collating ADC inputs graphically demonstrates the effectiveness of the design. Offset is evident in all sensors, provided the sensors do not make excursions too close to the top or bottom rail clipping will not occur and the data will be complete.

The magnetoresistive device is very sensitive to external magnetic fields and natural anomalies which can also produce an offset in either direction. Accordingly it would be sensible ensure the offset is adjusted to a minimum state centred about the mid rail voltage in the first instance. This would provide the maximum margin of safety and could be accomplished by inclusion in the design of individual magnetic sensor offset nulling as set out in subsection 10.5.2.

11.2 Determining heading from the data.

The output from the accelerometer and magnetic sensor provide the information necessary to construct magnetic bearing relative to magnetic north. The components of the magnetic field are represented in Figure 46

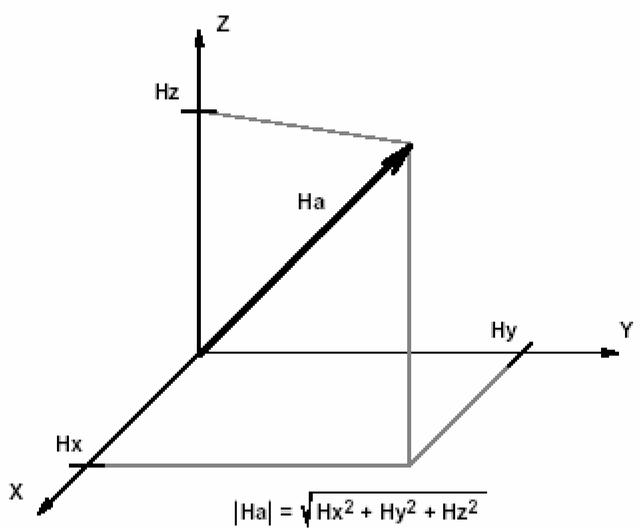

Figure 46 Diagrammatic representation of the components of magnetic field detected by the instrument and the relationship to the horizontal plane. AN200 (1996)

The process of determining magnetic bearing relative to north Ψ in degrees relies on the trigonometric relationship between the magnetic components Y_h and X_h taken in the horizontal plane (with roll angle Θ = 0 and pitch angle Φ = 0) and can be found by applying equation 9.5, reproduced here for convenience.

$$\Psi = \arctan\left(\frac{Y_h}{X_h}\right) \tag{9.5}$$

As equation 9.5 has defined limits (arctan), consideration must be given to the returned sign of X_h and Y_h in accordance with equations 11.1 to 11.5, following.

Conditional heading Ψ in degrees for

$$\Psi = 180^\circ - \arctan\left(\frac{Y_h}{X_h}\right) \qquad \text{for} \qquad (X_h < 0) \tag{11.1}$$

$$\Psi = -\arctan\left(\frac{Y_h}{X_h}\right) \qquad \text{for} \qquad (X_h > 0,\ Y_h < 0) \tag{11.2}$$

$$\Psi = 360^\circ - \arctan\left(\frac{Y_h}{X_h}\right) \qquad \text{for} \qquad (X_h > 0,\ Y_h > 0) \tag{11.3}$$

$$\Psi = 90^\circ \qquad \text{for} \qquad (X_h = 0,\ Y_h < 0) \tag{11.4}$$

$$\Psi = 270^\circ \qquad \text{for} \qquad (X_h = 0,\ Y_h > 0) \tag{11.5}$$

Allowing the instrument to be at any angle of pitch or roll it is necessary to use all of the sensor information to arrive at the bearing.

From the accelerometer: the calculated roll and pitch in degrees

- Roll angle Θ
- Pitch angle Φ

From the magnetoresistive device: magnetic field strength relative to the instrument orientation

- Magnetic field strength X^*
- Magnetic field strength Y^*
- Magnetic field strength Z^*

Converting the readings into the horizontal plane using equations 11.6 and 11.7 as correction factors.

$$X_h = X^*\cos(\Phi) + Y^*\sin(\Theta)^*\sin(\Phi) - Z^*\cos(\Theta)^*\sin(\Phi) \tag{11.6}$$

$$Y_h = Y^*\cos(\Phi) + Z^*\sin(\Theta) \tag{11.7}$$

We then apply equation (9.5) and arrive at the magnetic bearing Ψ in degrees.

11.3 Determining Pitch and Roll from the data

The instrument produces two ADC readings from the accelerometer X^{Φ} and Y^{Θ} which are used to determine the pitch angle Φ and roll angle Θ. The accelerometer if smoothly rotated will trace a sinusoidal response curve (neglecting quantization) evident in Figure 45. To convert the ADC readings to an angle the sinusoid needs to be modelled. To do this the maximum and minimum ADC values for each X^{Φ} and Y^{Θ} are required in order to determine the peak to peak value and then determine the amplitude component of the sinusoid. Once determined, equations 11.8 to 11.10 can be used to determine the pitch angle Φ and equations 11.11 to 11.13 to determine roll angle Θ.

11.3.1 Determining pitch angle Φ

To determine the pitch angle Φ the following steps are taken

Given:

X^{Φ}_{Max} = Maximum ADC value
X^{Φ}_{Min} = Minimum ADC value
X^{Φ} = ADC Reading

Determine the amplitude of the sinusoid using equation 11.8

$$X^{\Phi}_{Amp} = \left(\frac{X^{\Phi}_{Max} - X^{\Phi}_{Min}}{2} \right) \tag{11.8}$$

Determine the midrange ADC value using equation 11.9

$$X^{\Phi}_{Mid} = \left(\frac{X^{\Phi}_{Max} + X^{\Phi}_{Min}}{2} \right) \tag{11.9}$$

Determine the angle of pitch Φ determined from the *x* axis component of the accelerometer using equation 11.10.

$$\Phi = \arcsin\left(\frac{X^{\Phi} - X^{\Phi}_{Mid}}{X^{\Phi}_{Amp}} \right) \tag{11.10}$$

11.3.2 Determining roll angle Θ

To determine the roll angle Θ the following steps are taken

Given:

Y^{Θ}_{Max} = Maximum ADC value

Y^{Θ}_{Min} = Minimum ADC value

Y^{Θ} = ADC Reading

Determine the amplitude of the sinusoid using equation 11.11

$$Y^{\Theta}_{Amp} = \left(\frac{Y^{\Theta}_{Max} - Y^{\Theta}_{Min}}{2} \right) \tag{11.11}$$

Determine the midrange ADC value using equation 11.12

$$Y^{\Theta}_{Mid} = \left(\frac{Y^{\Theta}_{Max} + Y^{\Theta}_{Min}}{2} \right) \tag{11.12}$$

Determine the angle of pitch Θ determined from the *y* axis component of the accelerometer using equation 11.13.

$$\Theta = \arcsin\left(\frac{Y^{\Theta} - Y^{\Theta}_{Mid}}{Y^{\Theta}_{Amp}} \right) \tag{11.13}$$

11.3.3 Determining if the device is inverted

Using a similar approach to determining the roll and pitch angles the Z^* response variable is used to determine if the device is inverted, that is if either the roll or pitch exceeds ±90˚.

Given:

Z^*_{Max} = Maximum ADC value

Z^*_{Min} = Minimum ADC value

Z^* = ADC Reading

Determine the midrange ADC value using equation 11.14

$$Z^*_{Mid} = \left(\frac{Z^*_{Max} + Z^*_{Min}}{2} \right) \tag{11.14}$$

Determine the test value of inversion ζ via magnetoresistive Z^* component using equation 11.15.

$$\zeta = \left(Z^* - Z^*_{Mid} \right) \tag{11.15}$$

The device is inverted if ζ is returned as a positive number.

11.3.4 Interpreting the results pitch Φ and roll Θ

The following references to position are taken from Figure 10 in conjunction with the component position shown in Figure 15.

For results returning Φ as a positive angle this indicates a nose down position.
For results returning Φ as a negative number this indicates a nose up position.
For results returning Θ as a positive angle this indicates right wing down position.
For results returning Θ as a positive angle this indicates right wing up position.
To determine when the instrument becomes inverted we need test for inversion using ζ.

11.4 Treatment of Compassing Error

The resolution of the instrument is mostly limited by the 10 bit ADC quantization and a gain of 300 in the magnetoresistive circuit, producing a maximum *resolution* of **0.71**° (as calculated in 7.4.2) the requirements to pursue fine scale analysis of compassing error requires consideration.
Repeatability was calculated by taking the readings obtained in experiment No.6 and using equations 11.1 to 11.5 and equation 9.5 to determine the compass bearing for each run. This permitted the variation between experimental runs to be explored in degrees. The results of this exploration produced a standard deviation over three runs of 0.5°. It would be fair to say the *repeatability* of the device is in the order of 0.5°.
Calculating compassing error is intensively discussed by Caruso (2004) and following the analysis given by Caruso, Table 24 was derived.

Table 24 Compassing Error Results. The total error indicates the difference between the instruments reading and magnetic north.

Parameter	Specification	Heading Error
Magnetic Sensor Resolution	Section 10.6	0.71˚
Noise (BW=10Hz)	85 µ gauss	<0.01˚
Linearity	0.05%FS (FS=400 µ gauss)	0.03˚
Hysteresis	0.08 % FS	0.11˚
Repeatability	Section 11.4	0.47˚
Temperature Effects	Caruso (2000)	0.29˚
Signal Conditioning	Caruso (2000)	0.05˚
Tilt error	Table 21	0.74˚† 10.4‡
	Total (RMS)	0.93 (min) 10.4(max)

† Best case accelerometer uncertainty RMS of Static + Dynamic errors.

‡ Worse case accelerometer uncertainty RMS of Static + Dynamic errors.

11.5 Discrimination Summary

The angle of pitch Φ and roll Θ is gathered from the accelerometer output according to equations 11.10 and 11.13 respectively. The degree of accuracy is predominantly determined by the quantization of the ADC and is the RMS of static error and dynamic errors calculated in sections 9.3.5.1 and 9.3.5.3.

The discrimination achieved by the instrument in terms of measuring pitch and roll is expressed by equations 11.16 and 11.7.

$$\text{Pitch} = \Phi \pm 10.4\sin(\Phi) \tag{11.16}$$

$$\text{Roll} = \Theta \pm 10.4\sin(\Theta) \tag{11.17}$$

The effect of this error is best demonstrated graphically as shown in Figure 47.

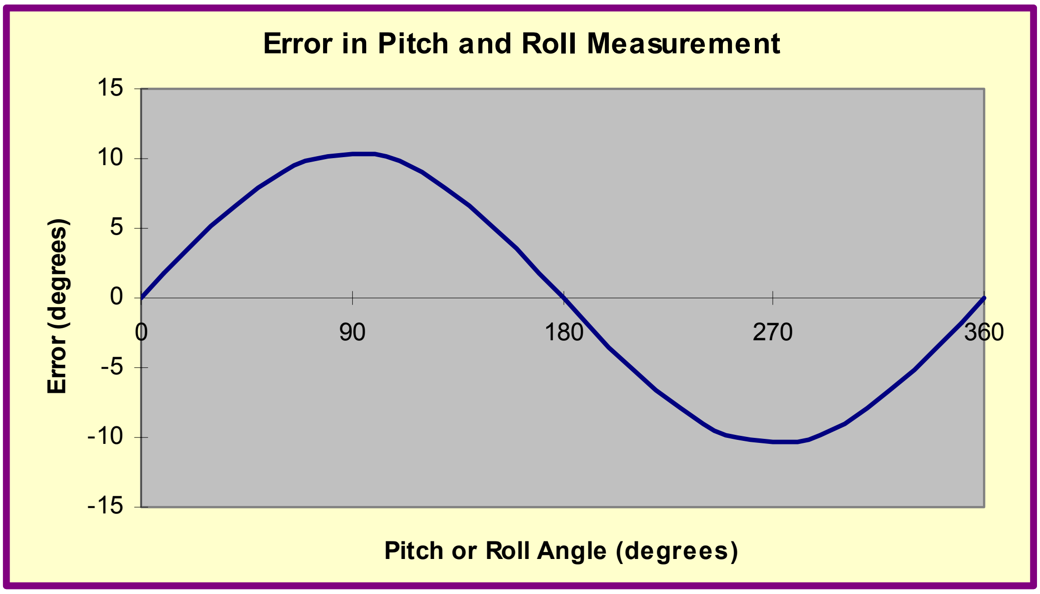

Figure 47 The error in pitch and roll clearly shows the device is more accurate for small values of tilt and increases to a maximum at ±90˚ tilt.

Examination of Table 24 shows the significance of the tilt error in determining bearing error. This is because the bearing correction equations 11.6 and 11.7 introduce the tilt error into the calculation of the magnetic bearing.

As such the discrimination achieved by the magnetic bearing is best described by equations 11.18 and 11.19 to demonstrate the best and worse case scenarios.

$$\text{Compass Bearing} = \Psi \pm 1^\circ \qquad \text{for} \quad \Phi \text{ or } \theta \text{ close to } 0^\circ \qquad (11.18)$$

$$\text{Compass Bearing} = \Psi \pm 10.4^\circ \qquad \text{for} \quad \Phi \text{ or } \theta \text{ close to } 90^\circ \qquad (11.19)$$

Chapter 12 Conclusion

12.1 Conclusion

This dissertation describes the design and construction of a data logging device, interfaced with specialist sensors to track the southern elephant seal on its journey across the southern ocean and return data into the hands of biologists for further analysis. The underlying physics exploited to achieve this feat was the ability to measure earth's magnetic field and the direction of gravity. Together, using simple trigonometry, these quantities can reveal the magnetic bearing of the animal in the water column, relative to magnetic north and roll and pitch relative to gravity. The progress of the instrument through the stages of component selection, circuit development, software design and prototype finally converged at an evaluation stage that supported the choice of underlying principals and satisfied the overall project specification.

The necessity to construct a device specifically to perform this task was driven by the lack of existing solutions and the extreme conditions of service such a device is expected to endure. The device is designed to cope with temperatures below 0˚ C and be capable of accurate time keeping in the order of ±1 minute per year. As the device is required to survive repetitive submersion to depths approaching two kilometres the simplest design was pursued using the least component count to maximise reliability. The utilization of a microcontroller interfaced with flash memory provides a low cost solution to data storage and also provides the functionality of an integrated analog to digital converter, real time clock and communications capabilities. The device is capable of storing four million bytes of information and has an energy budget capable of powering the device with a four-fold margin of safety.

The process taken to develop the instrument has successfully arrived at an instrument capable of producing the positional data required by biologists and with a calculated degree of accuracy.

12.2 Achievement of Project Objectives

The success of the project is measured against the Project Specification given in Appendix A. Tasks 1 to 9 are reproduced here and achievements noted.

1. *Research available literature and engage in personal communication with seal researchers to develop an insight into the biological aspects of the southern elephant seal.*

This objective was achieved with the valuable assistance of research biologists Steve Wall, Michelle Thums, Clair Holland and Dr Mark Hindell. Their personal communication with the author was invaluable and put the biological aspects into context which assisted greatly during the literature review of the biological journals evident in Chapter 2. The literature review was guided by personal communication which may have introduced some bias in the process but in this case the bias was regarded as a positive influence.

2. *Examine the nature of data already being obtained via trackers to permit seamless integration of positional data.*

Chapter 2 looks closely at the existing trackers both electrically and as regards the data returned. This investigation identified the need for a highly accurate local clock to permit seamless integration between the existing trackers and the new instrument based on time. As a result a precision clocking oscillator was selected for integration with the microcontroller. The limitations of existing data were also examined which confirmed the need for a new instrument to gather fine scale positional information of an animal whilst at sea, something that had not yet been achieved for an elephant seal.

3. *Investigate compassing technologies especially with respect to magneto-resistive devices.*

A literature review described in Chapter 3 confirmed the suitability of using magnetoresistive devices to produce a compassing solution and also indicated the requirement to provide tilt measurement for correction purposes. The technology was found to be well developed and employed widely in industrial applications, navigation and even some wrist watches. To further explore the use of magnetoresistive devices a compassing demonstration unit (HMR3000) was obtained and trialled. This evaluation underwrote the use of a magnetoresistive device and accelerometer as the principle sensors in the development of the instrument.

4. *Consider microcontrollers and non volatile memory to form the foundation of a data recording device.*

A literature review was conducted amongst the dozens of companies that manufacture microcontrollers and memory devices. The result of that review carried out in Chapter 3 culminated in the selection of a microcontroller from Freescale Inc. and flash memory from Atmel. At the time of selection there was recognition that the devices may not represent the best choice but reality dictated making a decision early to allow the project to proceed. At this stage in the development of the instrument the choice has returned a successful outcome and neither a rival microcontroller nor memory device has surfaced.

5. *Design circuit schematics and create PCB design.*

Component selection was based on functional modules listed in Table 3 and the expansion into electronic schematics followed the same modular approach as described in Chapter 3. The circuit schematics and printed circuit board design were developed using DXP2004 by Altium. The PCB track layout on the instrument was done manually as the inbuilt track routing software *Situs*, was not able to handle the highly congested connections effectively. A critical error in PCB design (incorrect component footprint) made the second prototype mandatory rather than optional in order to proceed with the project. The error reaffirmed the unforgiving nature of PCB errors when using surface mounted components and produced a benefit to the project in the implementation of a more rigorous quality control system.

6. *Explore and develop a microcontroller operating programme.*

The software written was modular in design as discussed in Chapter 5 and was specifically aimed at permitting evaluation of the instrument and providing the building blocks for future operating system designs. A structured approach was adopted to efficiently arrive at easily modified programs with good readability and suitable for future maintenance.

7. *Construct prototype board and evaluate, debug and refine hardware design.*

The construction phase of the operation described in Chapters 7, 8 and 9 was an interesting proposition as fine pitch components were specified by design. The methods engaged to populate a PCB with surface mounted devices demanded a new set of skills that once practiced produced a very good result. Two prototypes were developed, the second carrying the identified improvements from the first.

8. *Load microcontroller program, debug and refine.*

The code modules, once designed were loaded and tested individually on the microcontroller and used to evaluate the instrument. Debugging the modules required many revisions to produce the final effective code modules. The written code modules confirmed the electronic functionality of the instrument, activated microcontroller ports, accessed flash memory, energised sensors and returned data enabling the discrimination of the device to be explored in Chapters 10 and 11.

9. *Develop a non-aquatic test regime to evaluate the positional discrimination achieved.*

The final objective of the project and the most important element in the design process is the evaluation of the positional discrimination reached as discussed in Chapter 11. To achieve this goal two phases were employed, the first the development of an experimental design that divulges the data the instrument can produce and the second an analysis of that data to provide a measure of its worth. The experimental design recognised the differences between static testing and dynamic testing and made allowances for this factor when formulating the discrimination specifications. The analysis of data looked for variation in the response and implemented strategies for reducing the variation in both hardware and software. The resulting discrimination of the device is heavily influenced by the quantization limitations of using a 10 bit ADC in the design.

12.3 Further Work

The evolution of the instrument to this point has proven the underlying principles of the device and indicated a sound basis to continue development with a positive outlook for success. In the global evolution of the instrument I estimate, based on my experience, this point represents the half way mark on the way to a final product. Two objectives were considered in the project specification if time were to permit,

10. *Design a rugged construction method capable of withstanding deployment on a seal.*
11. *Devise an alignment method to promote correct orientation with respect to axis of seal.*

Bonus objectives *10* and *11* were not reached within the time limits and further work is required to find solutions to these issues.

Additional objectives have been identified during the progress of the project and are listed below.

12. Implement circuit recommendations discovered during evaluation, construct another prototype in a configuration that is acceptable for commercial manufacture and conduct a final round of evaluation.
13. Engage in discussions with biologists for operational advice in order to compile the software necessary to drive the final design. (Using the developed code modules designed to facilitate this step).
14. Develop a user friendly automated program to download the flash memory into a database structure for further analysis, perhaps using Visual Basic as the programming language.
15. Write an *Instruction Manual* at an appropriate technical level to facilitate repair and maintenance by technicians.
16. Write a *Users Manual* covering
    - the general operation of the instrument to allow isolated field based personnel to effectively deploy the instrument and retrieve the data.
    - A section on how to interpret the returned data and extract the bearing, pitch and roll information.

12.4 Ethical Consideration

The **Limitations of Use** provided at the beginning of this document provides a universal statement as to the fitness of the information within the dissertation for other purposes.
In addition to this general advice I must include a more specific statement as the author of this work.
The second prototype, with minimal effort, perhaps simply encasing the unit is resin, is capable of delivering useful data to scientists. However until the issues raised in Section 12.3 are fully addressed it would be unwise to deploy the instrument (before the vision is complete). This is especially important, as without further development and evaluation the trustworthiness of the instrument is not quantifiable and therefore, presenting the device to an animal ethics committee as a reliable entity would be false.
The point made here is to accept the instrument is not fully developed and I trust any persons considering the contents of this dissertation accept this viewpoint.

References

1,2 and 3 Axis Magnetic Sensors Application Data Sheet (2004) [Online] Available: http://www.ssec.honeywell.com [Accessed: 12 Nov 2004]

+5V Powered, Multichannel RS232 Drivers/Receivers Application Data Sheet (2004) [Online] Available: http://www.maxim-ic.com [Accessed: 3 Jan 2005]

±10g Duel Axis Micromachined Accelerometer Application Data Sheet (2004) [Online] Available: http://www.freescale.com [Accessed: 23 Dec 2004]

32.768kHz Temperature Compensated Crystal Oscillator Application Data Sheet (2004) [Online] Available: Available :http://www.maxim-ic.com [Accessed: 9 Feb 2005]

32-megabit (2M x16/4M x8) 3-volt Only Flash Memory Application Data Sheet (2004) [Online] Available: http://www.atmel.com [Accessed: 4 Dec 2004]

Airaudi, T. In-Circuit Programming of Flash Memory using the Monitor Mode for the MC68HC908JL/JK Application Data Sheet (2000) [Online] Available: http://www.freescale.com [Accessed: 2 Jan 2005]

Arendarik, S. Generating Clocks for the HC908 MCU Families, AN2508.pdf Application Data Sheet (2003) [Online] Available: http://www.freescale.com [Accessed: 12 Dec 2004]

Atkinson, A. C. and A. N. Donev (1992). Optimal Experimental Design. Oxford, Oxford University Press.

Atmel AT29 Flash Memories Application Data Sheet (1998) [Online] Available: http://www.atmel.com [Accessed: 4 Dec 2004]

Box, G. E. P., W. G. Hunter, et al. (1978). Statistics for Experimenters, An introduction to Design, Data Analysis and Model Building. Toronto, John Wiley and Sons Inc.

Caruso, J. A. Applications of magnetic sensors for Low Cost Compass Systems Application Data Sheet (2004) [Online] Available: http://www.ssec.honeywell.com [Accessed: 16 Dec 2004]

Compass Heading using Magnetometers Application Data Sheet (2004) [Online] Available: http://www.ssec.honeywell.com [Accessed: 14 Nov 2004]

CPU08 Central Processor Unit Reference Manual Application Data Sheet (2001) [Online] Available: http://www.freescale.com [Accessed: 12 Dec 2004]

Digital Compass Module Users Guide Application Data Sheet (2004) [Online] Available: http://www.ssec.honeywell.com [Accessed: 14 Nov 2004]

DS32kHz Temperature- Compensated Crystal Oscillator Application Data Sheet (2004) [Online] Available: http//:www.maxim-ic.com [Accessed: 4 April 2005]

Fan, R. In-Circuit Programming of Flash Memory in the MC68HC908JL3 Application Data Sheet (2000) [Online] Available: http://www.freescale.com [Accessed: 2 Jan 2005]

Fitchen, F. C. and C. D. Motchenbacher (1973). Low Noise Electronic Design. Toronto, John Wiley & Sons.

Greenwood, A. (2002). Research Methods for Post Graduates. New York, Oxford University Press.

HE-TXO-10C1 Temperature Compensated Oscillator Application Data Sheet (2004) [Online] Available: http://www.hoorayusa.com [Accessed: 9 Dec 2004]

Hindell, M. A., R. G. Harcourt, et al. (2002). "Fine-scale, three-dimensional spatial use of diving by lactating female Weddell seals *Leptonychotes weddellii.*" Marine Ecology Progress Series **242**: 275-284.

HMR3000 Digital Compass Module Application Data Sheet (2004) [Online] Available: http://www.ssec.honeywell.com [Accessed: 14 Nov 2004]

John, J. A. and M. H. Quenouille (1977). Experimental Design and Analysis. High Wycombe, Bucks, Englund, Charles Griffin & Company.

Laws, R. M. (1994). History and present status of southern elephant seal populations. Elephant seals: Population Ecology, Behavior and Physiology. L. R. M and L. B. J. Berkley, University of California Press**:** 49-56.

MAX3222E-MAX3246E RS232 Drivers/Receivers Application Data Sheet (2004) [Online] Available: http://www.maxim-ic.com [Accessed: 20 April 2005]

MC68HC908LJ24 Data Sheet Application Data Sheet (2004) [Online] Available: http://www.freescale.com [Accessed: 26 Nov 2004]

Miller, G. H. (1999). Microcomputer Engineering. New Jersey, Tom Robbins Prentice-Hall Inc.

Mounting Tips for LCC Magnetic Sensors Application Data Sheet (2004) [Online] Available: http://www.ssec.honeywell.com [Accessed: 16 Dec 2004]

Ott, H. W. (1988). Noise Reduction Techniques in Electronic Systems. New York, John Wiley & Sons.

Pant, B. and M. Caruso Magnetic Sensor Cross Axis Effect Application Data Sheet (1996) [Online] Available: http//:www.ssec-honeywell.com [Accessed: 3 June 2005]

Recommended Reprogramming Procedure for Atmels's Flash Memories Application Data Sheet (2000) [Online] Available: http://www.atmel.com [Accessed: 4 Dec 2004]

Schultz, P. ±1.5g Duel Axis Micromachined Accelerometer Power Supply Rejection Ration (PSRR) Sugestions Application Data Sheet (2004) [Online] Available: http://www.freescale.com [Accessed: 9 Dec 2004]

Sonnenschein Lithium Batteries Technical Brochure Application Data Sheet (2003) [Online] Available: http://www.sonnenschein-lithium.de [Accessed: 1 Jan 2005]

Suchyta, J. Programming and Debugging Options for M68HC08 MCUs Application Data Sheet (2002) [Online] Available: http://www.freescale.com [Accessed: 26 Nov 2004]

Technical Data M68HC08 Microcontrollers Application Data Sheet (2002) [Online] Available: http://www.freescale.com [Accessed: 2 Jan 2005]

Thionyl Chloride Lithium Battery (Li/SOC12) Application Data Sheet (2004) [Online] Available: http://www.gmbattery.com [Accessed: 9 Dec 2004]

TIM08 Timer Interface Module Application Data Sheet (1996) [Online] Available: http://www.freescale.com [Accessed: 21 Dec 2004]

Zamon, J. E., C. H. Greene, et al. (1996). "Acoustic characterization of the three-dimensional prey field of foraging chinstrap penguins." Marine Ecology Progress Series **131**(1-10).

Appendix A Project Specification

A.1 Issue C, 17 March 2005.

University of Southern Queensland
Faculty of Engineering and Surveying

ENG 4111/2 Research Project
PROJECT SPECIFICATION

FOR:	**Peter Deith**
TOPIC:	Instrumentation to Track the Southern Elephant Seal..
SUPERVISOR:	Dr Nigel Hancock
ENROLMENT:	ENG4111 – S1, X, 2005. ENG4112 – S2, D, 2005.
PROJECT AIM:	Application of a magneto-resistive coordinate sensor and microprocessor controlled data storage system to assist in determining three dimensional fine scale habitat use and behaviour of the Southern Elephant Seal (*Mirounga Leonina).*

PROGRAMME: Issue C , 17 March 2005.

1. Research available literature and engage in personal communication with seal researchers to develop an insight into the biological aspects of the southern elephant seal.

2. Examine the nature of data already being obtained via trackers to permit seamless integration of positional data.

3. Investigate compassing technologies especially with respect to magneto-resistive devices.

4. Consider microcontrollers and non volatile memory to form the foundation of a data recording device.

5. Design circuit schematics and create PCB design.

6. Explore and develop a microcontroller operating programme.

7. Construct prototype board and evaluate, debug and refine hardware design.

8. Load microcontroller program, debug and refine.

9. Develop a non-aquatic test regime to evaluate the positional discrimination achieved.

As time permits.

10. Design a rugged construction method capable of withstanding deployment on a seal.

11. Devise an alignment method to promote correct orientation with respect to axis of seal.

AGREED :______________________(Student) ________________________(Supervisor)

Dated 17/ 3 /05 Dated 17/ 3 /05

A.2 Issue B , 13 March 2005

University of Southern Queensland
Faculty of Engineering and Surveying

ENG 4111/2 Research Project
PROJECT SPECIFICATION

FOR:	**Peter Deith**
TOPIC:	Fine scale habitat use of the Southern Elephant Seal, *Mirounga Leonina.*
SUPERVISOR:	Dr Nigel Hancock
ENROLMENT:	ENG4111 – S1, X, 2005. ENG4112 – S2, D, 2005.
PROJECT AIM:	Application of a magneto-resistive coordinate sensor and microprocessor controlled data storage system to assist in determining three dimensional fine scale habitat use and behaviour of the Southern Elephant Seal (*Mirounga Leonina).*

PROGRAMME: Issue B , 13 March 2005.

1. Research available literature and engage in personal communication with seal researchers to develop an insight into the biological aspects of the southern elephant seal.

2. Examine the nature of data already being obtained via trackers to permit seamless integration of positional data.

3. Investigate compassing technologies especially with respect to magneto-resistive devices.

4. Consider microcontrollers and non volatile memory to form the foundation of a data recording device.

5. Design circuit schematics and create PCB design.

6. Explore and develop a microcontroller operating programme.

7. Construct prototype board and evaluate, debug and refine hardware design.

8. Load microcontroller program, debug and refine.

As time permits.

9. Employ a rugged construction method capable of withstanding actual deployment on a seal.

10. Arrange with seal researchers the deployment and retrieval of instrument.

11. Analyse data retrieved from the animal and develop a 3D software package to demonstrate fine scale habitat use of the Southern Elephant seal. (Can not be done as part of project due to time constraints.)

AGREED :______________________(Student) ________________________(Supervisor)

Dated 13/ 3 /05 Dated 13/ 3 /05

A.3 Issue A , 3 February 2005

University of Southern Queensland
Faculty of Engineering and Surveying

ENG 4111/2 Research Project
PROJECT SPECIFICATION

FOR:	**Peter Deith**
TOPIC:	Fine scale habitat use of the Southern Elephant Seal, *Mirounga Leonina.*
SUPERVISOR:	Dr John Leis
ENROLMENT:	ENG4111 – S1, X, 2005. ENG4112 – S2, D, 2005.
PROJECT AIM:	Application of a magneto-resistive coordinate sensor and microprocessor controlled data storage system to assist in determining three dimensional fine scale habitat use and behaviour of the Southern Elephant Seal (*Mirounga Leonina).*

PROGRAMME: Issue A , 3 February 2005.

1. Research available literature and engage in personal communication with seal researchers to develop an insight into the biological aspects of the southern elephant seal.

2. Examine the nature of data already being obtained via trackers to permit seamless integration of positional data.

3. Investigate compassing technologies especially with respect to magneto-resistive devices.

4. Consider microcontrollers and non volatile memory to form the foundation of a data recording device.

5. Design circuit schematics and create PCB design.

6. Explore and develop a microcontroller operating programme.

7. Construct prototype board and evaluate, debug and refine hardware design.

8. Load microcontroller program, debug and refine.

As time permits.

9. Employ a rugged construction method capable of withstanding actual deployment on a seal.

10. Arrange with seal researchers the deployment and retrieval of instrument.

11. Analyse data retrieved from the animal and develop a 3D software package to demonstrate fine scale habitat use of the Southern Elephant seal. (Can not be done as part of project due to time constraints.)

AGREED :________________________(Student) __________________________(Supervisor)

Dated __/ 2 /05 Dated __/ 2 /05

Appendix B   Prototype No.1 Drawings

Contents

B.1 Microcontroller page 103

B.2 Flash Memory page 104

B.3 Magnetoresistive Sensor page 105

B.4 Accelerometer page 106

B.5 Communication page 107

Note. In each case the printed drawing is unavoidably compressed but may be viewed with clarity in the software (.pdf) version of this dissertation

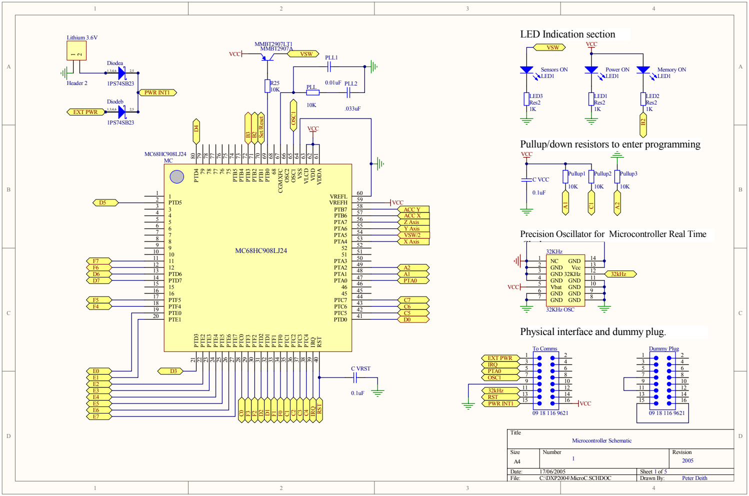

LED Indication section
Pullup/down resistors to enter programming
Precision Oscillator for Microcontroller Real Time
Physical interface and dummy plug.
MC68HC908LJ24
Lithium 3.6V
Header 2
Diodea
Diodeb
1PS74SB23
EXT PWR
PWR INT1
MMBT2907LT1
MMBT2907A
VSW
VCC
R25
10K
PLL1
PLL2
0.01uF
.033uF
Sensors ON
Power ON
Memory ON
LED1
LED2
LED3
Res2
1K
Pullup1
Pullup2
Pullup3
C VCC
0.1uF
32KHz
32KHz OSC
32kHz
C VRST
To Comms
Dummy Plug
09 18 116 9621
Title
Microcontroller Schematic
Size
A4
Number
1
Revision
2005
Date:
17/06/2005
Sheet 1 of 5
File:
C:\DXP2004\MicroC.SCHDOC
Drawn By:
Peter Deith

Micro Controller Port C/ Flash Pin
C0 C1 C2 C3 C4 C5 C6 C7
A11 A17 A7 A6 A5 A2 A3 A4

Micro Controller Port D/ Flash Pin
D0 D1 D2 D3 D4 D5 D6 D7
A1 A19 A8 A0 A15 A14 A13 A12

Micro Controller Port E/ Flash Pin
E0 E1 E2 E3 E4 E5 E6 E7
io0 ie1 io2 io3 io4 io5 io6 io7

Micro Controller Port F/ Flash Pin
F0 F1 F2 F3 F4 F5
A18 A20 A9 A10 A-1 A16

CONTROL PORTS/ Flash Pin
F6 B3 F7
OE WE CE

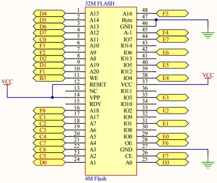

Title		
Flash Memory		
Size: A4	Number: 1	Revision: 2005
Date: 17/06/2005		Sheet 2 of 5
File: C:\DXP2004\FMemory.SCHDOC		Drawn By: Peter Deith

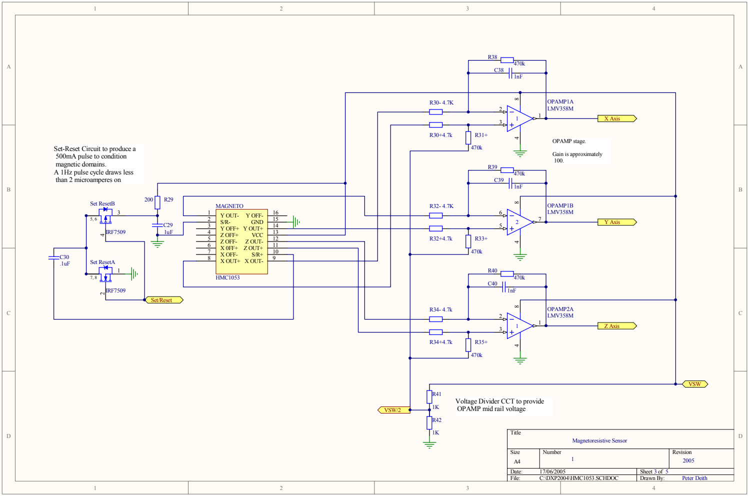
Set-Reset Circuit to produce a 500mA pulse to condition magnetic domains.
A 1Hz pulse cycle draws less than 2 microamperes on
Set ResetB
IRF7509
Set ResetA
IRF7509
C30 .1uF
200 R29
C29 1uF
Set/Reset
MAGNETO
HMC1053
Y OUT- Y OFF-
S/R- GND
Y OFF+ Y OUT+
Z OFF+ VCC
Z OFF- Z OUT-
X OFF+ Z OUT+
X OFF- S/R+
X OUT+ X OUT-
R38 470k
C38 1nF
R30- 4.7K
R30+4.7k
R31+ 470k
OPAMP1A LMV358M
X Axis
OPAMP stage.
Gain is approximately 100.
R39 470k
C39 1nF
R32- 4.7K
R32+4.7k
R33+ 470k
OPAMP1B LMV358M
Y Axis
R40 470k
C40 1nF
R34- 4.7k
R34+4.7k
R35+ 470k
OPAMP2A LMV358M
Z Axis
VSW
VSW/2
R41 1K
R42 1K
Voltage Divider CCT to provide OPAMP mid rail voltage
Title
Magnetoresistive Sensor
Size A4
Number 1
Revision 2005
Date: 17/06/2005
Sheet 3 of 5
File: C:\DXP2004\HMC1053.SCHDOC
Drawn By: Peter Deith

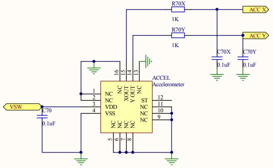

Title	Accelerometer		
Size A4	Number 1		Revision 2005
Date:	17/06/2005	Sheet 4 of 5	
File:	C:\DXP2004\AccelMMA6233Q.SCHDOC	Drawn By:	Peter Deith

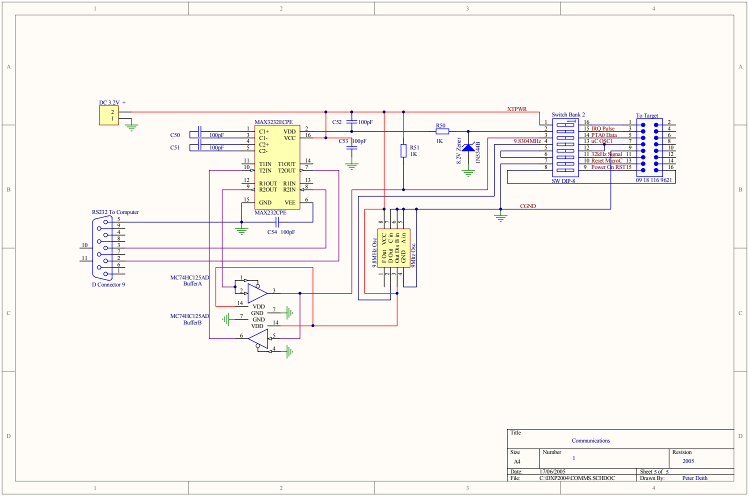
DC 3.2V +
XTPWR
MAX3232ECPE
C1+ C1- C2+ C2- VDD VCC
T1IN T2IN T1OUT T2OUT
R1OUT R2OUT R1IN R2IN
GND VEE
MAX232CPE
C50 100pF
C51 100pF
C52 100pF
C53 100pF
C54 100pF
R50 1K
R51 1K
8.2V Zener
1N5344B
9.8304MHz
Switch Bank 2
SW DIP-8
15 IRQ Pulse
14 PTA0 Data
13 uC OSC1
11 32kHz Signal
10 Reset MicroC
9 Power On RST
To Target
09 18 116 9621
CGND
RS232 To Computer
D Connector 9
9.8MHz Osc
9Mhz Osc
F Out
D Out
Out Dis
GND
VCC
C in
B in
A in
MC74HC125AD
BufferA
MC74HC125AD
BufferB
VDD
GND
Title
Communications
Size
A4
Number
1
Revision
2005
Date: 17/06/2005
Sheet 5 of 5
File: C:\DXP2004\COMMS.SCHDOC
Drawn By: Peter Deith

Appendix C   Prototype No.2 Drawings

Contents

C.1 Microcontroller Board page 109

C.2 Sensor Board page 110

C.3 Communications Board page 111

Note. In each case the printed drawing is unavoidably compressed but may be viewed with clarity in the software (.pdf) version of this dissertation

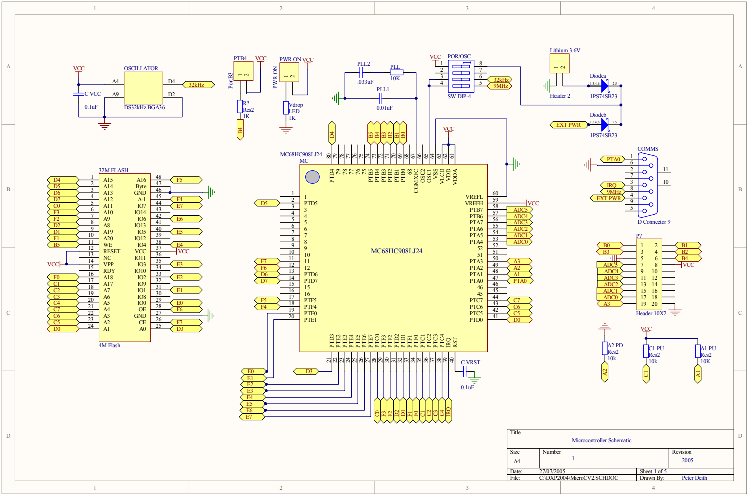
OSCILLATOR
DS32kHz BGA36
32kHz
C VCC
0.1uF
PTB4
PortB3
R?
Res2
1K
PWR ON
VCC
Vdrop
LED
PLL2
.033uF
PLL
10K
PLL1
0.01uF
POR/OSC
SW DIP-4
32kHz
9MHz
Lithium 3.6V
Header 2
Diodea
1PS74SB23
Diodeb
EXT PWR
COMMS
PTA0
IRQ
D Connector 9
32M FLASH
4M Flash
MC68HC908LJ24
MC
C VRST
0.1uF
P?
Header 10X2
A2 PD
C1 PU
A1 PU
Res2
10k
Title
Microcontroller Schematic
Size
A4
Number
1
Revision
2005
Date:
27/07/2005
Sheet 1 of 5
File:
C:\DXP2004\MicroCV2.SCHDOC
Drawn By:
Peter Deith

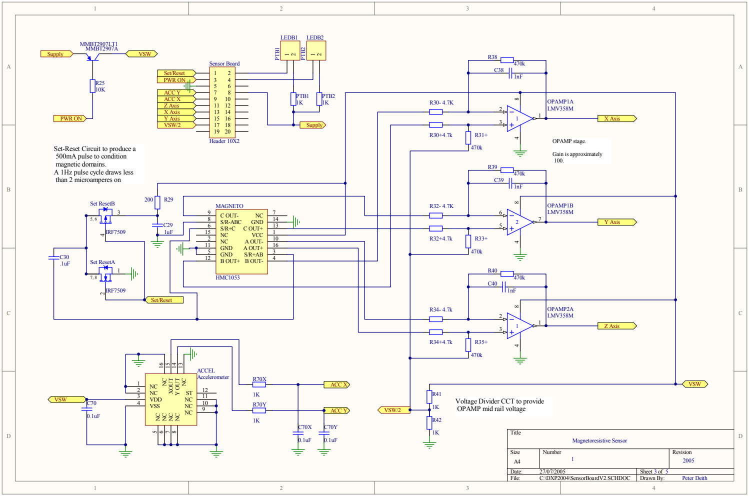
MMBT2907LT1
MMBT2907A
Supply
VSW
R25
10K
PWR ON
LEDB1
LEDB2
PTB1
PTB2
Sensor Board
Set/Reset
PWR ON
ACC Y
ACC X
Z Axis
X Axis
Y Axis
VSW/2
Header 10X2
PTB1 1K
PTB2 1K
Supply
Set-Reset Circuit to produce a 500mA pulse to condition magnetic domains.
A 1Hz pulse cycle draws less than 2 microamperes on
Set ResetB
IRF7509
200
R29
C29
1uF
C30
.1uF
Set ResetA
IRF7509
Set/Reset
MAGNETO
C OUT-
S/R-ABC
S/R+C
NC
NC
GND
GND
B OUT+
NC
GND
C OUT+
VCC
A OUT-
A OUT+
S/R+AB
B OUT-
HMC1053
R38
470k
C38
1nF
R30- 4.7K
R30+4.7k
R31+
470k
OPAMP1A
LMV358M
X Axis
OPAMP stage.
Gain is approximately 100.
R39
470k
C39
1nF
R32- 4.7K
R32+4.7k
R33+
470k
OPAMP1B
LMV358M
Y Axis
R40
470k
C40
1nF
R34- 4.7K
R34+4.7k
R35+
470k
OPAMP2A
LMV358M
Z Axis
ACCEL
Accelerometer
VDD
VSS
XOUT
Y OUT
ST
VSW
C70
0.1uF
R70X
1K
R70Y
1K
ACC X
ACC Y
C70X
0.1uF
C70Y
0.1uF
VSW/2
R41
1K
R42
1K
VSW
Voltage Divider CCT to provide OPAMP mid rail voltage
Title
Magnetoresistive Sensor
Size
A4
Number
1
Revision
2005
Date:
27/07/2005
Sheet 3 of 5
File:
C:\DXP2004\SensorBoardV2.SCHDOC
Drawn By:
Peter Deith

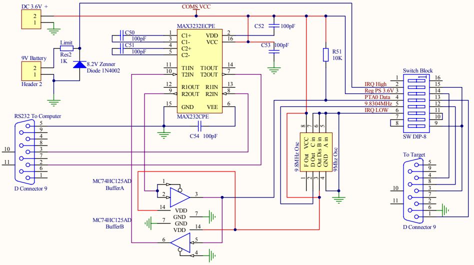

Title			
Communications			
Size: A4	Number: 1		Revision: 2005
Date: 27/07/2005		Sheet 5 of 5	
File: C:\DXP2004\COMMSV2.SCHDOC		Drawn By: Peter Deith	

Appendix D Code Listing

D.1 Code Modules.

D 1.1 Write to External Memory

```
****************Write to External Flash  Memory*************
*
*Author: Peter Deith
*Subject: Research Project Eng4111/2
*Project: Instrumentation to track the Southern Elephant Seal
*Version 9.2
*Date 9 August 2005
*
*This code is an example of modular design where each small functional
*section of code is isolated and transformed into a subroutine or otherwise
*segregated from the general operating section of the program. This has
*the advantage of making the code transportable between different
*programs using the same processor and assists in maintenance.
*
*******************************************************

*********** List Constants  Module**************************
RamStart     EQU  $0080    ; Memory Map RAM
Romstart     EQU  $9000    ; Memory Map ROM
VectorStart  EQU  $FFD8  ; Memory Map Interupt Addresses.

$Include 'lj24regs.inc'          ; List memory of addresses

***********List Variables in RAM  Module********************

      org  RamStart

ONES    EQU  $FF       ; 1111 1111
ZEROS   EQU  $00       ; 0000 0000
HYBY    EQU  $3F       ; 0011 1111
MEM1    EQU  $00
MEM2    EQU  $00
MEM3    EQU  $00
count_lo     ds   1
count_hi     ds   1

************************************************************
* Main_Int - This is the point where code starts executing  *
*          after a RESET.                        *
************************************************************

        org   RomStart

;************************************************************
; Blink LEDS    Indicating Module                         *
;************************************************************

BLINK_LEDS:

      jsr    SEN_ON             ;blink the heartbeat LED
      jsr    EXTMEM_ON
```

```
      jsr    Wait500ms
      jsr    SEN_OFF
      jsr    EXTMEM_OFF
      jsr    Wait500ms
      rts

*************************************************************
*  External Atmel MEMORY Initialisation Module.
*************************************************************

EXTDATABUS_int:
        mov  ZEROS,DDRE      ;Set port E as input port.
        clr  PortE          ;Set Register E to Hex 00
        rts
EXTADDBUS_int:
        mov  ONES,DDRC       ;Set Port C as output port.
        mov  ONES,DDRD       ;Set Port D as output port.
        mov  HYBY,DDRF       ;Set Port F0-f5 as output port.
        rts
EXTCONTBUS_int:
        BSET 6,PortF        ; OE Output Enable Output Hi Z
        BSET 7,PortF        ; CE Chip Enable   Output Hi Z
        BSET 3,PortB        ; WE Write Enable
        BSET 6,DDRF           ; OE
        BSET 7,DDRF           ; CE
        BSET 3,DDRB           ; WE
        rts

*************************************************************
*  Turn Sensors ON  Module
*************************************************************

SEN_ON:

      BSET    0,LEDB         ; Ensure 15ma sink on.
      BCLR    0,PortB        ; Set B0 to logic 0
      BSET    0,DDRB         ; Set B0 to output
      rts

*************************************************************
*  Turn Sensors OFF   Module
*************************************************************

SEN_OFF:

      BSET    0,LEDB         ; Ensure 15ma sink on
      BSET    0,PortB        ; Set B0 to logic 1
      BSET    0,DDRB         ; Set B0 to Output
      rts


*************************************************************
*  Turn Set/Reset ON Module   (Condition Magnetoresistive device)
*************************************************************

SET/RESET_ON:

      BSET    1,LEDB         ; Ensure 15ma sink on.
      BCLR    1,PortB        ; Set B1 to logic 0
      BSET    1,DDRB         ; Set B1 to output
```

```
      rts


**************************************************************
*  Turn Set/Reset OFF  Module (Condition Magnetoresistive device)
**************************************************************

SET/RESET_OFF:

      BSET    1,LEDB          ; Ensure 15ma sink on
      BSET    1,PortB         ; Set B1 to logic 1
      BSET    1,DDRB          ; Set B1 to Output
      rts

**************************************************************
*  External Memory ON Module (LED indicator)
**************************************************************

EXTMEM_ON:

      BSET    2,LEDB          ; Ensure 15ma sink on.
      BCLR    2,PortB         ; Set B2 to logic 0
      BSET    2,DDRB          ; Set B2 to output
      rts

**************************************************************
*  External Memory OFF Module (LED indicator)
**************************************************************

EXTMEM_OFF:

      BSET    2,LEDB          ; Ensure 15ma sink on
      BSET    2,PortB         ; Set B2 to logic 1
      BSET    2,DDRB          ; Set B2 to Output
      rts

;**************************************************************
; Timing Module Time500ms -- (4x250) x 500us = 500ms
;**************************************************************

Time500ms:
      lda     #1
      sta     count_hi
w500m1: lda    #$10
      sta     count_lo
w500m2: jsr    Time500us
      dbnz    count_lo,w500m2
      dbnz    count_hi,w500m1
      rts

;***********************************************************************
; Timing Module500us -- Delay 500us
;***********************************************************************
Time500us:
      lda     #$79
w500u:  deca
      nop
      bne     w500u
      rts
```

```
************** Interupt vectors initialised below ***********

***********************************************************
* DUMMY_ISR - Dummy Interrupt Service Routine.          *
*       Just does a return from interrupt.        *
***********************************************************
dummy_isr:

    rti       ; return
***********************************************************
*                  The main program Module.
* This section of codes calls up the subroutines to, in this case write to the
* external flash memory.
***********************************************************

Main_int:
    sei                    ;disable all interrupts
    ldhx    #$01FF              ;initialize
    txs                    ;the stack pointer
    jsr     EXTDATABUS_int       ;INITALISE DATA BUS
    jsr     EXTADDBUS_int       ;INITALISE ADDRESS BUS
    jsr     EXTCONTBUS_int       ;INITALISE CONTROL BUS
    mov     #$ab,PortE        ;Put hex 'ab' on port E
    mov     #$0f,PortC        ;Set A0-A7 to 0F
    mov     #$0a,PortD        ;Set A8-A15 to 0A
    mov     #$2f,PortF        ;Set A16-A21 to 2f


***********************************************************
* Vectors - Timer Interrupt Service Routine.          *
*       after a RESET.                  *
***********************************************************
  org  VectorStart

    dw  dummy_isr   ; Real-time Clock Vector
    dw  dummy_isr   ; ADC Conversion Complete
    dw  dummy_isr   ; Keyboard Vector
    dw  dummy_isr   ; MMIIC Vector
    dw  dummy_isr   ; SCI Transmit Vector
    dw  dummy_isr   ; SCI Receive Vector
    dw  dummy_isr   ; SCI Error Vector
    dw  dummy_isr   ; SPI Receive Vector
    dw  dummy_isr   ; SPI Transmit Vector
    dw  dummy_isr   ; TIM2 Overflow Vector
    dw  dummy_isr   ; TIM2 Channel 1 Vector
    dw  dummy_isr   ; TIM2 Channel 0 Vector
    dw  dummy_isr   ; TIM1 Overflow Vector
    dw  dummy_isr   ; TIM1 Channel 1 Vector
    dw  dummy_isr   ; TIM1 Channel 0 Vector
    dw  dummy_isr   ; PLL Vector
    dw  dummy_isr   ; LVI Vector
    dw  dummy_isr   ; ~IRQ1 Vector
    dw  dummy_isr   ; SWI Vector
    dw  Main_int    ; Reset Vector
```

D 1.2 Selected Read ADC Modules

```
* Interupt Disabled (COCO test controlled),One Conversion

ADC_VSW/2     EQU    #$00   ;ADC0  move into ADSCR to select
ADC_MZ        EQU    #$01   ;ADC1           "
ADC_MY        EQU    #$02   ;ADC2           "
ADC_MX        EQU    #$03   ;ADC3           "
ADC_AY        EQU    #$04   ;ADC4           "
ADC_AX        EQU    #$05   ;ADC5           "
ADC_DISABLE   EQU    #$1F   ;Disable ADC    "

ADC_VSW/2_data rmb   1
ADC_MZ_data    rmb   1
ADC_MY_data    rmb   1
ADC_MX_data    rmb   1
ADC_AY_data    rmb   1
ADC_AX_data    rmb   1


*************************************************************
* Init_AtoD - Sets up the AtoD clock                        *
*************************************************************
ADC_ON:
     mov  #$10,ADCLK        ; Internal Bus Clock
                            ; 8 Bit Truncated Mode
     mov
     rts

*************************************************************
* Turn Off ADC and disable interupt                         *
*************************************************************

ADC_OFF;
      mov  ADC_DISABLE_INT,ADSCR
      rts

*************************************************************
*  Test COCO BIT for conversion complete                    *
*************************************************************

COCO_TEST      nop
         brclr  7,ADSCR,COCO_TEST
         rts

 *************************************************************
* READ Analogue to Digital Converter.                       *
*************************************************************

READ_ADC:
         jsr    ADC_ON            ;Get Mid Voltage Level.
         mov    ADC_VSW/2,ADSCR
         jsr    COCO_TEST
         mov    ADRL,ADC_VSW/2_data

         jsr    ADC_ON            ;Get Mag Z reading
         mov    ADC_MZ,ADSCR
         jsr    COCO_TEST
         mov    ADRL,ADC_MZ_data
```

```
            jsr    ADC_ON           ;Get Mag Y reading
            mov     ADC_MY,ADSCR
            jsr    COCO_TEST
            mov     ADRL,ADC_MY_data

            jsr    ADC_ON           ;Get Mag X reading
            mov     ADC_MX,ADSCR
            jsr    COCO_TEST
            mov     ADRL,ADC_MX_data

            jsr    ADC_ON           ;Get Acc Y reading
            mov     ADC_AY,ADSCR
            jsr    COCO_TEST
            mov     ADRL,ADC_AY_data

            jsr    ADC_ON           ;Get Axx X reading
            mov     ADC_AX,ADSCR
            jsr    COCO_TEST
            mov     ADRL,ADC_AX_data


************************************************************
* Main_Init - This is the point where code starts executing  *
*           after a RESET.                                  *
************************************************************

Main_Init:
    rsp             ; Reset Stack Pointer
    clra            ; Initialize A,X so that interrupt
    clrx            ; processing doesn't stop with
                    ; uninitialized register warning
                    ; when push A,X on the stack
                    ; Initialize peripherals
    bsr Init_AtoD       ; Initialise ADC
    mov                ,ADCSR
                    ; Start a single ADC conversion
                    ; which will generate an interrupt.
    cli             ; Allow interrupts to happen

    mov #$01,Config1    ; Disable Watchdog

main_loop:
    bra main_loop

************************************************************
* AtoD_ISR - ADC Conversion Complete Interrupt              *
*          Place valeu in ADC_VALUE byte                    *
************************************************************

AtoD_ISR:

    lda  adrl         ; Get the converted value
    sta  ADC_VALUE      ; save it in temp_byte
    rti
```

```
***********************************************************
* Vectors - Timer Interrupt Service Routine.              *
*           after a RESET.                                *
***********************************************************

  org  VectorStart
     dw  AtoD_isr     ; ADC Conversion Complete
     dw  main_init    ; Reset Vector
```

Appendix E Experimental Method and Data

Contents

E.1 Laboratory testing of Tracker....122
E.1.1 Testing apparatus. 122
E.1.2. Testing Precautions 122
E.1.3. Controlling the testing environment....122
E.1.4. Set Up Procedure....123
E.1.5 Experimental Method....123
E 2.1 Experiment No.1 Magnetic X and Y axis. 125
E 2.2 Experiment No.2 Magnetic X and Y axis. 129
E 2.3 Experiment No.3. Magnetic X and Y axis. 135
E 2.4 Experiment No 4. Magnetic X and Y axis 141
E 2.5 Experiment No.5 Magnetic X and Y axis. 147
E 2.6 Experiment No.6 Magnetic X and Y axis. 149
E 2.7 Experiment No.7 Magnetic X axis....155
E 2.8 Experiment No.8 Magnetic Y axis....157
E 2.9 Experiment No.9 Accelerometer Y axis and Magnetic Z axis 159
E 2.10 Experiment No.10 Accelerometer X axis and Magnetic Z axis 161

List of Tables

TABLE E. 1 SAMPLE A RAW DATA. CONDITIONS: NO SET/RESET, 3.5V REGULATED SUPPLY, 9MHZ OSCILLATOR IN CIRCUIT....125
TABLE E. 2 SAMPLE A NORMALISED DATA. (OFFSET REMOVED.) 126
TABLE E. 3 SAMPLE B RAW DATA. CONDITIONS: NO SET/RESET, 3.5V REGULATED SUPPLY, 9MHZ OSCILLATOR IN CIRCUIT....127
TABLE E. 4 SAMPLE B NORMALISED DATA. (OFFSET REMOVED.) 128
TABLE E. 5 SAMPLE A RAW DATA. CONDITIONS: NO SET/RESET, 3.5V REGULATED SUPPLY, 9MHZ OSCILLATOR IN CIRCUIT....129
TABLE E. 6 SAMPLE A NORMALISED DATA. (OFFSET REMOVED.)....130
TABLE E. 7 SAMPLE B RAW DATA. CONDITIONS: NO SET/RESET, 3.5V REGULATED SUPPLY, 9MHZ OSCILLATOR IN CIRCUIT. 131
TABLE E. 8 SAMPLE B NORMALISED DATA. (OFFSET REMOVED.)....132
TABLE E. 9 SAMPLE C RAW DATA. CONDITIONS: NO SET/RESET, 3.5V REGULATED SUPPLY, 9MHZ OSCILLATOR IN CIRCUIT....133
TABLE E. 10 SAMPLE C NORMALISED DATA. (OFFSET REMOVED.)....134
TABLE E. 11 SAMPLE A RAW DATA. CONDITIONS: SET/RESET EMPLOYED, 3.5V REGULATED SUPPLY, 9MHZ OSCILLATOR IN CIRCUIT. 135
TABLE E. 12 SAMPLE A NORMALISED DATA. (OFFSET REMOVED.) 136
TABLE E. 13 SAMPLE B RAW DATA. CONDITIONS: SET/RESET EMPLOYED, 3.5V REGULATED SUPPLY, 9MHZ OSCILLATOR IN CIRCUIT. 137
TABLE E. 14 SAMPLE B NORMALISED DATA. (OFFSET REMOVED.)....138
TABLE E. 15 SAMPLE C RAW DATA. CONDITIONS: SET/RESET EMPLOYED, 3.5V REGULATED SUPPLY, 9MHZ OSCILLATOR IN CIRCUIT. 139
TABLE E. 16 SAMPLE C NORMALISED DATA. (OFFSET REMOVED.)....140
TABLE E. 17 SAMPLE A RAW DATA. CONDITIONS: SET/RESET EMPLOYED, 3.5V REGULATED SUPPLY, 9MHZ OSCILLATOR DISCONNECTED FROM CIRCUIT....141
TABLE E. 18 SAMPLE A NORMALISED DATA. (OFFSET REMOVED.) 142
TABLE E. 19 SAMPLE B RAW DATA. CONDITIONS: SET/RESET EMPLOYED, 3.5V REGULATED SUPPLY, 9MHZ OSCILLATOR DISCONNECTED FROM CIRCUIT....143
TABLE E. 20. SAMPLE B NORMALISED DATA. (OFFSET REMOVED.) 144

TABLE E. 21 SAMPLE C RAW DATA. CONDITIONS: SET/RESET EMPLOYED, 3.5V REGULATED SUPPLY, 9MHZ OSCILLATOR DISCONNECTED FROM CIRCUIT..145
TABLE E. 22 SAMPLE C NORMALISED DATA. (OFFSET REMOVED.) 146
TABLE E. 23 SAMPLE A RAW DATA. CONDITIONS: SET EMPLOYED, 3.5V REGULATED SUPPLY, 9MHZ OSCILLATOR DISCONNECTED FROM CIRCUIT...147
TABLE E. 24 SAMPLE A NORMALISED DATA. (OFFSET REMOVED.) 148
TABLE E. 25 SAMPLE A RAW DATA. CONDITIONS: SET/RESET EMPLOYED, 3.6V LITHIUM BATTERY, 9MHZ OSCILLATOR DISCONNECTED FROM CIRCUIT..149
TABLE E. 26. SAMPLE A NORMALISED DATA. (OFFSET REMOVED.) 150
TABLE E. 27 SAMPLE B RAW DATA. CONDITIONS: SET/RESET EMPLOYED, 3.6V LITHIUM BATTERY, 9MHZ OSCILLATOR DISCONNECTED FROM CIRCUIT..151
TABLE E. 28. SAMPLE B NORMALISED DATA. (OFFSET REMOVED.) 152
TABLE E. 29 SAMPLE C RAW DATA. CONDITIONS: SET/RESET EMPLOYED, 3.6V LITHIUM BATTERY, 9MHZ OSCILLATOR DISCONNECTED FROM CIRCUIT..153
TABLE E. 30. SAMPLE C NORMALISED DATA. (OFFSET REMOVED.) 154
TABLE E. 31. SAMPLE A RAW DATA. CONDITIONS: SET/RESET EMPLOYED, 3.6V LITHIUM BATTERY, 9MHZ OSCILLATOR DISCONNECTED FROM CIRCUIT..155
TABLE E. 32 SAMPLE A NORMALISED DATA. (OFFSET REMOVED.) 156
TABLE E. 33. SAMPLE A RAW DATA. CONDITIONS: SET/RESET EMPLOYED, 3.6V LITHIUM BATTERY, 9MHZ OSCILLATOR DISCONNECTED FROM CIRCUIT..157
TABLE E. 34 SAMPLE A NORMALISED DATA. (OFFSET REMOVED.) 158
TABLE E. 35 SAMPLE A RAW DATA. CONDITIONS: SET/RESET EMPLOYED, 3.6V LITHIUM BATTERY, 9MHZ OSCILLATOR DISCONNECTED FROM CIRCUIT..159
TABLE E. 36. SAMPLE A NORMALISED DATA. (OFFSET REMOVED.) 160
TABLE E. 37. SAMPLE A RAW DATA. CONDITIONS: SET/RESET EMPLOYED, 3.6V LITHIUM BATTERY, 9MHZ OSCILLATOR DISCONNECTED FROM CIRCUIT..161
TABLE E. 38. SAMPLE A NORMALISED DATA. (OFFSET REMOVED.) 162

E.1 Laboratory testing of Tracker

E.1.1 Testing apparatus.

The equipment needed for testing in the laboratory.

1. Tektronix 2213 60MHz Oscilloscope and test leads.
2. Electronics Australia Bench top Power Supply 3-20V adjustable
3. Fluke 77 Series 2 Digital Multimeter.
4. Leica Aluminium Surveyors Tripod.
5. Topcon Surveyors sight, with bubble level.
6. Compound spirit level.
7. Compaq EVO N1020v laptop computer.
8. Win IDE Version 1.22, HCO8 Development software from P&E Microcomputer Systems Inc.
9. Perspex sheet 160x160mm to mount tracker.
10. Data logger with sensor board attached.
11. Communications Interface board.
12. Testing Software Module for microcontroller "Individual ADC Test"
12. Connecting RS232 cables, Power cables, Lithium 3.6V battery.

E.1.2. Testing Precautions

The sensors employed by the tracker are sensitive to both acceleration and magnetic disturbances. In order to limit unwanted effects of these quantities and to lessen the effects of EMC noise the following procedures were developed.

E.1.3. Controlling the testing environment.

All magnetic materials, ferrous tables, chairs and other equipment were excluded in a >1m radius from the instrument under test. Electrical equipment was distanced from the device with only essential power and communications cables permitted using screened leads where possible. To reduce any acceleration due to vibration the device was securely attached to the surveyor's sight using cable ties and insulation tape.

E.1.4. Set Up Procedure

- Clear area of all magnetic material and electronic equipment to a radius of >1m.
- Unfold aluminium surveyors tripod and ensure legs are sufficiently wide to provide a stable platform.
- Secure Topcon Surveyors sight to tripod and level using the integral bubble level. See Figure E.1.
- Attach Perspex sheet to Topcon Surveyors sight and level using spirit level.
- Attach tracker to Perspex sheet using blue tack.
- Plug communications cable into tracker and secure cable to movable section of surveyors sight
- Attach Communications PCB board to tripod leg using insulating tape.
- Attach remaining communications plug to communications PCB.
- Adjust height of communications PCB to permit full 360° rotation of tracker given length of communications cable may hinder this rotation.
- Plug RS232 extension cable from computer to communications PCB.
- Attach regulated 3.6V DC supply to communications PCB.
- Adjust regulated supply to 3.6V and switch on.
- Set DIP switches for communication on tracker and communications PCB.
- Start Win IDE software and make contact with tracker.
- Ensure tracker memory is erased.
- Select in software “Individual ADC Test” which ADC inputs you wish to monitor.
- Compile then load software on to tracker.
- Open In-Circuit Simulator (Debugger) and observe ADC registers.
- Perform experiments.

E.1.5 Experimental Method.

Set surveyors sight at 0° on the incremental ring of the sight.

Record ADC measurements

Rotate surveyors sight 10° CW using thumb wheel

Record ADC measurement

Continue process until 350° is reached.

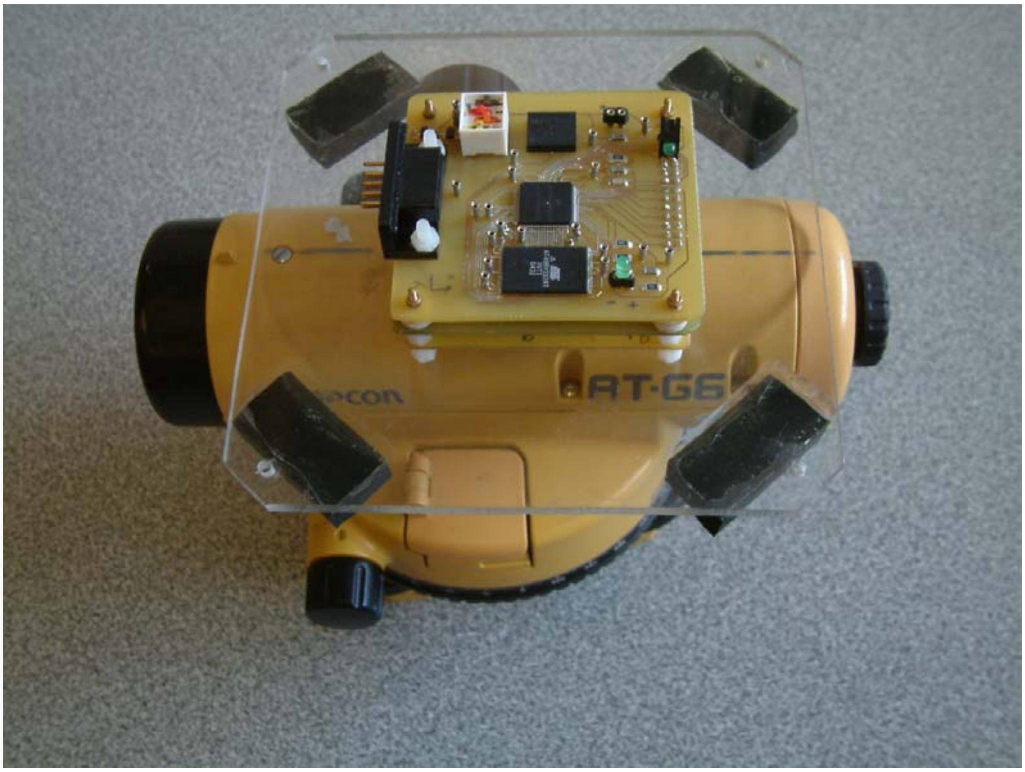

Figure E. 1 Topcon Surveyors Level with instrument in position prior to securing using cable ties and insulating tape.

E 2.1 Experiment No.1 Magnetic X and Y axis.

Table E. 1 Sample A Raw data. Conditions: No set/reset, 3.5V regulated Supply, 9MHz oscillator in circuit.

5.8.05	VCC 3.5V					
Sight Angle	High Byte	Low Byte	High Byte	Low Byte	Decimal	Decimal
Angle	Xmag High	X Low	Ymag High	Y Low	x ABS	y ABS
0	2	10	0	227	522	227
10	2	17	0	227	529	227
20	2	22	0	236	534	236
30	2	26	0	240	538	240
40	2	35	0	232	547	232
50	2	40	0	236	552	236
60	2	47	0	232	559	232
70	2	53	0	225	565	225
80	2	64	0	226	576	226
90	2	64	0	220	576	220
100	2	71	0	207	583	207
110	2	74	0	207	586	207
120	2	76	0	196	588	196
130	2	73	0	184	585	184
140	2	78	0	180	590	180
150	2	74	0	171	586	171
160	2	67	0	163	579	163
170	2	68	0	160	580	160
180	2	58	0	155	570	155
190	2	52	0	151	564	151
200	2	43	0	158	555	158
210	2	41	0	151	553	151
220	2	34	0	152	546	152
230	2	23	0	159	535	159
240	2	20	0	160	532	160
250	2	9	0	168	521	168
260	2	8	0	163	520	163
270	2	0	0	176	512	176
280	1	254	0	180	510	180
290	1	252	0	179	508	179
300	1	243	0	192	499	192
310	1	245	0	203	501	203
320	1	251	0	199	507	199
330	1	250	0	207	506	207
340	2	2	0	216	514	216
350	2	1	0	226	513	226

Table E. 2 Sample A Normalised data. (Offset removed.)

Sight Angle	Range Values X	Range Values Y	90 Phase Shift.
Angle	NormalX	NormalY	Y+90 phase
0	23	76	25
10	30	76	29
20	35	85	28
30	39	89	41
40	48	81	52
50	53	85	48
60	60	81	56
70	66	74	65
80	77	75	75
90	77	69	76
100	84	56	76
110	87	56	85
120	89	45	89
130	86	33	81
140	91	29	85
150	87	20	81
160	80	12	74
170	81	9	75
180	71	4	69
190	65	0	56
200	56	7	56
210	54	0	45
220	47	1	33
230	36	8	29
240	33	9	20
250	22	17	12
260	21	12	9
270	13	25	4
280	11	29	0
290	9	28	7
300	0	41	0
310	2	52	1
320	8	48	8
330	7	56	9
340	15	65	17
350	14	75	12

Table E. 3 Sample B Raw data. Conditions: No set/reset, 3.5V regulated Supply, 9MHz oscillator in circuit

Sight Angle Angle	High Byte Xmag High	Low Byte X Low	High Byte Ymag High	Low Byte Y Low	Decimal x ABS	Decimal y ABS
0	2	0	0	219	512	219
10	2	12	0	232	524	232
20	2	15	0	231	527	231
30	2	24	0	235	536	235
40	2	27	0	227	539	227
50	2	38	0	227	550	227
60	2	44	0	223	556	223
70	2	51	0	227	563	227
80	2	58	0	223	570	223
90	2	59	0	209	571	209
100	2	65	0	203	577	203
110	2	67	0	195	579	195
120	2	65	0	200	577	200
130	2	71	0	188	583	188
140	2	69	0	184	581	184
150	2	67	0	176	579	176
160	2	64	0	168	576	168
170	2	57	0	160	569	160
180	2	51	0	153	563	153
190	2	44	0	160	556	160
200	2	39	0	147	551	147
210	2	36	0	156	548	156
220	2	25	0	152	537	152
230	2	18	0	147	530	147
240	2	12	0	160	524	160
250	2	7	0	157	519	157
260	2	4	0	161	516	161
270	2	0	0	168	512	168
280	1	249	0	176	505	176
290	1	242	0	175	498	175
300	1	239	0	184	495	184
310	1	239	0	196	495	196
320	1	247	0	199	503	199
330	1	250	0	208	506	208
340	1	243	0	207	499	207
350	1	251	0	218	507	218

Table E. 4 Sample B Normalised data. (Offset removed.)

Sight Angle	Range Values X	Range Values Y	90 Phase Shift.
Angle	NormalX	NormalY	Y+90 phase
0	17	72	21
10	29	85	29
20	32	84	28
30	41	88	37
40	44	80	49
50	55	80	52
60	61	76	61
70	68	80	60
80	75	76	71
90	76	62	72
100	82	56	85
110	84	48	84
120	82	53	88
130	88	41	80
140	86	37	80
150	84	29	76
160	81	21	80
170	74	13	76
180	68	6	62
190	61	13	56
200	56	0	48
210	53	9	53
220	42	5	41
230	35	0	37
240	29	13	29
250	24	10	21
260	21	14	13
270	17	21	6
280	10	29	13
290	3	28	0
300	0	37	9
310	0	49	5
320	8	52	0
330	11	61	13
340	4	60	10
350	12	71	14

E 2.2 Experiment No.2 Magnetic X and Y axis.

Table E. 5 Sample A Raw data. Conditions: No set/reset, 3.5V regulated Supply, 9MHz oscillator in circuit.

	VCC					
6.8.05	3.5V					
Sight Angle	High Byte	Low Byte	High Byte	Low Byte	Decimal	Decimal
Angle	Xmag High	X Low	Ymag High	Y Low	x ABS	y ABS
0	2	0	0	160	512	160
10	1	255	0	165	511	165
20	1	247	0	171	503	171
30	1	243	0	184	499	184
40	1	249	0	185	505	185
50	1	246	0	199	502	199
60	1	244	0	197	500	197
70	1	247	0	208	503	208
80	1	246	0	216	502	216
90	1	249	0	222	505	222
100	2	4	0	223	516	223
110	2	3	0	228	515	228
120	2	15	0	238	527	238
130	2	24	0	227	536	227
140	2	28	0	231	540	231
150	2	38	0	236	550	236
160	2	40	0	234	552	234
170	2	52	0	224	564	224
180	2	56	0	223	568	223
190	2	60	0	213	572	213
200	2	66	0	207	578	207
210	2	68	0	199	580	199
220	2	67	0	200	579	200
230	2	67	0	190	579	190
240	2	70	0	183	582	183
250	2	70	0	171	582	171
260	2	59	0	163	571	163
270	2	64	0	159	576	159
280	2	59	0	160	571	160
290	2	54	0	159	566	159
300	2	40	0	156	552	156
310	2	34	0	149	546	149
320	2	27	0	147	539	147
330	2	24	0	155	536	155
340	2	11	0	159	523	159
350	2	9	0	160	521	160

Table E. 6 Sample A Normalised data. (Offset removed.)

Sight Angle	Range Values X	Range Values Y	90 Phase Shift.
Angle	NormalX1	NormalY1	Y+90 phase1
0	13	13	12
10	12	18	13
20	4	24	12
30	0	37	9
40	6	38	2
50	3	52	0
60	1	50	8
70	4	61	12
80	3	69	13
90	6	75	13
100	17	76	18
110	16	81	24
120	28	91	37
130	37	80	38
140	41	84	52
150	51	89	50
160	53	87	61
170	65	77	69
180	69	76	75
190	73	66	76
200	79	60	81
210	81	52	91
220	80	53	80
230	80	43	84
240	83	36	89
250	83	24	87
260	72	16	77
270	77	12	76
280	72	13	66
290	67	12	60
300	53	9	52
310	47	2	53
320	40	0	43
330	37	8	36
340	24	12	24
350	22	13	16

Table E. 7 Sample B Raw data. Conditions: No set/reset, 3.5V regulated Supply, 9MHz oscillator in circuit.

	VCC					
6.8.05	3.5V					
Sight Angle	High Byte	Low Byte	High Byte	Low Byte	Decimal	Decimal
Angle	Xmag High	X Low	Ymag High	Y Low	x ABS	y ABS
0	2	1	0	166	513	166
10	1	255	0	167	511	167
20	1	252	0	176	508	176
30	1	244	0	182	500	182
40	1	247	0	192	503	192
50	1	246	0	196	502	196
60	1	242	0	197	498	197
70	1	240	0	208	496	208
80	1	245	0	218	501	218
90	1	252	0	224	508	224
100	1	255	0	229	511	229
110	2	5	0	221	517	221
120	2	14	0	228	526	228
130	2	24	0	227	536	227
140	2	32	0	231	544	231
150	2	39	0	236	551	236
160	2	42	0	227	554	227
170	2	48	0	224	560	224
180	2	53	0	226	565	226
190	2	64	0	216	576	216
200	2	68	0	212	580	212
210	2	67	0	200	579	200
220	2	66	0	196	578	196
230	2	70	0	185	582	185
240	2	69	0	180	581	180
250	2	68	0	178	580	178
260	2	66	0	174	578	174
270	2	60	0	159	572	159
280	2	51	0	160	563	160
290	2	47	0	155	559	155
300	2	39	0	151	551	151
310	2	31	0	152	543	152
320	2	26	0	156	538	156
330	2	24	0	151	536	151
340	2	15	0	151	527	151
350	2	6	0	155	518	155

Table E. 8 Sample B Normalised data. (Offset removed.)

Sight Angle	Range Values X	Range Values Y	90 Phase Shift.
Angle	NormalX2	NormalY2	Y+90 phase2
0	17	15	8
10	15	16	9
20	12	25	4
30	4	31	0
40	7	41	1
50	6	45	5
60	2	46	0
70	0	57	0
80	5	67	4
90	12	73	15
100	15	78	16
110	21	70	25
120	30	77	31
130	40	76	41
140	48	80	45
150	55	85	46
160	58	76	57
170	64	73	67
180	69	75	73
190	80	65	78
200	84	61	70
210	83	49	77
220	82	45	76
230	86	34	80
240	85	29	85
250	84	27	76
260	82	23	73
270	76	8	75
280	67	9	65
290	63	4	61
300	55	0	49
310	47	1	45
320	42	5	34
330	40	0	29
340	31	0	27
350	22	4	23

Table E. 9 Sample C Raw data. Conditions: No set/reset, 3.5V regulated Supply, 9MHz oscillator in circuit.

	VCC					
6.8.05	3.5V					
Sight Angle	High Byte	Low Byte	High Byte	Low Byte	Decimal	Decimal
Angle	Xmag High	X Low	Ymag High	Y Low	x ABS	y ABS
0	2	0	0	164	512	164
10	1	254	0	163	510	163
20	1	248	0	170	504	170
30	1	242	0	176	498	176
40	1	245	0	190	501	190
50	1	241	0	192	497	192
60	1	245	0	199	501	199
70	1	248	0	203	504	203
80	1	250	0	216	506	216
90	1	254	0	222	510	222
100	1	255	0	224	511	224
110	2	3	0	224	515	224
120	2	10	0	236	522	236
130	2	20	0	231	532	231
140	2	30	0	232	542	232
150	2	35	0	227	547	227
160	2	39	0	223	551	223
170	2	48	0	228	560	228
180	2	60	0	223	572	223
190	2	64	0	211	576	211
200	2	67	0	208	579	208
210	2	72	0	200	584	200
220	2	67	0	191	579	191
230	2	71	0	183	583	183
240	2	72	0	180	584	180
250	2	65	0	175	577	175
260	2	65	0	167	577	167
270	2	59	0	166	571	166
280	2	56	0	160	568	160
290	2	47	0	157	559	157
300	2	46	0	151	558	151
310	2	36	0	154	548	154
320	2	32	0	151	544	151
330	2	22	0	151	534	151
340	2	15	0	156	527	156
350	2	14	0	158	526	158

Table E. 10 Sample C Normalised data. (Offset removed.)

Sight Angle	Range Values X	Range Values Y	90 Phase Shift.
Angle	NormalX3	NormalY3	Y+90 phase3
0	15	13	15
10	13	12	9
20	7	19	6
30	1	25	0
40	4	39	3
50	0	41	0
60	4	48	0
70	7	52	5
80	9	65	7
90	13	71	13
100	14	73	12
110	18	73	19
120	25	85	25
130	35	80	39
140	45	81	41
150	50	76	48
160	54	72	52
170	63	77	65
180	75	72	71
190	79	60	73
200	82	57	73
210	87	49	85
220	82	40	80
230	86	32	81
240	87	29	76
250	80	24	72
260	80	16	77
270	74	15	72
280	71	9	60
290	62	6	57
300	61	0	49
310	51	3	40
320	47	0	32
330	37	0	29
340	30	5	24
350	29	7	16

E 2.3 Experiment No.3. Magnetic X and Y axis.

Table E. 11 Sample A Raw data. Conditions: Set/reset employed, 3.5V regulated Supply, 9MHz oscillator in circuit.

6.8.05	VCC 3.5V					
Sight Angle	High Byte	Low Byte	High Byte	Low Byte	Decimal	Decimal
Angle	Xmag High	X Low	Ymag High	Y Low	x ABS	y ABS
0	2	6	0	159	518	159
10	1	249	0	170	505	170
20	1	248	0	167	504	167
30	1	252	0	184	508	184
40	1	243	0	187	499	187
50	1	246	0	191	502	191
60	1	244	0	204	500	204
70	1	243	0	203	499	203
80	1	252	0	213	508	213
90	1	248	0	221	504	221
100	2	2	0	219	514	219
110	2	10	0	232	522	232
120	2	18	0	225	530	225
130	2	22	0	227	534	227
140	2	30	0	236	542	236
150	2	40	0	227	552	227
160	2	43	0	223	555	223
170	2	54	0	228	566	228
180	2	56	0	219	568	219
190	2	59	0	218	571	218
200	2	65	0	212	577	212
210	2	67	0	197	579	197
220	2	76	0	192	588	192
230	2	72	0	184	584	184
240	2	74	0	179	586	179
250	2	67	0	178	579	178
260	2	69	0	172	581	172
270	2	59	0	159	571	159
280	2	55	0	160	567	160
290	2	52	0	150	564	150
300	2	43	0	155	555	155
310	2	40	0	152	552	152
320	2	34	0	147	546	147
330	2	24	0	152	536	152
340	2	20	0	157	532	157
350	2	11	0	155	523	155

Table E. 12 Sample A Normalised data. (Offset removed.)

Sight Angle Angle	Range Values X NormalX4	Range Values Y NormalY4	90 Phase Shift. Y+90 phase4
0	19	12	12
10	6	23	13
20	5	20	3
30	9	37	8
40	0	40	5
50	3	44	0
60	1	57	5
70	0	56	10
80	9	66	8
90	5	74	12
100	15	72	23
110	23	85	20
120	31	78	37
130	35	80	40
140	43	89	44
150	53	80	57
160	56	76	56
170	67	81	66
180	69	72	74
190	72	71	72
200	78	65	85
210	80	50	78
220	89	45	80
230	85	37	89
240	87	32	80
250	80	31	76
260	82	25	81
270	72	12	72
280	68	13	71
290	65	3	65
300	56	8	50
310	53	5	45
320	47	0	37
330	37	5	32
340	33	10	31
350	24	8	25

Table E. 13 Sample B Raw data. Conditions: Set/reset employed, 3.5V regulated Supply, 9MHz oscillator in circuit.

Sight Angle Angle	High Byte Xmag High	Low Byte X Low	High Byte Ymag High	Low Byte Y Low	Decimal x ABS	Decimal y ABS
0	2	3	0	160	515	160
10	2	0	0	164	512	164
20	1	249	0	173	505	173
30	1	245	0	176	501	176
40	1	245	0	183	501	183
50	1	244	0	193	500	193
60	1	248	0	202	500	202
70	1	243	0	207	499	207
80	1	247	0	211	503	211
90	1	250	0	216	506	216
100	1	252	0	218	508	218
110	2	2	0	226	514	226
120	2	10	0	230	522	230
130	2	14	0	232	526	232
140	2	21	0	232	533	232
150	2	37	0	234	549	234
160	2	43	0	227	555	227
170	2	55	0	226	567	226
180	2	55	0	222	567	222
190	2	64	0	216	576	216
200	2	64	0	209	576	209
210	2	73	0	199	585	199
220	2	72	0	196	584	196
230	2	71	0	184	583	184
240	2	72	0	179	584	179
250	2	72	0	176	584	176
260	2	63	0	167	575	167
270	2	59	0	164	571	164
280	2	60	0	154	572	154
290	2	52	0	156	564	156
300	2	47	0	152	559	152
310	2	38	0	152	550	152
320	2	32	0	147	544	147
330	2	24	0	155	536	155
340	2	16	0	150	528	150
350	2	10	0	159	522	159

Table E. 14 Sample B Normalised data. (Offset removed.)

Sight Angle Angle	Range Values X NormalX5	Range Values Y NormalY5	90 Phase Shift. Y+90 phase5srs
0	16	13	17
10	13	17	7
20	6	26	9
30	2	29	5
40	2	36	5
50	1	46	0
60	1	55	8
70	0	60	3
80	4	64	12
90	7	69	13
100	9	71	17
110	15	79	26
120	23	83	29
130	27	85	36
140	34	85	46
150	50	87	55
160	56	80	60
170	68	79	64
180	68	75	69
190	77	69	71
200	77	62	79
210	86	52	83
220	85	49	85
230	84	37	85
240	85	32	87
250	85	29	80
260	76	20	79
270	72	17	75
280	73	7	69
290	65	9	62
300	60	5	52
310	51	5	49
320	45	0	37
330	37	8	32
340	29	3	29
350	23	12	20

Table E. 15 Sample C Raw data. Conditions: Set/reset employed, 3.5V regulated Supply, 9MHz oscillator in circuit.

Sight Angle Angle	High Byte Xmag High	Low Byte X Low	High Byte Ymag High	Low Byte Y Low	Decimal x ABS	Decimal y ABS
0	2	3	0	160	515	160
10	2	0	0	164	512	164
20	1	249	0	173	505	173
30	1	245	0	176	501	176
40	1	245	0	183	501	183
50	1	244	0	193	500	193
60	1	248	0	202	500	202
70	1	243	0	207	499	207
80	1	247	0	211	503	211
90	1	250	0	216	506	216
100	1	252	0	218	508	218
110	2	2	0	226	514	226
120	2	10	0	230	522	230
130	2	14	0	232	526	232
140	2	21	0	232	533	232
150	2	37	0	234	549	234
160	2	43	0	227	555	227
170	2	55	0	226	567	226
180	2	55	0	222	567	222
190	2	64	0	216	576	216
200	2	64	0	209	576	209
210	2	73	0	199	585	199
220	2	72	0	196	584	196
230	2	71	0	184	583	184
240	2	72	0	179	584	179
250	2	72	0	176	584	176
260	2	63	0	167	575	167
270	2	59	0	164	571	164
280	2	60	0	154	572	154
290	2	52	0	156	564	156
300	2	47	0	152	559	152
310	2	38	0	152	550	152
320	2	32	0	147	544	147
330	2	24	0	155	536	155
340	2	16	0	150	528	150
350	2	10	0	159	522	159

Table E. 16 Sample C Normalised data. (Offset removed.)

Sight Angle Angle	Range Values X NormalX5	Range Values Y NormalY5	90 Phase Shift. Y+90 phase5srs
0	16	13	17
10	13	17	7
20	6	26	9
30	2	29	5
40	2	36	5
50	1	46	0
60	1	55	8
70	0	60	3
80	4	64	12
90	7	69	13
100	9	71	17
110	15	79	26
120	23	83	29
130	27	85	36
140	34	85	46
150	50	87	55
160	56	80	60
170	68	79	64
180	68	75	69
190	77	69	71
200	77	62	79
210	86	52	83
220	85	49	85
230	84	37	85
240	85	32	87
250	85	29	80
260	76	20	79
270	72	17	75
280	73	7	69
290	65	9	62
300	60	5	52
310	51	5	49
320	45	0	37
330	37	8	32
340	29	3	29
350	23	12	20

E 2.4 Experiment No 4. Magnetic X and Y axis

Table E. 17 Sample A Raw data. Conditions: Set/reset employed, 3.5V regulated Supply, 9MHz oscillator disconnected from circuit.

	VCC					
6.8.05	3.5V					
Sight Angle	High Byte	Low Byte	High Byte	Low Byte	Decimal	Decimal
Angle	Xmag High	X Low	Ymag High	Y Low	x ABS	y ABS
0	2	7	0	159	519	159
10	2	0	0	169	512	169
20	1	254	0	171	510	171
30	1	249	0	176	505	176
40	1	248	0	185	504	185
50	1	245	0	194	501	194
60	1	245	0	199	501	199
70	1	246	0	209	502	209
80	1	250	0	211	506	211
90	2	0	0	220	512	220
100	2	3	0	221	515	221
110	2	10	0	227	522	227
120	2	13	0	232	525	232
130	2	24	0	234	536	234
140	2	31	0	231	543	231
150	2	36	0	227	548	227
160	2	45	0	225	557	225
170	2	53	0	223	565	223
180	2	57	0	216	569	216
190	2	61	0	213	573	213
200	2	69	0	210	581	210
210	2	72	0	199	584	199
220	2	70	0	196	582	196
230	2	71	0	189	583	189
240	2	74	0	179	586	179
250	2	68	0	172	580	172
260	2	65	0	163	577	163
270	2	61	0	163	573	163
280	2	55	0	154	567	154
290	2	51	0	156	563	156
300	2	43	0	153	555	153
310	2	40	0	149	552	149
320	2	32	0	152	544	152
330	2	27	0	154	539	154
340	2	20	0	151	532	151
350	2	10	0	155	522	155

Table E. 18 Sample A Normalised data. (Offset removed.)

Sight Angle Angle	Range Values X NormalX4	Range Values Y NormalY4	90 Phase Shift. Y+90 phase4srs
0	18	10	14
10	11	20	5
20	9	22	7
30	4	27	4
40	3	36	0
50	0	45	3
60	0	50	5
70	1	60	2
80	5	62	6
90	11	71	10
100	14	72	20
110	21	78	22
120	24	83	27
130	35	85	36
140	42	82	45
150	47	78	50
160	56	76	60
170	64	74	62
180	68	67	71
190	72	64	72
200	80	61	78
210	83	50	83
220	81	47	85
230	82	40	82
240	85	30	78
250	79	23	76
260	76	14	74
270	72	14	67
280	66	5	64
290	62	7	61
300	54	4	50
310	51	0	47
320	43	3	40
330	38	5	30
340	31	2	23
350	21	6	14

Table E. 19 Sample B Raw data. Conditions: Set/reset employed, 3.5V regulated Supply, 9MHz oscillator disconnected from circuit.

	VCC					
6.8.05	3.5V					
Sight Angle	High Byte	Low Byte	High Byte	Low Byte	Decimal	Decimal
Angle	Xmag High	X Low	Ymag High	Y Low	x ABS	y ABS
0	2	3	0	158	515	158
10	2	0	0	167	512	167
20	1	249	0	173	505	173
30	1	251	0	176	507	176
40	1	243	0	182	499	182
50	1	243	0	196	499	196
60	1	245	0	197	501	197
70	1	245	0	208	501	208
80	1	251	0	213	507	213
90	1	255	0	219	511	219
100	2	3	0	223	515	223
110	2	10	0	230	522	230
120	2	13	0	232	525	232
130	2	20	0	228	532	228
140	2	29	0	230	541	230
150	2	35	0	233	547	233
160	2	44	0	228	556	228
170	2	53	0	223	565	223
180	2	57	0	219	569	219
190	2	64	0	213	576	213
200	2	70	0	208	582	208
210	2	70	0	203	582	203
220	2	72	0	196	584	196
230	2	73	0	188	585	188
240	2	73	0	182	585	182
250	2	72	0	176	584	176
260	2	65	0	168	577	168
270	2	64	0	159	576	159
280	2	59	0	153	571	153
290	2	49	0	151	561	151
300	2	42	0	152	554	152
310	2	38	0	147	550	147
320	2	33	0	151	545	151
330	2	24	0	152	536	152
340	2	20	0	154	532	154
350	2	13	0	160	525	160

Table E. 20. Sample B Normalised data. (Offset removed.)

Sight Angle Angle	Range Values X NormalX5	Range Values Y NormalY5	90 Phase Shift. Y+90 phase5srs
0	16	11	12
10	13	20	6
20	6	26	4
30	8	29	5
40	0	35	0
50	0	49	4
60	2	50	5
70	2	61	7
80	8	66	13
90	12	72	11
100	16	76	20
110	23	83	26
120	26	85	29
130	33	81	35
140	42	83	49
150	48	86	50
160	57	81	61
170	66	76	66
180	70	72	72
190	77	66	76
200	83	61	83
210	83	56	85
220	85	49	81
230	86	41	83
240	86	35	86
250	85	29	81
260	78	21	76
270	77	12	72
280	72	6	66
290	62	4	61
300	55	5	56
310	51	0	49
320	46	4	41
330	37	5	35
340	33	7	29
350	26	13	21

Table E. 21 Sample C Raw data. Conditions: Set/reset employed, 3.5V regulated Supply, 9MHz oscillator disconnected from circuit.

6.8.05	VCC 3.5V					
Sight Angle	High Byte	Low Byte	High Byte	Low Byte	Decimal	Decimal
Angle	Xmag High	X Low	Ymag High	Y Low	x ABS	y ABS
0	2	2	0	162	514	162
10	2	0	0	167	512	167
20	1	251	0	171	507	171
30	1	248	0	178	504	178
40	1	249	0	188	505	188
50	1	246	0	196	502	196
60	1	243	0	199	499	199
70	1	249	0	203	505	203
80	1	249	0	211	505	211
90	1	251	0	215	507	215
100	2	6	0	219	518	219
110	2	7	0	228	519	228
120	2	16	0	230	528	230
130	2	22	0	232	534	232
140	2	31	0	235	543	235
150	2	35	0	232	547	232
160	2	43	0	232	555	232
170	2	54	0	226	566	226
180	2	55	0	216	567	216
190	2	62	0	213	574	213
200	2	67	0	210	579	210
210	2	69	0	199	581	199
220	2	72	0	198	584	198
230	2	75	0	186	587	186
240	2	74	0	176	586	176
250	2	69	0	171	581	171
260	2	64	0	163	576	163
270	2	62	0	164	574	164
280	2	57	0	158	569	158
290	2	52	0	155	564	155
300	2	46	0	152	558	152
310	2	37	0	150	549	150
320	2	30	0	153	542	153
330	2	22	0	151	534	151
340	2	20	0	151	532	151
350	2	12	0	155	524	155

Table E. 22 Sample C Normalised data. (Offset removed.)

Sight Angle Angle	Range Values X NormalX6	Range Values Y NormalY6	90 Phase Shift. Y+90 phase6srs
0	15	12	14
10	13	17	8
20	8	21	5
30	5	28	2
40	6	38	0
50	3	46	3
60	0	49	1
70	6	53	1
80	6	61	5
90	8	65	12
100	19	69	17
110	20	78	21
120	29	80	28
130	35	82	38
140	44	85	46
150	48	82	49
160	56	82	53
170	67	76	61
180	68	66	65
190	75	63	69
200	80	60	78
210	82	49	80
220	85	48	82
230	88	36	85
240	87	26	82
250	82	21	82
260	77	13	76
270	75	14	66
280	70	8	63
290	65	5	60
300	59	2	49
310	50	0	48
320	43	3	36
330	35	1	26
340	33	1	21
350	25	5	13

E 2.5 Experiment No.5 Magnetic X and Y axis.

Table E. 23 Sample A Raw data. Conditions: Set employed, 3.5V regulated Supply, 9MHz oscillator disconnected from circuit.

Sight Angle Angle	High Byte Xmag High	Low Byte X Low	High Byte Ymag High	Low Byte Y Low	Decimal x ABS	Decimal y ABS
0	2	21	1	168	533	424
10	2	16	1	171	528	427
20	2	13	1	169	525	425
30	2	11	1	170	523	426
40	2	8	1	171	520	427
50	2	7	1	175	519	431
60	2	11	1	178	523	434
70	2	9	1	178	521	434
80	2	12	1	184	524	440
90	2	11	1	185	523	441
100	2	20	1	185	532	441
110	2	26	1	184	538	440
120	2	29	1	188	541	444
130	2	33	1	185	545	441
140	2	41	1	183	553	439
150	2	45	1	186	557	442
160	2	49	1	186	561	442
170	2	57	1	182	569	438
180	2	64	1	180	576	436
190	2	67	1	182	579	438
200	2	70	1	176	582	432
210	2	72	1	178	584	434
220	2	72	1	177	584	433
230	2	69	1	175	581	431
240	2	72	1	170	584	426
250	2	66	1	168	578	424
260	2	65	1	169	577	425
270	2	62	1	168	574	424
280	2	56	1	166	568	422
290	2	54	1	166	566	422
300	2	46	1	163	558	419
310	2	44	1	164	556	420
320	2	40	1	166	552	422
330	2	32	1	165	544	421
340	2	29	1	163	541	419
350	2	20	1	168	532	424

Table E. 24 Sample A Normalised data. (Offset removed.)

Sight Angle Angle	Range Values X NormalX7	Range Values Y NormalY7	90 Phase Shift. Y7+90 phase4srs
0	14	5	5
10	9	8	3
20	6	6	3
30	4	7	0
40	1	8	1
50	0	12	3
60	4	15	2
70	2	15	0
80	5	21	5
90	4	22	5
100	13	22	8
110	19	21	6
120	22	25	7
130	26	22	8
140	34	20	12
150	38	23	15
160	42	23	15
170	50	19	21
180	57	17	22
190	60	19	22
200	63	13	21
210	65	15	25
220	65	14	22
230	62	12	20
240	65	7	23
250	59	5	23
260	58	6	19
270	55	5	17
280	49	3	19
290	47	3	13
300	39	0	15
310	37	1	14
320	33	3	12
330	25	2	7
340	22	0	5
350	13	5	6

E 2.6 Experiment No.6 Magnetic X and Y axis.

Table E. 25 Sample A Raw data. Conditions: Set/reset employed, 3.6V Lithium Battery, 9MHz oscillator disconnected from circuit.

	VCC					
7.8.05	3.4V					
	Battery					
Sight	High	Low	High	Low		
Angle	Byte	Byte	Byte	Byte	Decimal	Decimal
	Xmag		Ymag			
Angle	High	X Low	High	Y Low	x ABS	y ABS
0	2	6	0	161	518	161
10	1	255	0	165	511	165
20	1	251	0	171	507	171
30	1	248	0	178	504	178
40	1	247	0	185	503	185
50	1	246	0	192	502	192
60	1	248	0	198	504	198
70	1	249	0	205	505	205
80	1	252	0	211	508	211
90	2	0	0	216	512	216
100	2	5	0	220	517	220
110	2	11	0	224	523	224
120	2	18	0	226	530	226
130	2	25	0	227	537	227
140	2	33	0	227	545	227
150	2	40	0	225	552	225
160	2	47	0	223	559	223
170	2	53	0	219	565	219
180	2	59	0	214	571	214
190	2	64	0	208	576	208
200	2	68	0	201	580	201
210	2	70	0	194	582	194
220	2	72	0	187	584	187
230	2	72	0	180	584	180
240	2	70	0	173	582	173
250	2	68	0	167	580	167
260	2	64	0	161	576	161
270	2	59	0	157	571	157
280	2	54	0	153	566	153
290	2	48	0	150	560	150
300	2	42	0	147	554	147
310	2	34	0	147	546	147
320	2	28	0	147	540	147
330	2	21	0	149	533	149
340	2	15	0	152	527	152
350	2	9	0	155	521	155

Table E. 26. Sample A Normalised data. (Offset removed.)

Sight Angle Angle	Range Values X NormalX8	Range Values Y NormalY8	90 Phase Shift. Y+90 phase8srs
0	16	14	10
10	9	18	6
20	5	24	3
30	2	31	0
40	1	38	0
50	0	45	0
60	2	51	2
70	3	58	5
80	6	64	8
90	10	69	14
100	15	73	18
110	21	77	24
120	28	79	31
130	35	80	38
140	43	80	38
150	50	78	51
160	57	76	58
170	63	72	64
180	69	67	69
190	74	61	73
200	78	54	77
210	80	47	79
220	82	40	80
230	82	33	80
240	80	26	78
250	78	20	76
260	74	14	72
270	69	10	67
280	64	6	61
290	58	3	54
300	52	0	47
310	44	0	40
320	38	0	33
330	31	2	26
340	25	5	20
350	19	8	14

Table E. 27 Sample B Raw data. Conditions: Set/reset employed, 3.6V Lithium Battery, 9MHz oscillator disconnected from circuit.

6.8.05	VCC 3.5V					
Sight Angle Angle	High Byte Xmag High	Low Byte X Low	High Byte Ymag High	Low Byte Y Low	Decimal x ABS	Decimal y ABS
0	2	3	0	160	515	160
10	1	255	0	166	511	166
20	1	251	0	171	507	171
30	1	248	0	178	504	178
40	1	247	0	185	503	185
50	1	246	0	192	502	192
60	1	247	0	199	503	199
70	1	249	0	205	505	205
80	1	252	0	211	508	211
90	2	1	0	216	513	216
100	2	6	0	221	518	221
110	2	11	0	224	523	224
120	2	18	0	227	530	227
130	2	25	0	227	537	227
140	2	32	0	227	544	227
150	2	40	0	226	552	226
160	2	47	0	223	559	223
170	2	53	0	219	565	219
180	2	59	0	214	571	214
190	2	64	0	208	576	208
200	2	67	0	201	579	201
210	2	71	0	194	583	194
220	2	72	0	187	584	187
230	2	72	0	180	584	180
240	2	70	0	173	582	173
250	2	68	0	166	580	166
260	2	64	0	161	576	161
270	2	60	0	156	572	156
280	2	54	0	152	566	152
290	2	48	0	150	560	150
300	2	42	0	148	554	148
310	2	35	0	147	547	147
320	2	28	0	148	540	148
330	2	21	0	149	533	149
340	2	15	0	152	527	152
350	2	8	0	155	520	155

Table E. 28. Sample B Normalised data. (Offset removed.)

Sight Angle Angle	Range Values X NormalX9	Range Values Y NormalY9	90 Phase Shift. Y+90 phase9srs
0	13	13	9
10	9	19	5
20	5	24	3
30	2	31	1
40	1	38	0
50	0	45	1
60	1	52	2
70	3	58	5
80	6	64	8
90	11	69	13
100	16	74	19
110	21	77	24
120	28	80	31
130	35	80	38
140	42	80	45
150	50	79	52
160	57	76	58
170	63	72	64
180	69	67	69
190	74	61	74
200	77	54	77
210	81	47	80
220	82	40	80
230	82	33	80
240	80	26	79
250	78	19	76
260	74	14	72
270	70	9	67
280	64	5	61
290	58	3	54
300	52	1	47
310	45	0	40
320	38	1	33
330	31	2	26
340	25	5	19
350	18	8	14

Table E. 29 Sample C Raw data. Conditions: Set/reset employed, 3.6V Lithium Battery, 9MHz oscillator disconnected from circuit.

6.8.05	VCC 3.5V					
Sight Angle Angle	High Byte Xmag High	Low Byte X Low	High Byte Ymag High	Low Byte Y Low	Decimal x ABS	Decimal y ABS
0	2	3	0	160	515	160
10	1	255	0	166	511	166
20	1	251	0	171	507	171
30	1	249	0	178	505	178
40	1	247	0	184	503	184
50	1	246	0	192	502	192
60	1	247	0	199	503	199
70	1	249	0	205	505	205
80	1	252	0	211	508	211
90	2	0	0	217	512	217
100	2	7	0	221	519	221
110	2	11	0	224	523	224
120	2	18	0	226	530	226
130	2	25	0	227	537	227
140	2	32	0	227	544	227
150	2	40	0	226	552	226
160	2	47	0	223	559	223
170	2	53	0	219	565	219
180	2	59	0	214	571	214
190	2	63	0	208	575	208
200	2	67	0	201	579	201
210	2	70	0	194	582	194
220	2	71	0	187	583	187
230	2	72	0	180	584	180
240	2	70	0	173	582	173
250	2	68	0	168	580	168
260	2	64	0	161	576	161
270	2	59	0	156	571	156
280	2	54	0	152	566	152
290	2	49	0	150	561	150
300	2	42	0	148	554	148
310	2	35	0	147	547	147
320	2	28	0	148	540	148
330	2	21	0	150	533	150
340	2	15	0	152	527	152
350	2	9	0	156	521	156

Table E. 30. Sample C Normalised data. (Offset removed.)

Sight Angle Angle	Range Values X NormalX10	Range Values Y NormalY10	90 Phase Shift. Y+90 phase10srs
0	13	13	9
10	9	19	5
20	5	24	3
30	3	31	1
40	1	37	0
50	0	45	1
60	1	52	3
70	3	58	5
80	6	64	9
90	10	70	13
100	17	74	19
110	21	77	24
120	28	79	31
130	35	80	37
140	42	80	45
150	50	79	52
160	57	76	58
170	63	72	64
180	69	67	70
190	73	61	74
200	77	54	77
210	80	47	79
220	81	40	80
230	82	33	80
240	80	26	79
250	78	21	76
260	74	14	72
270	69	9	67
280	64	5	61
290	59	3	54
300	52	1	47
310	45	0	40
320	38	1	33
330	31	3	26
340	25	5	21
350	19	9	14

E 2.7 Experiment No.7 Magnetic X axis.

Table E. 31. Sample A Raw data. Conditions: Set/reset employed, 3.6V Lithium Battery, 9MHz oscillator disconnected from circuit.

Sight Angle Angle	High Byte X1mag High	Low Byte X Low	High Byte X2mag High	Low Byte X Low	Decimal x1ABS	Decimal X2 ABS
0	1	192	1	192	448	448
10	1	234	1	234	490	490
20	2	19	2	19	531	531
30	2	59	2	58	571	570
40	2	93	2	94	605	606
50	2	122	2	122	634	634
60	2	146	2	146	658	658
70	2	163	2	163	675	675
80	2	173	2	173	685	685
90	2	176	2	176	688	688
100	2	171	2	171	683	683
110	2	157	2	157	669	669
120	2	138	2	138	650	650
130	2	112	2	112	624	624
140	2	81	2	80	593	592
150	2	45	2	44	557	556
160	2	6	2	6	518	518
170	1	220	1	220	476	476
180	1	178	1	177	434	433
190	1	134	1	133	390	389
200	1	92	1	92	348	348
210	1	53	1	54	309	310
220	1	19	1	20	275	276
230	0	245	0	246	245	246
240	0	222	0	222	222	222
250	0	205	0	206	205	206
260	0	195	0	195	195	195
270	0	192	0	192	192	192
280	0	198	0	197	198	197
290	0	209	0	209	209	209
300	0	230	0	229	230	229
310	0	254	0	254	254	254
320	1	30	1	30	286	286
330	1	66	1	65	322	321
340	1	106	1	106	362	362
350	1	148	1	149	404	405

Table E. 32 Sample A Normalised data. (Offset removed.)

Sight Angle Angle	Range Values X NormalX10a	Range Values X NormalX11
0	256	256
10	298	298
20	339	339
30	379	378
40	413	414
50	442	442
60	466	466
70	483	483
80	493	493
90	496	496
100	491	491
110	477	477
120	458	458
130	432	432
140	401	400
150	365	364
160	326	326
170	284	284
180	242	241
190	198	197
200	156	156
210	117	118
220	83	84
230	53	54
240	30	30
250	13	14
260	3	3
270	0	0
280	6	5
290	17	17
300	38	37
310	62	62
320	94	94
330	130	129
340	170	170
350	212	213

E 2.8 Experiment No.8 Magnetic Y axis

Table E. 33. Sample A Raw data. Conditions: Set/reset employed, 3.6V Lithium Battery, 9MHz oscillator disconnected from circuit.

Sight Angle Angle	High Byte Y1mag High	Low Byte Y1 Low	High Byte Y2mag High	Low Byte X Low	Decimal Y1ABS	Decimal Y2 ABS
0	1	251	1	251	507	507
10	1	209	1	209	465	465
20	1	169	1	169	425	425
30	1	131	1	131	387	387
40	1	97	1	97	353	353
50	1	68	1	67	324	323
60	1	46	1	46	302	302
70	1	29	1	29	285	285
80	1	19	1	19	275	275
90	1	16	1	16	272	272
100	1	22	1	21	278	277
110	1	33	1	33	289	289
120	1	51	1	51	307	307
130	1	75	1	75	331	331
140	1	107	1	107	363	363
150	1	142	1	142	398	398
160	1	181	1	181	437	437
170	1	222	1	223	478	479
180	2	7	2	7	519	519
190	2	48	2	48	560	560
200	2	89	2	89	601	601
210	2	127	2	127	639	639
220	2	160	2	160	672	672
230	2	189	2	189	701	701
240	2	212	2	212	724	724
250	2	229	2	230	741	742
260	2	239	2	239	751	751
270	2	242	2	242	754	754
280	2	238	2	238	750	750
290	2	225	2	225	737	737
300	2	207	2	207	719	719
310	2	181	2	181	693	693
320	2	152	2	153	664	665
330	2	118	2	118	630	630
340	2	79	2	79	591	591
350	2	38	2	38	550	550

Table E. 34 Sample A Normalised data. (Offset removed.)

Sight Angle Angle	Range Values X NormalY12a	Range Values Y NormalY13
0	235	235
10	193	193
20	153	153
30	115	115
40	81	81
50	52	51
60	30	30
70	13	13
80	3	3
90	0	0
100	6	5
110	17	17
120	35	35
130	59	59
140	91	91
150	126	126
160	165	165
170	206	207
180	247	247
190	288	288
200	329	329
210	367	367
220	400	400
230	429	429
240	452	452
250	469	470
260	479	479
270	482	482
280	478	478
290	465	465
300	447	447
310	421	421
320	392	393
330	358	358
340	319	319
350	278	278

E 2.9 Experiment No.9 Accelerometer Y axis and Magnetic Z axis

Table E. 35 Sample A Raw data. Conditions: Set/reset employed, 3.6V Lithium Battery, 9MHz oscillator disconnected from circuit.

Sight Angle Angle	High Byte Y1Acc High	Low Byte Y1 Low	High Byte Zmag High	Low Byte X Low	Decimal Y1AccABS	Decimal Z2 ABS
0	1	241	1	212	497	468
10	1	201	1	214	457	470
20	1	162	1	214	418	470
30	1	124	1	213	380	469
40	1	91	1	213	347	469
50	1	63	1	214	319	470
60	1	39	1	215	295	471
70	1	23	1	216	279	472
80	1	12	1	217	268	473
90	1	10	1	221	266	477
100	1	12	1	224	268	480
110	1	24	1	226	280	482
120	1	41	1	227	297	483
130	1	64	1	230	320	486
140	1	94	1	229	350	485
150	1	127	1	233	383	489
160	1	165	1	233	421	489
170	1	205	1	237	461	493
180	1	245	1	236	501	492
190	2	30	1	235	542	491
200	2	69	1	236	581	492
210	2	106	1	235	618	491
220	2	139	1	235	651	491
230	2	169	1	232	681	488
240	2	191	1	229	703	485
250	2	208	1	231	720	487
260	2	218	1	227	730	483
270	2	222	1	227	734	483
280	2	217	1	225	729	481
290	2	207	1	224	719	480
300	2	190	1	222	702	478
310	2	166	1	217	678	473
320	2	137	1	218	649	474
330	2	103	1	215	615	471
340	2	66	1	213	578	469
350	2	26	1	213	538	469

Table E. 36. Sample A Normalised data. (Offset removed.)

Sight Angle Angle	Range Values Y NormalY12a	Range Values Z NormalY13
0	225	196
10	185	198
20	146	198
30	108	197
40	75	197
50	47	198
60	23	199
70	7	200
80	-4	201
90	-6	205
100	-4	208
110	8	210
120	25	211
130	48	214
140	78	213
150	111	217
160	149	217
170	189	221
180	229	220
190	270	219
200	309	220
210	346	219
220	379	219
230	409	216
240	431	213
250	448	215
260	458	211
270	462	211
280	457	209
290	447	208
300	430	206
310	406	201
320	377	202
330	343	199
340	306	197
350	266	197

E 2.10 Experiment No.10 Accelerometer X axis and Magnetic Z axis

Table E. 37. Sample A Raw data. Conditions: Set/reset employed, 3.6V Lithium Battery, 9MHz oscillator disconnected from circuit.

Sight Angle Angle	High Byte X1Acc High	Low Byte X1 Low	High Byte Zmag High	Low Byte X Low	Decimal X1AccABS	Decimal Z2 ABS
0	1	198	1	212	454	468
10	1	156	1	211	412	467
20	1	114	1	211	370	467
30	1	78	1	210	334	466
40	1	42	1	212	298	468
50	1	12	1	211	268	467
60	0	245	1	212	245	468
70	0	228	1	214	228	470
80	0	217	1	216	217	472
90	0	216	1	219	216	475
100	0	220	1	222	220	478
110	0	232	1	222	232	478
120	0	250	1	224	250	480
130	1	19	1	225	275	481
140	1	49	1	225	305	481
150	1	84	1	231	340	487
160	1	124	1	232	380	488
170	1	166	1	233	422	489
180	1	208	1	235	464	491
190	1	251	1	233	507	489
200	2	35	1	233	547	489
210	2	73	1	232	585	488
220	2	109	1	233	621	489
230	2	137	1	232	649	488
240	2	161	1	231	673	487
250	2	179	1	227	691	483
260	2	190	1	228	702	484
270	2	192	1	226	704	482
280	2	188	1	222	700	478
290	2	176	1	222	688	478
300	2	157	1	218	669	474
310	2	133	1	218	645	474
320	2	101	1	217	613	473
330	2	65	1	213	577	469
340	2	28	1	213	540	469
350	1	240	1	210	496	466

Table E. 38. Sample A Normalised data. (Offset removed.)

Sight Angle Angle	Range Values X NormalX12a	Range Values Z NormalZ13
0	182	196
10	140	195
20	98	195
30	62	194
40	26	196
50	-4	195
60	-27	196
70	-44	198
80	-55	200
90	-56	203
100	-52	206
110	-40	206
120	-22	208
130	3	209
140	33	209
150	68	215
160	108	216
170	150	217
180	192	219
190	235	217
200	275	217
210	313	216
220	349	217
230	377	216
240	401	215
250	419	211
260	430	212
270	432	210
280	428	206
290	416	206
300	397	202
310	373	202
320	341	201
330	305	197
340	268	197
350	224	194

Appendix F Miscellaneous

Table F 1 Battery Budget by functional modules.

Functional Circuit	Current Consumption	Average current (Period 10 sec)
Microcontroller		
On	3mA x 200ms	0.06
ADC On	4.5mA x 10ms	0.0045
Sleep	0.004mA x 9.790s	0.004
Memory		
Standby	0.013 x 10s	0.013
Write	25mA x 0.001s	0.0025
Oscillator	0.150mA x 10s	0.150
Magnetic Sensor	10mA x 0.2s	0.2
Accelerometer	1.2mA x 0.2s	0.024
	Total	0.9mA